Electrostatic Polysilicon Microrelays

A dissertation submitted to the Faculty of Sciences of the University of Neuchâtel, in fulfillment of the requirements for the degree of *"Docteur ès Sciences"*

by

Marc-Alexis Grétillat
Diplômé en électronique-physique
de l'Université de Neuchâtel

Institute of Microtechnology
University of Neuchâtel
Rue Jaquet-Droz 1, CH-2007 Neuchâtel
Switzerland

1997

à mes parents
à Florence

Contents

Abbreviation table:

Abbreviation	*Description*
μ-TAS	Miniaturized total analysis system
Al	Aluminum
Au	Gold
BHF	Buffered hydrofluoric acid
BC	Boundary condition
Cr	Chromium
CAD	Computer aided design
CVD	Chemical vapor deposition/deposited
DIL	Dual in line socket
FEM	Finite element modeling
H_2O_2	Hydrogen peroxide
H_2SO_4	Sulfuric acid
HF	Hydrofluoric acid
HNO_3	Nitric acid
IC	Integrated circuit
IMT	Institute of Microtechnology
ISFET	Ion sensitive field effect transistor
$K_2Cr_2O_7$	Potassium dichromate

Abbreviation	***Description***
LOCOS	Local oxidation of the silicon
LPCVD	Low pressure chemical vapor deposition/deposited
NMOS	n-channel MOSFETs
MEMS	Microelectromechanical system
MIT	Massachusetts Institute of Technology
MOSFET	Metal-oxide-semiconductor field effect transistor
Polysilicon	Polycrystalline silicon
RIE	Reactive ion etching
SEM	Scanning electron microscope
Si	Silicon
Si_3N_4	Silicon nitride
SiO_2	Silicon dioxide
SWAMI	Side-wall masked isolation
UniNe	University of Neuchâtel

Symbols and Units:

Symbol	*Description*	*Units*
Δf_{3dB}	Bandwidth at -3 dB	Hz
$\Omega_{\square}$	Sheet resistance	Ω
β	Gain of MOSFETs	A/V^2
ρ_s/t'	Density of a beam	kg/m^3
μ	Air viscosity	kg/(m·s)
σ_r	Residual stress	Pa
$\sigma_s(h)/t'$	Gap dependent stress	Pa
ν	Poisson's ratio	
ω	see f: $\omega=2\pi f$	rad/s
dB	Decibel: $20\cdot\log(V_{out}/V_{in})$	dB
E	Young modulus	Pa
f_0	Resonance frequency	Hz
F_D	Damping forces	N
F_E	Electrical forces	N
h	Gap between a beam and the substrate	m
I_d	Drain current of a transistor	A
[K]	Matrix of the spring constant	N/m
$[K_G]$	Generalized spring constant	
L	Length of the transistor channel	m
[M]	Matrix of the mass for each coordinate	kg
$[M_G]$	Generalized mass	
n	Subthreshold slope of MOSFETs	

Symbol	*Description*	*Units*
P_D	Pressure due to the damping	Pa
Q	Quality factor: $Q=f_0/\Delta f_{-3dB}$	
R_c	Contact resistance	Ω
R_L	Load resistance	Ω
R	Resistance	Ω
t	Time	s
t′	Beam thickness	m
{q}	Modal coordinates	
U_{DC}	D. C. Voltage	V
U_{AC}	A. C. Voltage: $U_{AC}= U_{ac}\cos(\omega t)$	V
V_{ad}	Voltage of the microrelay actuation port (diffusion)	V
V_{am}	Voltage of the microrelay actuation port (microbeam)	V
V_{ds}	Drain-source voltage of a transistor	V
V_{gs}	Gate-source voltage of the transistor	V
V_{off}	Offset voltage	V
$V_{p\text{-}in}$	Pull-in voltage	V
$V_{p\text{-}out}$	Pull-out voltage	V
V_s	Substrate voltage	V
V_t	Threshold voltage of MOSFETs	V
V_{w1}	Voltage of the microrelay working port (terminal 1)	V
V_{w2}	Voltage of the microrelay working port (terminal 2)	V
{x}	Position vector	m
{ẍ}	Acceleration vector	m/s
W	Width of the transistor channel	m

Résumé

Ce paragraphe devrait donner aux lecteurs francophones une idée de ma thèse. Parmi mes proches qui m'ont soutenu tout au long de ce travail, tous ne parlent pas la langue de Shakespeare.

Cette thèse dont le titre peut se traduire par "Relais électrostatiques en polysilicium" présente la réalisation de mécanismes de taille micrométrique (un micromètre: 1 µm correspond à un millième de millimètre: 0.001 mm). Ces structures sont fabriquées grâce à des techniques similaires à celles qui sont utilisées dans la micro-électronique (photolitographies et gravures chimiques). Ces procédés ont permis de réduire la taille des composants tels que résistances, transistors et capacités afin de réaliser sur des plaquettes en silicium des circuits électroniques de plus en plus complexes oppelés puces. Ces puces se trouvent dans nos ordinateurs, télévisions, téléphones, cartes banquaires, ...

La fabrication de micromécanismes comme des poutres, des microponts ou des membranes fait appel à des matériaux tel que le silicium polycristallin (polysilicium), le nitrure et l'oxyde de silicium. Ces couches sont utilisées tant pour leurs qualités électriques que mécaniques. Elles sont déposées dans des fours à haute température. Leur structuration se fait à l'aide de procédés photolithographiques et de gravures chimiques. Grâce à ces techniques nous avons pu réaliser des microrelais.

Le Chapitre 1 rappelle brièvement les motivations qui nous ont guidés dans notre travail. Il présente d'une part les avantages de la miniaturisation: réduction de la masse, vitesse plus élevée, intégration de plusieurs structures en même temps. D'autre part comme cette nouvelle technologie permet de très bien contrôler les dimensions des structures, elle a ouvert de nouvelles perspectives pour la réalisation de structures commandées por des forces électrostatiques. En effet la courbe de Paschen, qui définit la tension nécessaire pour tirer un arc électrique entre deux électrodes, possède un minimum pour une distance entre les électrodes de 9 µm (à pression ambiante, sous atmosphère d'azote: Figure 1.1). Ainsi pour des structures dont les dimensions

sont inférieures à 9 µm, nous nous trouvons dans une situation très favorable de ce point de vue puisqu'à aucun moment nous ne passons par ce minimum, ce qui est le cas par contre pour des structures macroscopiques.

Le Chapitre 2 explique l'usinage de surfoce du silicium ainsi que certains aspects de l'encapsulotion de structures méconiques. Différentes techniques sont présentées comme, l'usinage de surface de petits couvercles sur des résonateurs, l'usinage de capilloires en verre et l'encapsulation de capteurs de vitesse angulaire.

Basé sur le développement de structures résonantes en multicouche, nous avons conçu et fabriqué des microrelais dont les quatre terminaux sont complètement isolés électriquement. Le concept et la réalisation de ces structures sont expliquées dans le Chapitre 3, qui présente également leur coractérisation. Ces structures ont permis de démontrer la qualité du silicium polycristollin comme couche mécanique. En effet le microrelais dont la partie méconique octive (actionneur) est formée par une poutre multicouche en silicium polycristallin et en nitrure de silicium a permis de faire des tests de durée de vie. Il a été possible de les octionner 10^9 fois sons dommage. Ce résultat est très prometteur et laisse présager l'utilisation de ce matériau pour des micro-actionneurs industriels.

Le Chapitre 4 expose les simulations réalisées à Boston au "Massachusetts Institute of Technology" dans le groupe du Professeur Steve Senturia. Ces travaux ont été réalisés lors d'un stage de trois mois durant l'été 1996. Ils consistent en la combinaison de différents outils de simulation qui permettent de prédire le comportement des relais lorsqu'on les octionne. Ces prédictions ont été confrontées aux mesures.

Pour conclure, je peux dire que cette thèse m'a beaucoup aidé dans la façon d'aborder un nouveau problème. Grâce à cette expérience, chaque nouveau projet parait plus facile à entreprendre. J'espère que dans le futur, de port les nouveaux outils de simulation qui apparaissent maintenont sur le marché, nous aurons la possibilité de concevoir de nouveaux produits de haute technologie plus rapidement et ainsi d'améliorer la qualité de vie des gens.

1. Introduction

1.1 Short history of sensors, actuators and microsystems:

The miniaturization of mechanical devices has always been a goal of mechanics. The area of Neuchâtel has a long experience in watch factories where one target was to make complex but small watches. With fine mechanics these people were able to do very flat wrist watches with a thickness in the order of a coin [1.1]. The history of this field of activity illustrates well the tendency of decreasing the size of the components and increasing the complexity of the devices. Many mechanical watches are fabricated with very sophisticated mechanics to give the date. Some of them include the perpetual calendar, others indicate the phase of the moon. All these functions which where available on Church astronomical clocks (as in the cathedral of Strasbourg in France) have been miniaturized to take place in a wrist watch.

The technological revolution of the quartz technology has allowed more precise and stable watches to be made. Combined with electronics it has begun the age of the "computer-watch" which has induced a diversification of the watches to include new functions like calculators, altimeters, etc.

Based on the electronics technology, the silicon sensors field has started 35 years ago, around 1960 when a light detector was made in silicon. At about the same time articles on the Hall [1.2, 1.3] and piezoresistive [1.4, 1.5] effects have been published. These works allowed the integration of the first physical and chemical sensors in the seventies [1.6, 1.7]. Inspired by the success of these first silicon sensors, a myriad of smart sensors has been developed in many laboratories around the world [1.8, 1.9, 1.10, 1.11, 1.12]. The first surface micromachined device was the resonant gate transistor presented by Nathanson et al. in 1967 [1.13]. Mechanical switches have been reported by Petersen in 1979 [1.14]. The golden age of the surface micromachining has begun in 1983 [1.15]. Since then, many interesting surface micromachined devices have been developed [1.16, 1.17, 1.18, 1.19, 1.20, 1.21, 1.22, 1. 23, 1.24, 1.25, 1.26, 1.27, 1.28, 1.29, 1.30, 1.31, 1.32, 1.33, 1.34, 1.35, 1.36, 1.37, 1.38, 1.39, 1.40, 1.41].

1.2 Modeling of microsystems:

The evolution of the sensors, actuators and microsystems field is toward developing systems with many functions in a small volume. The integration of different devices requires that their characteristics are well known. For this purpose there is a growing need for more and more accurate systems to simulate these devices. As electromechanical coupling is highly nonlinear, the modeling of such devices is not very accurate with analytical formulas, so new computer based approaches are emerging [1.42, 1.43, 1.44, 1.45, 1.46, 1.47, 1. 48]. These allow, in particular for electrostatic devices, to get their main working parameters. Based on finite element modeling (FEM) quasi static simulations are performed. To simulate the dynamics of electromechanical devices, a macro-model approach is the best way to get results in accordance with measurements [1.49, 1.50, 1.51, 1.52].

Nevertheless, it is very important to extract the mechanical properties of every layer which make up the device to insure a good accuracy between the simulation and the measurements [1.53, 1.54, 1.55, 1.56, 1.57]. Moreover the effects of the residual stress [1.58, 1.59] have to be taken into account for the modeling of such microelectromechanical systems.

1.3 Advantages of the miniaturization:

The use of batch fabrication techniques enable the reduction of the size of the integrated devices which offer many advantages: high speed, the possibility to fabricate many devices at the same time, the possibility of building arrays of devices, etc. [1.60, 1.61]. As the mass and the stiffness do not scale down the same way, the reduction of the size allows to build devices which have a small inertia and which support large accelerations and shocks. Thanks to the surface micromachining technology, it allows to build thin and long beams which thickness is 1 μm and which length is up to 500 μm.

Moreover the surface micromachining allows to realize well controlled gaps between the device and the counter electrode in the substrate. This was used in some capacitive accelerometers to define the sensing capacitance with a good accuracy [1.32]. Electrostatic forces can also be used to drive micromachined devices [1.13]. As the gaps are small and well controlled a good reproducibility can be achieved with this technology. Moreover, it allows to get a high density of energy to drive the devices and thus a relatively low driving

voltage. As indicated in Figure 1.1, the minimum of the Paschen law is at about 9 µm for Nitrogen at ambient pressure [1.62,1.63]. For the microrelays presented in this Thesis the gaps were about 1.5 µm, being under this limit. For driving voltages up to 80V, no breakdown current has been observed, which points out that such a configuration is promising for electrostatic microrelay applications.

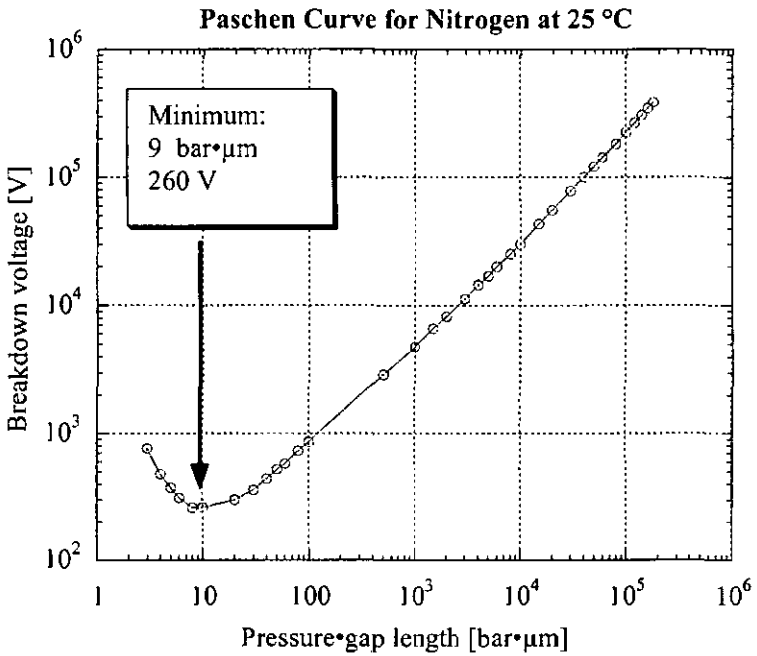

Figure 1.1: Paschen law for Nitrogen at 25 °C [1.63].

1.4 Objectives and outline of this work:

1.4.1 Objectives:

The first objective of this Ph.D. Thesis is to demonstrate the fabrication, the characterization and the modeling of electrostatic polysilicon microrelays. A relay is a four terminals switching device which controls the connection between two conductors. Two terminals are used for the driving port also called the input while the two other ones are intended for the contact port also called the output or the working circuit in this Ph.D. Thesis. A key point of such a device is that its terminals have to be fully isolated. A multilayer moving part is a solution to build such a device. This particular configuration will be described in this Ph.D. Thesis.

The main publications which have influence the microrelays design are given in Table 1-1. Some features such as the driving principle as well as the actuator and contact materials are compared with the approach which will be detailed in this Ph.D. Thesis.

The relays presented here are fabricated with the surface micromachining technique which uses a sacrificial layer to define the gap between the structure and the substrate. Thanks to the well controlled gaps under the actuator beams, this work has confirmed the possibility to use electrostatic forces to drive microrelays. Moreover it was possible to operate these devices for a large number of cycles and thus to test the mechanical stability of the polysilicon-nitride multilayer beam. These results have confirmed the low wear of the polysilicon-nitride multilayer beam which occurs when it is operated for a long period. An other interesting parameter investigated in this Ph.D. Thesis is the high switching speed of these microrelays which confirms the interest of the miniaturization.

A comparison between basic measured properties of the microrelays (switching voltage, resonant behavior and switching speed) and corresponding quasi-static and dynamic models is presented. The models presented here offer a good insight into the behavior of the polysilicon microrelay, including the squeeze film effect due to the air under the beam and the compliant beam supports.

Table 1-1: References which have influenced the relays design:

References	Driving	Actuator	Contact
Petersen [1.14]	Electrostatic	Gold/Silicon dioxide beam	Gold
Sakata [1.64]	Electrostatic	Silicon plate	Gold
Hosaka et al.[1.65]	Electromagnetic	Permalloy spiral spring	Gold, Silver and Palladium
This Ph.D. Thesis	Electrostatic	Polysilicon/Nitride beam	Polysilicon

1.4.2 Outline:

Chapter 1 is a brief introduction of the silicon micromachining. It gives the objectives and the outline of this work.

Chapter 2 starts with a description of the basic processing steps of the surface micromachining technology. It deals also with the encapsulation of microelectromechanical systems. The surface encapsulation and the glass micromachining are described. Some basic concepts of the encapsulation are explained including the fact that it has to be investigated at the beginning of the project, explaining the position of this chapter in this Thesis.

Chapter 3 explains the fabrication and the characterization of electrostatic polysilicon microrelays. These devices offer a high off-state to on-state impedance ratio. As the micromachining allows a reduction of size, these devices can be operated faster (100 kHz) than conventional mechanical relays (1 kHz).

Chapter 4 explains the modeling of the electrostatic microrelay which is presented in Chapter 3. These simulations have been done at the Massachusetts Institute of Technology (MIT) in the group of Professor Stephen Senturia. Chapter 4 describes the nonlinear behavior of the multilayer beam capacitor. The quasi-static and the dynamic behavior of these devices are investigated, including the pull-in voltage, the operate time versus the applied voltage, the resonance frequency as well as the spring softening effect.

Chapter 5 is the final conclusion which highlights the work performed in this Ph.D. Thesis and compares it to the main publications found in the literature on this topic.

1.5 References:

[1.1] International Museum of Watches, La Chaux-de-Fonds, Switzerland

[1.2] E. H. Putley, "The Hall Effect and Semiconductor Physics", Dover, New York, 1960.

[1.3] R. S. Popovic, "Hall Effect Devices", Sensors1. 3 & Actuators, 17 (1989), pp. 39-53

[1.4] W. G. Pfann and R. N. Thurston, "Semiconducting Stress Transducers Utilizing the Transverse and Shear Piezoresistance Effects", Journal of Applied physics, 32-10 (1961), pp. 2008-2019.

[1.5] B. Kloeck, "Design, Fabrication and Characterization of Piezoresistive Pressure Sensors, Including the Study of Electrochemical Etch-Stop", Ph.D. Thesis, Institute of Microtechnology, University of Neuchâtel, Switzerland, 1989.

[1.6] S. Middelhoek, "Quo-Vadis Silicon Sensors", Sensors & Actuators, A41-42 (1994), pp. 1-8.

[1.7] S. Middelhoek, "Silicon Sensors", Measurement Science & Technology, 6 (1995), pp. 1641-1658.

[1.8] "Microsensors", IEEE Press, Edited by R. S. Muller, R. T. Howe, S. D. Senturia, R. L. Smith and R. M. White, New York, 1991.

[1.9] J. W. Gardner, "Microsensors: Principles and Applications", John Wiley & Sons, Inc., Chichester, 1994.

[1.10] "Semiconductor Sensors", John Wiley & Sons, Inc., Edited by S. M. Sze, New-York, 1994.

[1.11] "Mechanical Sensors", Sensors-A Comprehensive Survey, Edited by H. H. Bau, N. F. de Rooij and B. Kloeck, Weinheim, Vol. 7, 1994.

[1.12] "Sensors Technology and Devices", Artech House, Edited by Lj. Ristic, Boston, 1994.

[1.13] H. C. Nathanson, W. E. Newell, R. A. Wickstrom and J. R. Davis Jr., "The Resonant Gate Transistor", IEEE Transactions on Electron Devices, Vol. 14-3 (1967), pp. 117-133.

[1.14] K. E. Petersen, "Micromechanical Membrane Switches on Silicon", IBM Journal of Research and Development, Vol. 23-4 (1979), pp. 376-385.

[1.15] R.T. Howe and R.S. Muller, "Polycristalline and Amorphous Silicon Micromechanical Beams: Annealing and Mechanical Properties", Sensors & Actuators, 4 (1983), pp. 447-454.

[1.16] R. T. Howe, "Resonant Microsensors", Digest of Technical Papers of the 4th International Conference on Solide-State Sensors and Actuators, Transducers '87, Tokyo, Japan, June 1987, pp. 843-848.

[1.17] M. Mehregany, K. J. Gabriel, W. S. N. Trimmer, "Integrated Fabrication of Polysilicon Mechanisms", IEEE Transactions on Electron Devices, Vol. 35 N°6 (1988), pp. 719-723.

[1.18] Y. C. Tai, R. S. Muller and R. T. Howe, "Polysilicon-Bridges for Anemometer Applications", Digest of Technical Papers of the 3rd International Conference on Solide-State Sensors and Actuators, Transducers '85, Philadelphia, PA, June 1985, pp. 354-357.

[1.19] M. W. Putty, S. C. Chang, R. T. Howe, A. L. Robinson and K. D. Wise, "One-Port Active Polysilicon Resonant Microstructures", Proceedings of the 2nd IEEE Workshop on Micro Electro Mechanical Systems, MEMS '89, Salt Lake City, UT, February 1989, pp. 60-65.

[1.20] L. S. Tavrow, S. F. Bart, J. H. Lang and M. F. Schlecht, "A LOCOS Process for an Electrostatic Microfabricated Motor", Sensors & Actuators, A21-A23 (1990), pp. 893-898.

[1.21] J. J. Sniegowski, H. Guckel and T. R. Christenson, "Performance characteristics of second generation polysilicon resonating beam force transducers", Technical Digest of IEEE Solid-State Sensor and Actuator Workshop, Hilton Head Island, SC, June 1990, pp. 9-12.

[1.22] T. S. J. Lammerink, M. Elwenspoek, R. H. Van Ouwerkerk, S. Bouwstra and J. H. J. Fluitman, "Performance of Thermally Excited Resonators", Sensors & Actuators, A21-A23 (1990), pp. 352-356.

[1.23] S. Bouwstra, "Resonating Microbridge Mass Flow Sensor", Ph.D. Thesis, University of Twente, The Netherlands, 1990.

[1.24] M. M. Farooqui and A. G. R. Evans, "Polysilicon microstructures", Proceedings of the 4th IEEE Workshop on Micro Electro Mechanical Systems, MEMS '91, Nara, Japan, January 1991, pp. 187-191.

[1.25] H. A. C. Tilmans, D. J. IJntema and J. H. J. Fluitman, "Single Element Excitation and Detection of (Micro-)Mechanical Resonators", Digest of Technical Papers of the 6th International Conference on Solide-State Sensors and Actuators, Transducers '91, San Francisco, CA, June 1991, pp. 533-537.

[1.26] C. Linder, L. Paratte, M.-A. Grétillat, V. P. Jaecklin and N. F. de Rooij, "Surface micromachining", Journal of Micromechanics and Microengineering, 2 (1992), pp. 122-132.

[1.27] K. S. J. Pister, "Hinged Polysilicon structures with Integrated CMOS TFTs", Technical Digest of IEEE Solid-State Sensor and Actuator Workshop, Hilton Head Island, SC, June 1992, pp. 136-139.

[1.28] Lj. Ristic, R. Gutteridge, B. Dunn, D. Mietus and P. Bennett, "Surface Micromachined Polysilicon Accelerometer", Technical Digest of IEEE Solid-State Sensor and Actuator Workshop, Hilton Head Island, SC, June 1992, pp. 118-121.

[1.29] L. C. Kong, B. G. Orr and K. D. Wise, "Integrated Electrostatically Resonant Scan Tip for an Atomic Force Microscope", Journal of Vacuum Science & Technology B, Vol. 11-3 (1993), pp. 634-641.

[1.30] D. F. Moore, M. I. Lutwyche and A. C. F. Hoole, "Fabrication of Freestanding Structures and Proposed Applications in Tunneling Sensors", Journal of Vacuum Science & Technology B, 11-6 (1993), pp. 2548-2551.

[1.31] K. Deng, M. Mehregany, A. S. Dewa, "A simple fabrication process for polysilicon side-drive micromotors", Journal of Microelectromechanical Systems, 3: 4 (1994), 126-133.

[1.32] W. Kuehnel and S. Sherman, "A Surface Micromachined Silicon Accelerometer with On-Chip Detection Circuitry", Sensors & Actuators, A45 (1994), pp. 7-16.

[1.33] H. A. C. Tilmans, R. Legtenberg, H. Schurer, D. J. Ijntema, M. Elwenspoek and J. H. J. Fluitman, "(Electro-)Mechanical Characteristics of Electrostatically Driven Vacuum Encapsulated Polysilicon Resonators", IEEE Transactions on Ultrasonics Ferroelectrics and Frequency Control, Vol. 41-1 (1994), pp. 4-6.

[1.34] J. Bernstein, S. Cho, A. T. King, A. Kourepenis, P. Maciel and M. Weinberg, "A Micromachined Comb-Drive Tuning Fork Rate Gyroscope", Proceedings of the 6th IEEE Workshop on Micro Electro Mechanical Systems, MEMS '93, Fort Lauderdale, FL, February 1994, pp. 143-148.

[1.35] J. W. Judy, R. S. Muller and H. H. Zappe, "Magnetic Microactuation of Polysilicon Flexure Structures", Technical Digest of IEEE Solid-State Sensor and Actuator Workshop, Hilton Head Island, SC, June 1994, pp. 43-48.

[1.36] C. Keller and M. Ferrari, "Milli- Scale Poysilicon Structures", Technical Digest of IEEE Solid-State Sensor and Actuator Workshop, Hilton Head Island, SC, June 1994, pp. 132-137.

[1.37] M. W. Putty and K. Najafi, "A Micromachined Vibrating Ring Gyroscope", Technical Digest of IEEE Solid-State Sensor and Actuator Workshop, Hilton Head Island, SC, June 1994, pp.213-220.

[1.38] P. Cheung, R. Horowitz and R. T. Howe, "Design, fabrication, position sensing, and control of an electrostatically-driven polysilicon microactuator", IEEE Transactions on Magnetics, Vol. 32-1 (1996), pp. 122-128.

[1.39] J. J. Sniegowski, "Moving the World with Surface Micromachining", Solid State Technology, February 1996, pp. 83-90.

[1.40] T. Akiyama, D. Collard and H. Fujita, "Scratch Drive Actuator with Mechanical Links for Self-Assembly of Three-Dimensional MEMS", Journal of Microelectromechanical Systems, Vol. 6 (1997), pp. 10-17.

[1.41] C. S. Pan and W. Hsu, "An Electro-Thermally and Laterally Driven Polysilicon Microactuator", Journal of Micromechanics and Microengineering, 7 (1997), pp. 7-13.

[1.42] P. Osterberg, H. Yie, X. Cai, J. White and S. D. Senturia, "Self-Consistent Simulation and Modeling of Electrostatically Deformed Diaphragms", Proceedings of the 7th IEEE Workshop on Micro Electro Mechanical Systems, MEMS '94, Oiso, Japan, January 1994, pp. 28-32.

[1.43] J. G. Korvink, J. Funk, M. Roos, G. Wachutka and H. Baltes, "SESES: A Comprehensive MEMS Modelling System", Proceedings of the 7th IEEE Workshop on Micro Electro Mechanical Systems, MEMS '94, Oiso, Japan, January 1994, pp. 22-27.

[1.44] J. R. Gilbert, R. Legtenberg and S. D. Senturia, "3D Coupled Electro-mechanics for MEMS: Applications of CoSolve-EM", Proceedings of the 8th IEEE Workshop on Micro Electro Mechanical Systems, MEMS '95, Amsterdam, the Netherlands, January 1995, pp. 122-127.

[1.45] P. M. Osterberg and S. D. Senturia, ""MemBuilder": An Automated 3D Solid Model Construction Program for Microelectromechanical Structures", Digest of Technical Papers of the 8th International Conference on Solide-State Sensors and Actuators, Transducers '95, Stockholm, Sweden, June 1995, vol.2: pp. 21-24.

[1.46] S. D. Senturia, "CAD for Microelectromechanical Systems", Digest of Technical Papers of the 8th International Conference on Solide-State Sensors and Actuators, Transducers '95, Stockholm, Sweden, June 1995, vol.2: pp. 5-8.

[1.47] Y. He, R. Harris, G. Napadenski and F. Maseeh, "A Virtual Prototype Manufacturing Software System for MEMS", Proceedings of the 9th IEEE Workshop on Micro Electro Mechanical Systems, MEMS '96, San Diego, CA, February 1996, pp. 122-126.

[1.48] MICROCOSM, Software solutions for MEMS design, 201 Willesden Drive, Cary, NC 27513, davec@memcad.com.

[1.49] R. K. Gupta, E. S. Hung, Y. J. Yang, G. K. Ananthasuresh and S. D. Senturia, "Pull-in Dynamics of Electrostatically-actuated Beams", Technical Digest of IEEE Solid-State Sensor and Actuator Workshop, Late news paper, Hilton Head Island, SC, June 1996, pp. 1-2.

[1.50] Y. J. Yang and S. D. Senturia, "Numerical Simulation of Compressible Squeezed-Film Damping", Technical Digest of IEEE Solid-State Sensor and Actuator Workshop, Hilton Head Island, SC, June 1996, pp. 76-79.

[1.51] G. K. Ananthasuresh, R. K. Gupta and S. D. Senturia, "An Approach to Macromodeling of MEMS for Nonlinear Dynamic Simulation", Proceedings of the ASME International Mechanical Engineering Congress and Exposition, Symposium on MEMS, Atlanta, GA, November 1996, pp. 18-22.

[1.52] Y. J. Yang, M.-A. Grétillat and S. D. Senturia, "Effect of Air Damping on the Dynamics of Nonuniform Deformations of Microstructures", Digest of Technical Papers of the 9th International Conference on Solide-State Sensors and Actuators, Transducers '97, Chicago, IL, June 1997, pp. 1093-1096.

[1.53] E. Obermeier, P. Kopystynski and R. Niessl, "Characteristics of polysilicon layers and their application in sensors", Technical Digest of IEEE Solid-State Sensor and Actuator Workshop, Hilton Head Island, SC, June 1986, pp. 1-4.

[1.54] H. Guckel, D. W. Burns, H. A. C. Tilmans, D. W. de Roo and C. R. Rutigliano, "Mechanical Properties of Fine Grained Polysilicon The Repeatability Issue", Technical Digest of IEEE Solid-State Sensor and Actuator Workshop, Hilton Head Island, SC, June 1988, pp. 96-99.

[1.55] P. Osterberg, R. K. Gupta, J. R. Gilbert and S. D. Senturia, "Quantitative Models for the Measurement of Residual Stress, Poisson Ratio and Young's Modulus Using Electrostatic Pull-in of Beams and Diaphragms", Technical Digest of IEEE Solid-State Sensor and Actuator Workshop, Hilton Head Island, SC, June 1994, pp. 184-188.

[1.56] R. K. Gupta, P. Osterberg and S. D. Senturia, "Material Property Measurement of Micromechanical Polysilicon Beams", Proceedings of the SPIE 1996 Conference: Microlithography and Metrology in Micromachining II, Austin, TX, October 1996, pp. 39-45.

[1.57] P. M. Osterberg and S. D. Senturia, "M-Test: A Test Chip of MEMS Material Property Measurement using Electrostatic Actuated Test

Structures", Journal of Microelectromechanical Systems, Vol. 6 N°2 (1997), pp. 107-118.

[1.58] B. P. Vandrieenhuizen, J. F. L. Goosen, P. J. French and R. F. Wolffenbuttel, "Comparison of Techniques for Measuring Both Compressive and Tensile Stress in Thin Films", Sensors & Actuators, A37-38 (1993), pp. 756-765.

[1.59] A. Benitez, J. Bausells, E. Cabruja, J. Esteve and J. Samitier, "Stress in Low Pressure Chemical Vapour Deposition Polycrystalline Silicon Thin Films Deposited Below 0.1 Torr", Sensors & Actuators, A37-38 (1993), pp. 723-726.

[1.60] W. E. Newell, "Miniaturization of Tuning Forks", Science, Vol. 161 (1968), pp. 1320-1326.

[1.61] W. Trimmer, "Micromechanical Systems", Integrated Micro-Motion Systems - Micromachining, Control and Applications, F. Harashima (Editor), 1990, pp. 1-15.

[1.62] F. Paschen, "Uber die zum Funkenübergang in Luft, Wasserstoff und Kohlensäure bei verschiedenen Drucken erforderliche Potentialdifferenz", Annalen der Physik, 37 (1887), pp. 69-96.

[1.63] T. W. Dakin, G. Luxa, G. Oppermann, J. Virgeux, G. Wind and H. Winkelnkemper, "Breakdown of Gasses in Uniform Fields - Paschen Curves for Nitrogen, Air and Sulfur Hexafluoride", Electra, N°32 (1974), pp. 61-82.

[1.64] M. Sakata, "An Electrostatic Microactuator For Electro-Mechanical Relay", Proceedings of the 2nd IEEE Workshop on Micro Electro Mechanical Systems, MEMS '89, Salt Lake City, UT, February 1989, pp. 149-151.

[1.65] H. Hosaka, H. Kuwano and K. Yanagisawa, "Electromagnetic Microrelays: Concept and Fundamental Characteristics", Proceedings of the 6th IEEE Workshop on Micro Electro Mechanical Systems, MEMS '93, Fort Lauderdale, FL, February 1993, pp. 12-17.

2. Surface micromachining and packaging technologies

2.1 Introduction:

This chapter presents some aspects on the packaging of silicon micromachined devices [2.1]. It has been placed before the microrelay fabrication, because it is a very important point which has to be investigated at the beginning of the work. Many papers published in the literature describe interesting devices, giving a lot of fabrication details but don't explain the encapsulation procedure used to test the devices, or simply test them on a test bench with probe needles [2.2, 2.3]. These kind of devices are interesting from an academic point of view, to test the feasibility of the process as well as some particular physical properties. But to push products on the market, it is evident that it is necessary to consider the packaging at the beginning of the project. Otherwise the time necessary to find an encapsulation will be too long and thus the costs will stop the project at the prototype level.

This chapter will deal with two packaging techniques: surface encapsulation and glass micromachining. The surface encapsulation is the combination of different sacrificial layers to obtain a free standing microstructure completely encapsulated by small polysilicon [2.4, 2.5, 2.6, 2.7, 2.8, 2.9, 2.10, 2.11, 2.12, 2.13, 2.14, 2.15, 2.16], silicon [2.17, 2.18] or silicon nitride [2.14, 2.19, 2.20] caps. This technology allows vacuum encapsulation, but is not strong enough to provide a mechanical protection. Thus it is often necessary to have a stronger way to package the devices [2.21]. Another way to encapsulate micromachined devices is the bonding of different wafers together [2.22, 2.23, 2.24, 2.25, 2.26, 2.27, 2.28]. Particular attention will be given to the glass micromachining. Combined with anodic bonding, this technology allows vacuum packaging of different sizes of devices [2.29, 2.30]. It has been demonstrated with the fabrication of capillary tubes [2.31, 2.32] and has been applied to the encapsulation of a silicon resonant gyroscope [2.33].

2.2 Surface micromachining:

2.2.1 Introduction:

Surface micromachining is a well known technology to realize sensors and actuators. Usually it utilizes low pressure chemical vapor deposited (LPCVD) polycrystalline silicon (polysilicon) as the building material and silicon dioxide (SiO_2) as the sacrificial layer [2.34, 2.35, 2.36, 2.37, 2.38, 2.39, 2.40, 2.41, 2.42, 2.43, 2.44, 2.45, 2.46, 2.47, 2.48]. A famous example of a surface micromachined commercially available device is the accelerometer of Analog Devices, which is build using this technique and integrated together with the sensing electronics [2.49, 2.50, 2.51]. Some work has also been realized at the Institute of Microtechnology (IMT) of the University of Neuchâtel (UniNe) where the mechanical structure is a single layer of polysilicon [2.52, 2.53, 2.4]. The latter has excellent mechanical properties which are similar to those of single-crystal silicon.

As the working circuit and the actuation circuit of microrelays have to be electrically insulated, the realization of multilayer beams is essential to build such devices.

This section will briefly describe the surface micromachining which will be used for the realization of microrelays. Some aspects such as the stress of the polysilicon as well as the metallization of released structures will be discussed.

2.2.2 Main processing steps of the surface micromachinig:

The surface micromachining technology developed at the IMT [2.4] uses silicon dioxide as the sacrificial layer. Figure 2.1 shows two approaches: the first one consists in the chemical vapor deposition (CVD) of a silicon dioxide layer at low temperature (400 °C), while the second one uses the local oxidation of the silicon (LOCOS) at high temperature (1100 °C) [2.54]. The masking material for the LOCOS process is a LPCVD silicon nitride (Si_3N_4) layer.
The mechanical structure is then deposited and patterned on top of the sacrificial layer. Finally it is released by the etching of the sacrificial silicon dioxide layer in buffered hydrofluoric acid (BHF) or in 50% hydrofluoric acid (50% HF). The etching rate of the latter depends on the type of silicon dioxide (CVD or thermal), on the annealing temperature and on the doping.

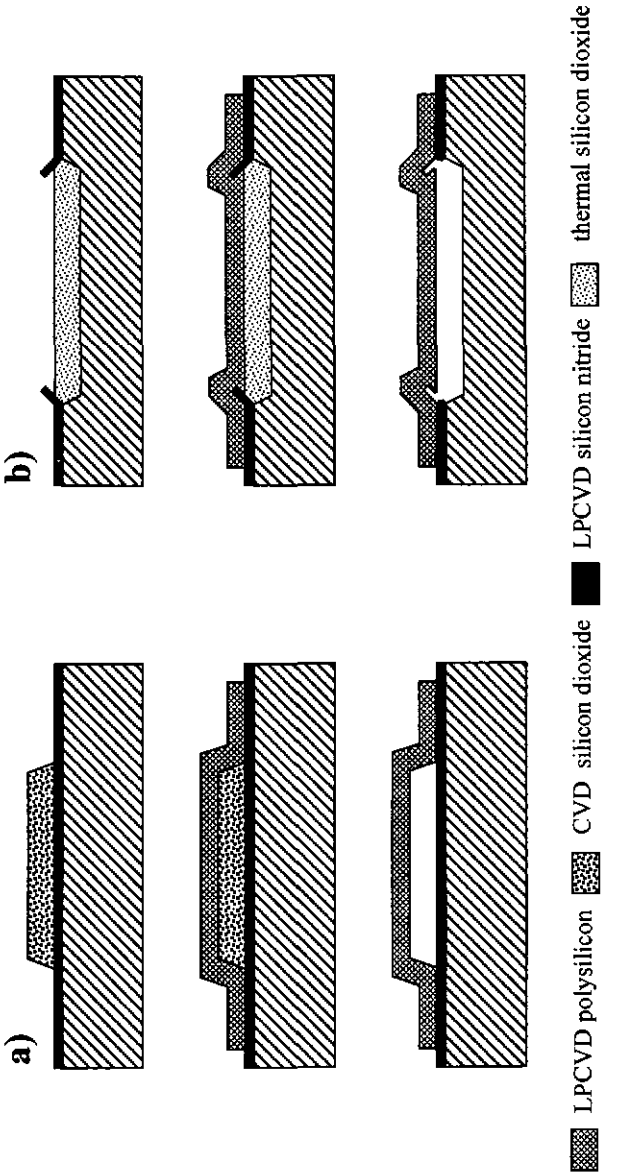

Figure 2.1: Key processing steps for the fabrication of free standing polysilicon beams a) using CVD silicon dioxide; b) using local thermal dioxide as sacrificial layer [2.52].

For phosphorus doped CVD silicon dioxide (≅ 4 wt.%) [2.52], the etch rate in BHF [7:1] is 0.3 μm/min while it is 0.1 μm/min for undoped thermal oxide.

The process using a CVD silicon dioxide as sacrificial layer is interesting because it allows the doping of the substrate to fabricate an electrode under the structure. It will be used in the realization of the polysilicon microrelays.

2.2.3 Polysilicon doping and residual stress:

The annealing and the doping of the polysilicon layer is very important to obtain free standing structures with good mechanical properties [2.34, 2.41, 2.55, 2.56, 2.57]. The deposition condition of LPCVD polysilicon layers at IMT are 600 °C and 200 mTorr. This deposition temperature is close to the transition temperature (580 °C at 200 mTorr [2.55]) from amorphous to polycristalline layers. To control the residual stress, the polysilicon layer is annealed 30 min at 1050 °C under nitrogen atmosphere [2.58, 2.52]. Undoped LPCVD polysilicon layers deposited at the IMT laboratory have a very small tensile residual stress (σ_r) of 1.7 MPa after the annealing step. However the electromechanical structures are working with electric fields, thus it is necessary to reduce their charging time (RC effect) by reducing their impedance. Figure 2.2 shows the influence of the doping on the residual stress for phosphorus doped polysilicon. The stress values have been obtained by measuring the curvature of the silicon wafer on which the layer was deposited. The thickness of the characterized polysilicon layer was 0.75 μm. An optimum has been obtained for n-doped polysilicon layers having a sheet resistance of about 850 Ω per square with a 8MPa tensile residual stress. As a comparison French et al. [2.57] found. 17 MPa compressive stress which is in the same order of magnitude. At smaller sheet resistances, the residual stress becomes compressive resulting in the breakage of the microstructures.

To dope the polysilicon layers the doping atoms are either deposited on top of the LPCVD polysilicon in a doped CVD silicon dioxide layer or directly implanted in the LPCVD polysilicon film. The implantation technique is more accurate and more reproducible than the CVD technique where the influence of the flow rates is very important on the characteristics of the deposited layer. The implantation parameters for the phosphorus impurities to give a sheet resistance of about 850 Ω per square are $1 \cdot 10^{15}$ atoms·cm^{-2} and 80 keV [2.57].

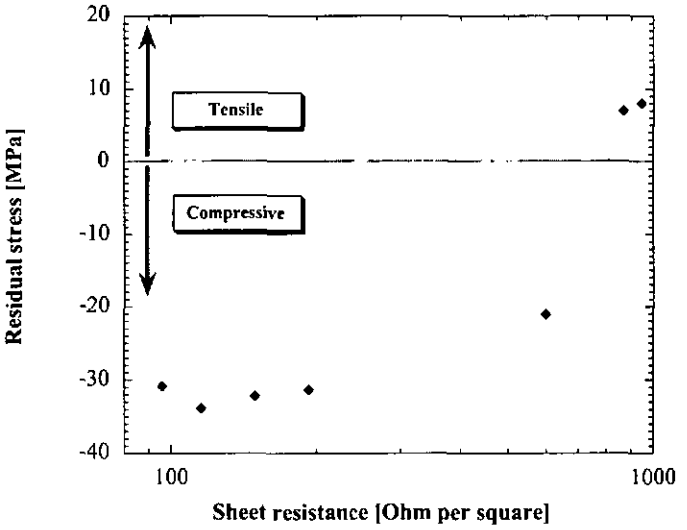

Figure 2.2: Graph of the residual stress [MPa] versus the sheet resistance of the phosphorus doped polysilicon layers after 30 min. annealing at 1050 °C under nitrogen atmosphere. The five left hand side points are obtained with the CVD doping method while the two right hand side points are obtained by implantation of phosphorus impurities. (boron doped polysilicon layers where not developed in our laboratory). The LPCVD polysilicon layer was deposited at 600 °C and 200 mTorr. Tensile residual stress is positive and compressive negative.

2.2.4 Metallization of released structures:

The final steps of the surface micromachining technology are to release the microstructures by removing the sacrificial layer. The etching of the sacrificial layer silicon dioxide is problematic, since the BHF attacks also other materials such as aluminum which is used for metallization. In order to avoid this effect, three different possibilities exist. The first approach consists in protecting the patterned metal by photoresist during the release of the beams [2.52]. However, one more mask is necessary. In addition, the protection by the photoresist is limited in time, thus restricting the width of the mechanical structures. The second possibility is to increase the selectivity of the aluminum etching

compared to the silicon dioxide by adding some chemicals (a polyhidric alcohol like glycerol or potassium dichromate) to the BHF [7:1] solution, but this protection is also limited in time and gives relatively rough aluminum surfaces. Details of this technique are given in [2.53]. The third technique, developed here, starts by the lateral etching of the sacrificial layer (220 minutes in BHF [7:1] for 40 μm wide beams), followed by the deposition of a thick aluminum layer. As shown in Figure 2.3, this aluminum layer must be thick enough to completely cover the mechanical structures (e.g. 1.5 μm). Thus it holds them during the subsequent photoresist spinning for the patterning of the aluminum. With this technique the lateral etching hardly affects the standard IC metallization process and, in addition, the width of the beams is not limited as in the case of the photoresist protection.

After each wet processing steps following the release of the microbeams, a particular attention has to be given to their rinsing and drying to avoid sticking phenomena [2.59]. The method used here consists in the rinsing of the devices in deionized water and in isopropanol alcohol (1 hour). Finally they are dried 15 minutes in an air pulsed oven at 200 °C [2.53].

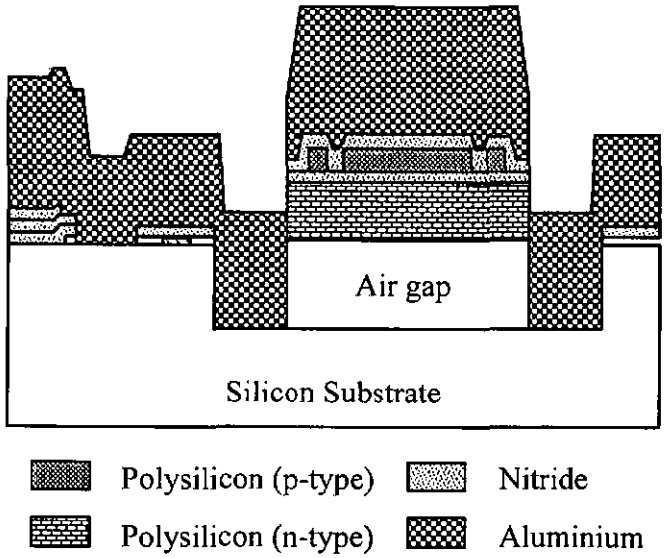

Figure 2.3: Cross section of the structure after the aluminum deposition. Note that the aluminum holds the free standing beam during the spinning process.

2.3 Surface encapsulation of polysilicon microresonators:

2.3.1 Introduction:

In this section a brief description of the surface encapsulation will be given. This surface encapsulation does not provide mechanical protection of the devices. Nevertheless, it protects the resonators from dust particles or other contamination during the packaging. Moreover it allows a vacuum sealing of these devices and thus the increasing of the quality factor of the resonators.

2.3.2 Technology:

Surface encapsulation is possible by extending sacrificial layer technology, described in section 2.2. After the deposition of a second sacrificial layer which covers completely the polysilicon resonator, a polysilicon cap can be deposited. Thin silicon dioxide channels underneath this second polysilicon layer allow the sacrificial silicon dioxide to be etched in hydrofluoric acid and thus release the resonators. The final steps consist in the sealing of the microcavity. This can be performed by a re-oxidation [e.g. 2.6, 2.7] or by a LPCVD silicon nitride deposition [e.g. 2.10, 2.11, 2.12]. A schematic of the process is given in Figure 2.4, while the SEMs pictures of Figure 2.5, Figure 2.6 and Figure 2.7 show examples of encapsulated resonant beams.

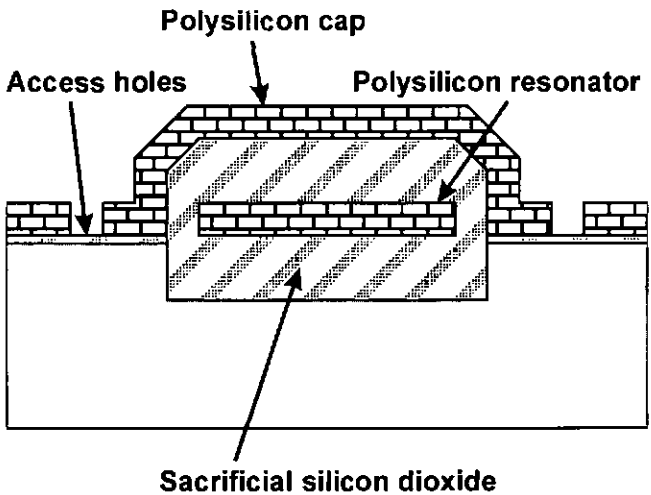

Figure 2.4: Schematic of the surface encapsulation.

Figure 2.5: SEM of a polysilicon beam encapsulated by a second polysilicon cover; the distance between cover, beam and substrate ore 2.2 µm and 1.8 µm respectively.

Figure 2.6: SEM close-up of a polysilicon beam encapsulated by a second polysilicon cover; the distance between cover, beam and substrate are 2.2 µm and 1.8 µm respectively. Note that the beam was not completely released.

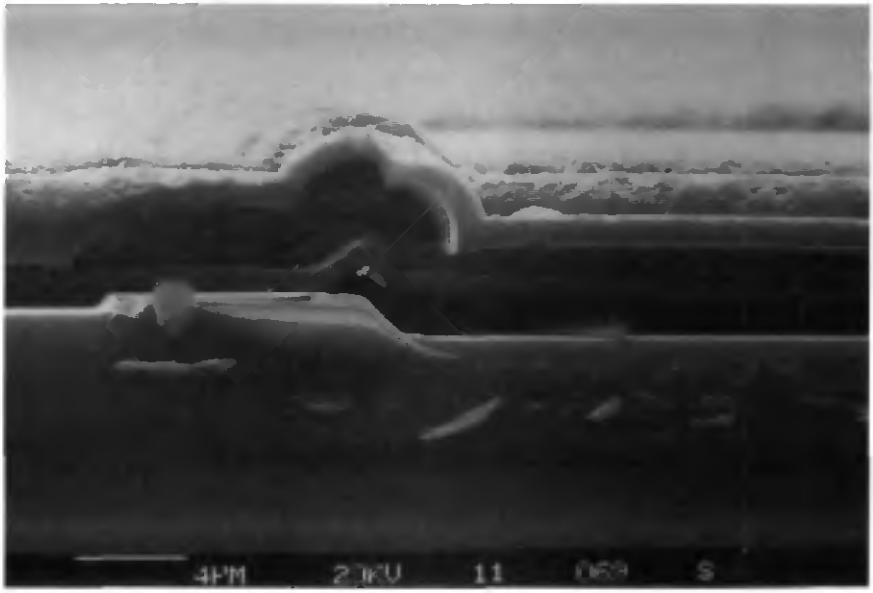

Figure 2.7: SEM showing side view of encapsulated LOCOS polysilicon beam.

This section points out the possibility to build smart electromechanical devices with a high level of integration. Such an integration is possible only if the different technological steps are fully controlled and need relatively long developments.

As can be seen from Figure 2.6 and Figure 2.7 every step on the substrate is faithfully translated on the polysilicon cap. This induces weak points in the covers and could be avoided by using planarized wafers. The use of an improved LOCOS technology as described in [2.46, 2.47] could also solve this problem.

The surface encapsulation has been also demonstrated for electrostatic devices where counter electrodes are used to sense or to actuate the device [2. 60]. Moreover such an encapsulation is very interesting because it allows the change of capacitance induced by vertical movements of the beam to be differentially measured.

2.4 Fabrication of glass micromachined capillary tubes [2.31, 2.32]:

2.4.1 Introduction:

In this section a new method for the micromachining of glass is presented. It is illustrated for the fabrication of borosilicate glass capillary tubes. As the interest of miniaturized Total chemical Analysis Systems (μ-TAS) is increasing, the need of fluidic paths is growing and thus the study of microchannels, microtubes and microcolumns is an important topic of the microfluidic area. μ-TAS have been developed to fulfill the following requirements: reduction of sample size, response time and reagent consumption [2.61]. On one hand, microtubes are necessary for the interconnection of the different modules (pumps, valves, flow sensors, chemical detectors...) of such complex systems [2.62, 2.63]. On the other hand, the fabrication of well defined capillary tubes is required for chemical analysis [2.64]. Different types of capillary tubes have been reported, which are realized in silicon [2.64] or quartz substrates [2.65, 2.66]. The capillary tubes, presented here, are fabricated by structuring and bonding three borosilicate glass wafers (7740 Corning Pyrex®). This material is usually employed for the encapsulation of silicon micromechanical systems because it allows anodic bonding to silicon [2.67]. The glass is also an interesting material for capillary tubes because it is transparent, hydrophilic and impermeable to oxygen. Some new photostructurable glass materials are emerging which are easy to define but have thermal expansion coefficients which are not compatible with the anodic bonding to silicon [2.21, 2.22, 2.23, 2.24, 2.25, 2.26, 2.27, 2.28, 2.29, 2.30, 2.68].

Here the fabrication and microscopic characterization of microchannels with lateral inlets and outlets will be presented. LPCVD polysilicon mask has been used to protect the glass surface during the etching in 50 % hydrofluoric acid (50 % HF), allowing well defined size and shape of the capillary tubes [2.69]. This mask allows also deeper etching than conventional chromium-gold mask [2.70, 2.71]. Several capillary tubes with widths from 340 to 940 μm have been realized as well as different section shapes, which can be circular, elliptic or quasi-rectangular. The main fabrication steps and SEM characterizations are reported. This technology can also be used for the packaging of silicon devices which need to be encapsulated in a controlled atmosphere or in vacuum.

2.4.2 Technology:

The capillary tubes are realized by the assembly of three structured glass wafers (500 µm thick). Figure 2.8 shows an exploded cross-section of the capillary tubes, where the middle glass wafer is patterned on both sides while the two others are only structured on one side. The micromachining of the different glass wafers has been performed in 50% HF at ambient temperature with an LPCVD polysilicon mask (5000 Å thick). As the glass wafers are held vertically in the furnace, a LPCVD polysilicon layer is deposited on both sides. A standard photolithography followed by a RIE (reactive ion etching) plasma etching allows to define the LPCVD polysilicon mask.

The fabrication of the capillary tubes consists in two different levels: first the structuring and second the assembly of the glass wafers. The glass micromachining begins with the fabrication of the access holes (2nd & 3rd glass

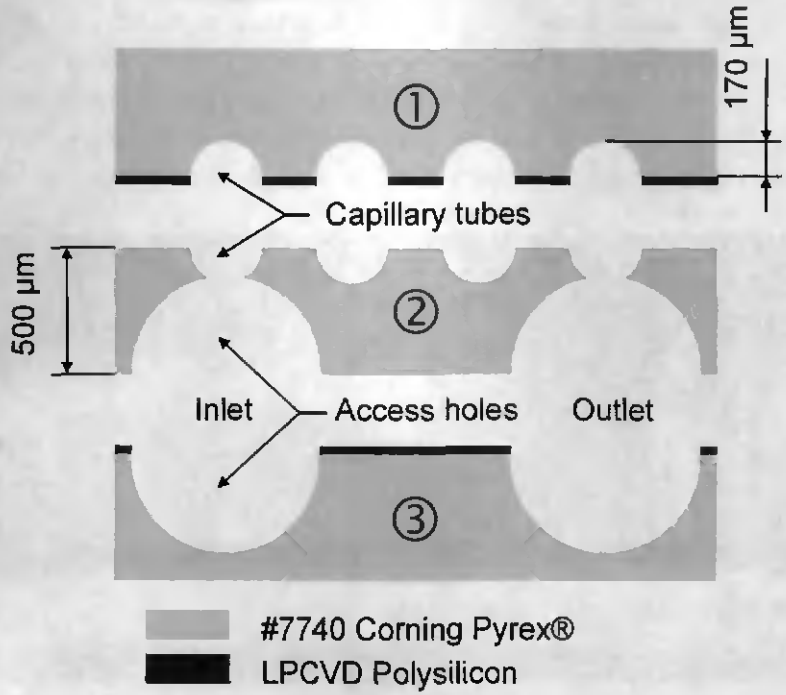

Figure 2.8: Exploded cross-section of the capillary tubes with inlet and outlet access holes just before bonding.

wafers). A partial etching is performed in 50% HF to obtain 350 µm deep grooves. Then the process continues with the definition of the capillary tubes (1^{st} & 2^{nd} glass wafers). The final size of the access holes (420 µm) is obtained while 170 µm deep capillary tubes are etched in the glass wafers.

The capillary tubes are obtained by the assembly of the three different structured wafers, which are joined together by anodic bonding technology at about 450 °C and 700 V. The adhesion of the two pyrex glasses is ensured by the remaining LPCVD polysilicon layer on one wafer side. The capillary tubes are assembled by fixing of the first and second glass wafers, then the lateral access holes are formed by the bonding of the third glass wafer to this glass sandwich. The unused polysilicon layers have been removed by RIE plasma etching before the bonding steps.

With the same technology, several capillary tubes have been realized by changing their length and their width. Figure 2.9 illustrates four widths of capillary tube cross-section. The widths are, from left to right, 340 µm, 440µm, 540 µm and 940 µm while the length is always 10 mm. These circular (Figure 2.10), elliptic and quasi rectangular shapes have been obtained with the same etching depth (170 µm) by changing the width of the mask. Several lengths of capillary tube have been also fabricated : 2 mm, 4 mm, 6 mm, 8 mm and 10 mm while the width is always 440 µm.

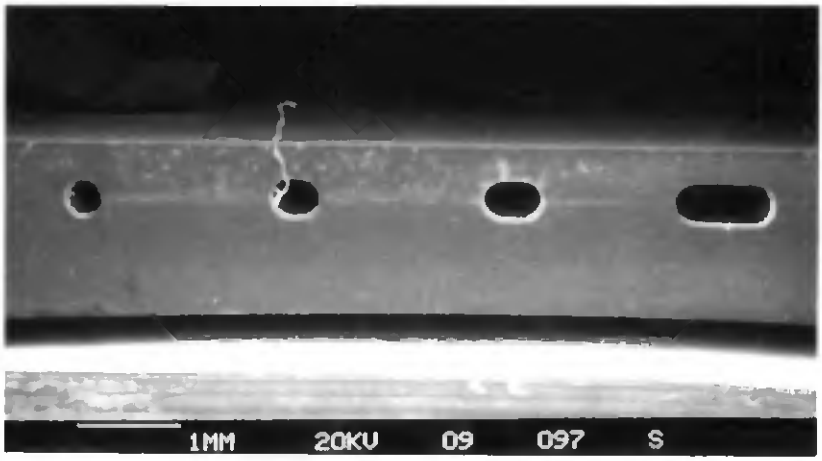

Figure 2.9: SEM of the cross-section of four capillary tubes. The widths are, from left to right: 340 µm, 440 µm, 540 µm and 940 µm.

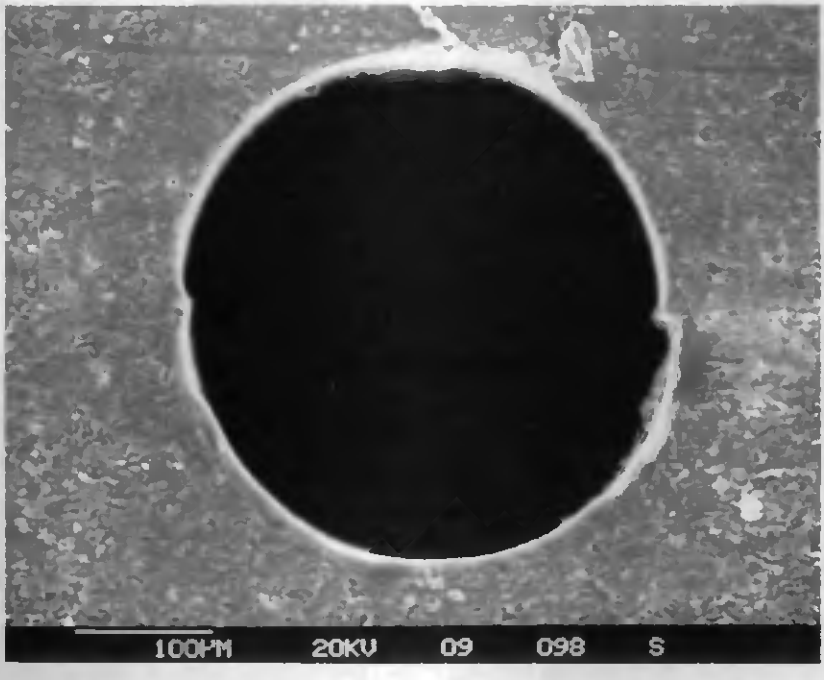

Figure 2.10: SEM of the cross-section of a circular capillary tube with 340 µm diameter.

Microcolumns have also been designed to study the shape of the corner with isotropic etching of glass by 50% HF (Figure 2.11). Corner shapes without any corner compensation have been fabricated with a roughness of the inner wall surface of less than 0.1 µm (Figure 2.12). This micro-column realization has demonstrated the possibility to built compact serpentine tubes with well defined corners.

All these fluidic paths have been connected by means of lateral holes (Figure 2.11 & Figure 2.13). This kind of access allows easier connection between several modules stacked together without any intermediate module. Moreover the fabrication of the inlet and outlet paths has been integrated with the technology used for the capillary tubes. Circular access tubes with 840 µm diameter have been realized, which can receive 800 µm diameter needles. For these deep glass etchings in 50% HF, an etch rate of about 6 µm/min has been obtained. By using thinner glass wafers, it is also possible to realize smaller capillary tubes with similar access holes.

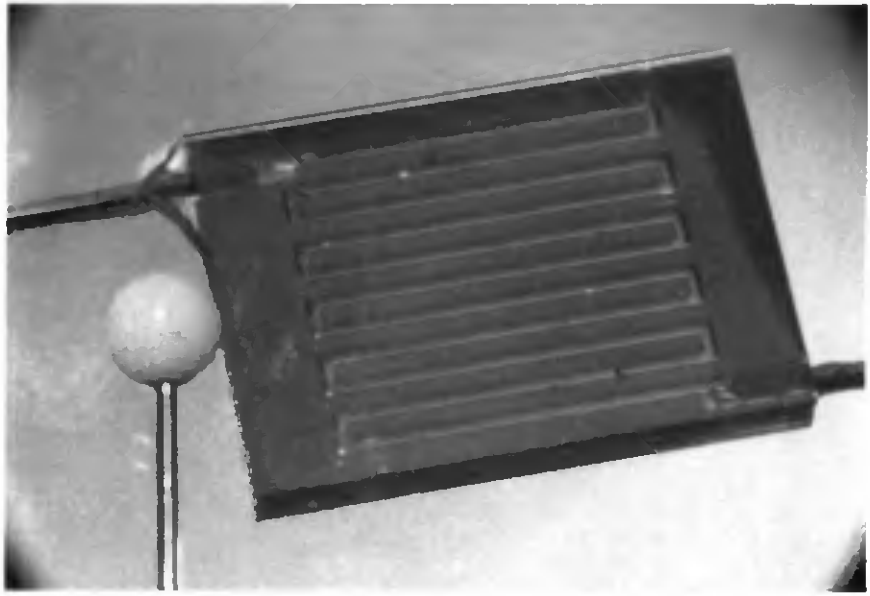

Figure 2.11: Micrograph of a microcolumn. The capillary tube is 118 mm long, with a circular cross-section (diameter: 340 μm).

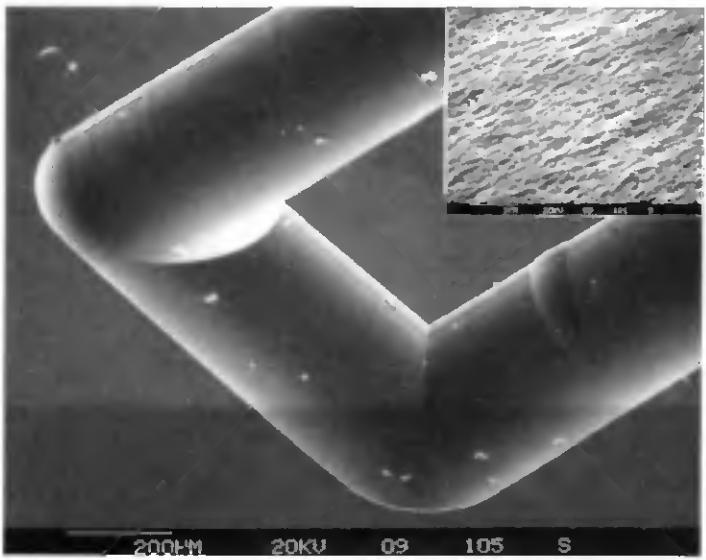

Figure 2.12: SEM of a half microcolumn corner before anodic bonding of the other part and detail of the inner wall surface roughness.

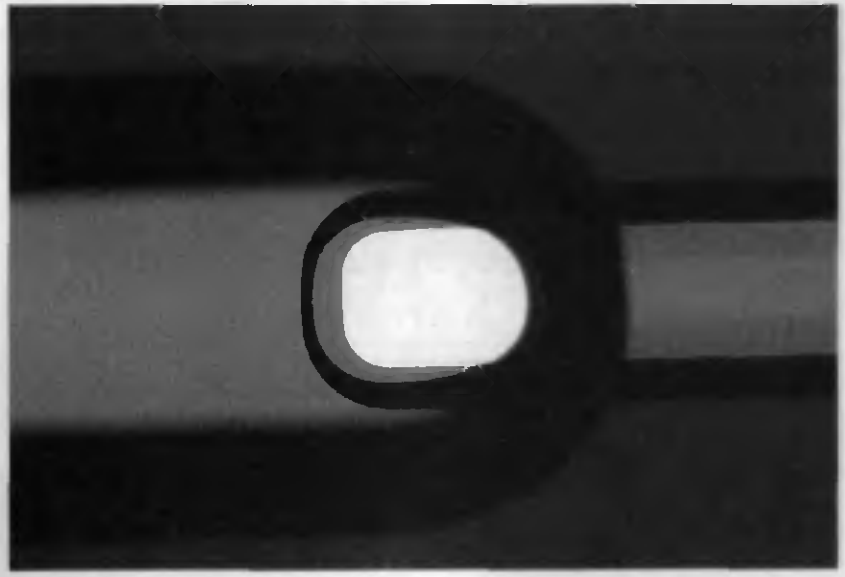

Figure 2.13: Top view of an interconnection between capillary tubes (right) and lateral inlet ar outlet (left). The wider tube (left) will receive a 800 μm diameter needle.

2.5 Packaging of a silicon resonant gyroscope [2.33]:

The technology of glass etching, presented in section 2.4, has been applied for the packaging of a silicon resonant gyroscope. This kind of device needs an over range protection of the same type used for accelerometers [2.70]. Thus it has been decided to bond three wafers together by realizing a glass-silicon-glass sandwich, where the mechanical structure is patterned in the silicon wafer. As described in Figure 2.14 the top glass wafer has been etched to provide this over range protection (20 μm). This technique allows also the device to be encapsulated in a controlled atmosphere. Thanks to this technique it has been possible to perform a wafer scale encapsulation and thus to be able to dice the wafers with a standard IC saw. This kind of encapsulation is also very interesting from an economic point of view, because the devices are protected before the final steps concerning their packaging (dicing, wire bonding, mounting on the IC sockets). Thus it has been possible to increase the yield of working devices from 10% to 80%. An example of such a packaged angular rate sensor is given in Figure 2.15.

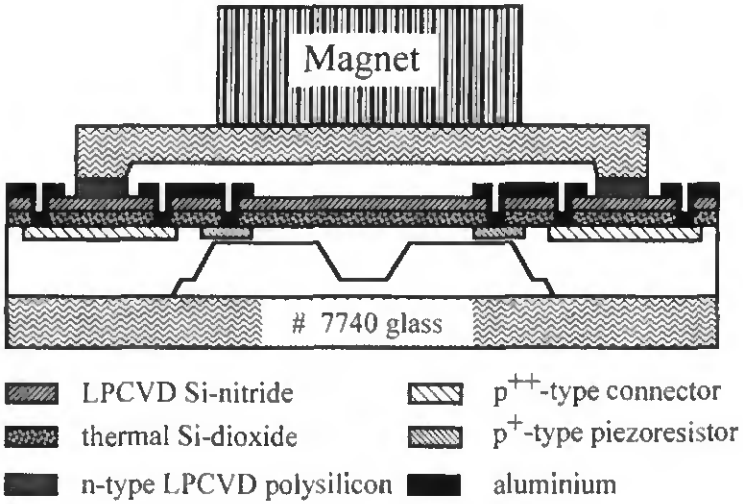

Figure 2.14: Schematic of the packaging of the silicon gyroscope. A magnet is glued on top of the device to provide an electromagnetic excitation.

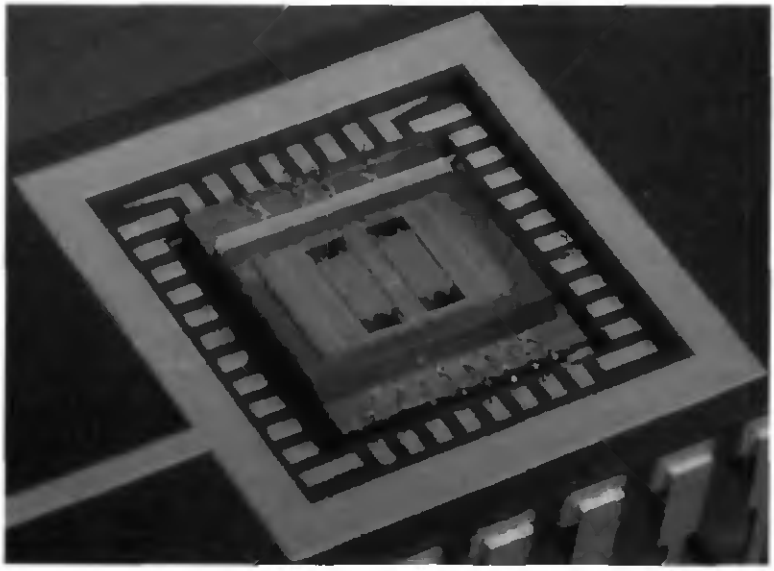

Figure 2.15: Micrograph of a silicon micromachined gyroscope with the glass encapsulation.

2.6 Conclusions:

In this chapter, different aspects of the encapsulation of mechanical devices have been presented as well as some technological aspects. A description of the surface micromachining technology was given as well as the polysilicon doping and the metallization of released structures.

The surface encapsulation of resonant beams has been briefly described as well as the realization of well defined capillary tubes with lateral inlets and outlets. Their realization has shown the possibility to etch 400 µm deep holes in Pyrex® glass by using polysilicon as the masking material. This glass etching technique has been applied to the encapsulation of a silicon gyroscope. Thanks to this work it has been possible to demonstrate its use for the encapsulation of micromechanical systems.

In Chapter 3, electrostatic polysilicon microrelays will be presented. These devices need to be operated in a nitrogen atmosphere. The encapsulation technique presented here could be used for this purpose.

2.7 References:

[2.1] S. D. Senturia and R. L. Smith, "Microsensor Packaging and System partitioning", Sensors & Actuators, 15 (1988), pp. 221-234.

[2.2] Digest of Technical Papers of the International Conferences on Solide-State Sensors and Actuators, Transducers, 1987-1995.

[2.3] Proceedings of the IEEE Workshops on Micro Electro Mechanical Systems, MEMS, 1989-1997.

[2.4] C. Linder, L. Paratte, M.-A. Grétillat, V. P. Jaecklin and N. F. de Rooij, "Surface micromachining", Journal of Micromechanics and Microengineering, Vol. 2 (1992), pp. 122-132.

[2.5] H. Guckel and D. W. Burns, "Planar Processed Sealed Cavities For Pressure Transducer Arrays", Technical Digest of IEDM, 1984, pp. 223-225.

[2.6] H. Guckel, J. J. Sniegowski and T. R. Christenson, "Construction and Performance Characteristics of Polysilicon Resonating Beam Force Transducers", Proceedings of the 3rd Toyota Conference, Nissin, Aishi, Japan, October 1989, pp. 23.1-23.10.

[2.7] H. Guckel, J. J. Sniegowski and T. R. Christenson, "Construction and Performance Characteristics of Polysilicon Resonating Beam Force Transducers", Integrated Micro-Motion Systems- Micromachining, Control and Applications, F. Harashima (Editor), 1990, pp. 393-404.

[2.8] H. Guckel, J. J. Sniegowski, T. R. Christenson and F. Raissi, "The Application of Fine-grained, Tensile Polysilicon to Mechanically Resonant Transducers", Sensors & Actuators, A21-A23 (1990), pp. 346-351.

[2.9] J. J. Sniegowski, H. Guckel and T. R. Christenson, "Performance characteristics of second generation polysilicon resonating beam force transducers", Technical Digest of IEEE Solid-State Sensor and Actuator Workshop, Hilton Head Island, SC, June 1990, pp. 9-12.

[2.10] H. A. C. Tilmans, R. Legtenberg, H. Schurer, D. J. Ijntema, M. Elwenspoek and J. H. J. Fluitman, "(Electro-)Mechanical Characteristics of Electrostatically Driven Vacuum Encapsulated Polysilicon Resonators", IEEE Transactions on Ultrasonics Ferroelectrics and Frequency Control, Vol. 41-1 (1994), pp. 4-6.

[2.11] R. Legtenberg and H. A. C. Tilmans, "Electrostatically driven vacuum-encapsulated polysilicon resonators .1. Design and fabrication", Sensors & Actuators, A45 (1994), pp. 57-66.

[2.12] H. A. C. Tilmans and R. Legtenberg, "Electrostatically driven vacuum-encapsulated polysilicon resonators .2. Theory and performance", Sensors & Actuators, A45 (1994), pp. 67-84.

[2.13] D. W. Burns, J. D. Zook, R. D. Horning, W. R. Herb and H. Guckel, "A Digital Pressure Sensor Based on Resonant Microbeams", Technical Digest of IEEE Solid-State Sensor and Actuator Workshop, Hilton Head Island, SC, June 1994, pp. 221-224.

[2.14] C. Liu and Y. C. Tai, "Studies on the Sealing of Surface Micromachined Cavities Using Chemical Vapour Deposition Materials", Technical Digest of IEEE Solid-State Sensor and Actuator Workshop, Hilton Head Island, SC, June 1994, pp. 103-106.

[2.15] D. W. Burns, J. D. Zook, R. D. Horning, W. R. Herb and H. Guckel, "Sealed-cavity resonant microbeam pressure sensor", Sensors & Actuators, A 48 (1995), pp. 179-186.

[2.16] C. Q. Gui, R. Legtenberg, M. Elwenspoek and J. H. Fluitman, "Q-factor dependence of one-port encapsulated polysilicon resonator on reactive sealing pressure", Journal of Micromechanics and Microengineering, 5 (1995), pp. 183-185.

[2.17] K. Ikeda, H. Kuwayama, T. Kobayashi, T. Watanabe, T. Nishikawa, T. Yoshida, and K. Harada, "Silicon Pressure Sensor Integrates Resonant Strain Gauge on Diaphragm", Sensors & Actuators, A21-A23 (1990), pp. 146-150.

[2.18] K. Ikeda, H. Kuwayama, T. Kobayashi, T. Watanabe, T. Nishikawa, T. Yoshida, and K. Harada, "Three-dimensional Micromachining of Silicon Pressure Sensor Integrating Resonant Strain Gauge on Diaphragm", Sensors & Actuators, A21-A23 (1990), pp. 1007-1010.

[2.19] C. H. Mastrangelo, J. H.-J. Yeh and R. S. Muller, "Electrical and Optical Characteristics of Vacuum-Sealed Polysilicon Microlamps", IEEE Transactions on Electron Devices, Vol. 39-6 (1992), pp. 1363-1375.

[2.20] Q. Mei, T. Tamagawa, C. Ye, Y. Lin, S. Zurn and D. L. Polla, "Planar-Processed Tungsten and Polysilicon Vacuum Microelectronic Devices with Integral Cavity Sealing", Journal of Vacuum Science & Technology B, 11-2 (1993), pp. 493-496.

[2.21] K. Dyrbye, T. Romedahl Brown and G. F. Eriksen, "Packaging of Physical Sensors for Aggressive Media Applications", Technical Digest of The 6th Workshop on Micromachining, Micromechanics and Microsystems, MME '95, Copenhagen, Denmark, September 1995, pp. 315-323.

[2.22] W. H. Ko, J. T. Sumitomo and G. J. Yeh, "Bonding Techniques for Microsensors", Micromachining and Micropackaging of Transducer's, Elsevier Science Publishers, Amsterdam, The Netherlands, 1985, pp. 41-61.

[2.23] M. Harz, "Anodic Bonding for the Third Dimension", Journal of Micromechanics and Microengineering, 2 (1992), pp. 161-163.

[2.24] M. Nese and A. Hanneborg, "Anodic Bonding of Silicon to Silicon Wafers Coated with Aluminum, Silicon Oxide, Polysilicon or Silicon Nitride", Sensors & Actuators, A37-38 (1993), pp. 61-67.

[2.25] C. Cabuz, S. Shoji, K. Fukatsu, E. Cabuz, K. Minami and M. Esashi, "Fabrication and Packaging of a Resonant Infrared Sensor Integrated in Silicon", Sensors & Actuators, A43 (1994), pp. 92-99.

[2.26] S. Schoji and M. Esashi, "Bonding and Assembling Methods for Realising a μTAS", Proceedings of Miniaturized Total Analysis Systems, μ-TAS94, Twente, The Netherlands, November 1994, pp. 165-179.

[2.27] T. Rogers and J. Kowal, "Selection of Glass, Anodic Bonding Conditions and Material Compatibility for Silicon-Glass Capacitive Sensors", Sensors & Actuators, A46-47 (1995), pp. 113-120.

[2.28] K. Hilgendorf, P. Krause and E. Obermeier, "Reduction of the Influence of the Anodic Bonding Process on the Behavior of Pressure Sensors by Using New Glass Substrates", Proceedings of the 5th International Conference on Micro Electro, Opto, Mechanic Systems and Components, Micro System Technologies 96, Potsdam, Germany, September 1996, pp. 331-336.

[2.29] H. Henmi, S. Shoji, Y. Shoji, K. Yoshimi and M. Esashi, "Vacuum Packaging for Microsensors by Glass-Silicon Anodic Bonding", Digest of Technical Papers of the 7th International Conference on Solide-State Sensors and Actuators, Transducers '93, Yokohama, Japan, June 1993, pp. 243-248.

[2.30] H. Henmi, S. Shoji, Y. Shoji, K. Yoshimi and M. Esashi, "Vacuum Packaging for Microsensors by Glass-Silicon Anodic Bonding", Sensors & Actuators, A43 (1994), pp. 243-248.

[2.31] M.-A Grétillat, F. Paoletti, P. Thiébaud, S. Roth, M. Koudelka-Hep and N.F. de Rooij, "A New Fabricaiton Method of Borosilicate Glass Capillary Tubes with Lateral Inlets and Outlets", Proceedings of the 10th European Conference on Solide-State Transducers, Eurosensor X, Leuven, Belgium, September 1996, pp. 259-262.

[2.32] M.-A Grétillat, F. Paoletti, P. Thiébaud, S. Roth, M. Koudelka-Hep and N.F. de Rooij, "A New Fabricaiton Method of Borosilicate Glass Capillary Tubes with Lateral Inlets and Outlets", Proceedings of Miniaturized Total Analysis Systems, μ-TAS96, Analytical Methods & Instrumentation, Basel, Switzerland, November 1996, p. 214.

[2.33] F. Paoletti, M.-A. Grétillat and N. F de Rooij, "A silicon micromachined vibrating gyroscope with piezoresistive detection and electromagnetic excitation", Proceedings of the 9th IEEE Workshop on Micro Electro Mechanical Systems, MEMS '96, San Diego, CA, February 1996, pp. 162-167.

[2.34] R.T. Howe and R.S. Muller, "Polycristalline and Amorphous Silicon Micromechanical Beams: Annealing and Mechanical Properties", Sensors & Actuators, 4 (1983), pp. 447-454.

[2.35] Y. C. Tai, R. S. Muller and R. T. Howe, "Polysilicon-Bridges for Anemometer Applications", Digest of Technical Papers of the 3rd International Conference on Solide-State Sensors and Actuators, Transducers '85, Philadelphia, PA, June 1985, pp. 354-357.

[2.36] H. Guckel and D. W. Burns, "Fabrication Techniques For Integrated Sensor Microstructures", Technical Digest of IEDM, 1986, pp. 176-179.

[2.37] M. A. Schmidt and R. H. Howe, "Resonant Structures for Integrated Sensors", Technical Digest of IEEE Solid-State Sensor and Actuator Workshop, Hilton Head Island, SC, June 1986.

[2.38] H. Guckel, D. W. Burns, C. R. Rutigliano, D. K. Showers and J.Uglow, "Fine Grained Polysilicon and Its Application to Planar Pressure Transducers", Digest of Technical Papers of the 4th International Conference on Solide-State Sensors and Actuators, Transducers '87, Tokyo, Japan, June 1987, pp. 277-282.

[2.39] Y. C. Tai and R. S. Muller, "Lightly Doped Polysilicon Bridge as an Anemometer", Digest of Technical Papers of the 4th International Conference on Solide-State Sensors and Actuators, Transducers '87, Tokyo, Japan, June 1987, pp. 360-363.

[2.40] P. J. French and A. G. R. Evans, "Polysilicon Strain Sensors Using Shear Piezoresistance", Sensors & Actuators, 15 (1988), pp. 257-272.

[2.41] Y. C. Tai and R. S. Muller, "Fracture Strain of LPCVD Polysilicon", Technical Digest of IEEE Solid-State Sensor and Actuator Workshop, Hilton Head Island, SC, June 1988, pp. 88-91.

[2.42] H. Guckel, J. J. Sniegowski, T. R. Christenson, S. Mohney and T. F. Kelly, "Fabrication of Micromechanical Devices from Polysilicon Films with Smooth Surfaces", Sensors & Actuators, 20 (1989), pp. 117-122.

[2.43] M. M. Farooqui and A. G. R. Evans, "Polysilicon microstructures", Proceedings of the 4th IEEE Workshop on Micro Electro Mechanical Systems, MEMS '91, Nara, Japan, January 1991, pp. 187-191.

[2.44] C. Linder, M.-A. Grétillat and N.F. de Rooij, "Realization of different polysilicon resonators with integrated excitation and detection elements", Microelectronic Engineering, 15 (1991), pp. 411-414.

[2.45] A. Kovacs and A. Stoffel, "Process Optimization of Free-Standing Polysilicon Microstructures", Technical Digest of The 3rd Workshop on Micromachining, Micromechanics and Microsystems, MME '92, Leuven, Belgium, June 1992, pp. 114-117.

[2.46] M.-A. Grétillat, C. Linder and N.F. de Rooij, "Multilayer Polysilicon Resonators Including Shielding for Excitation and Detection", Digest of Technical Papers of the 7th International Conference on Solide-State Sensors and Actuators, Transducers '93, Yokohama, Japan, June 1993, pp. 292-295.

[2.47] M.-A. Grétillat, C. Linder and N.F. de Rooij, "Integrated Shielding Lines on Multilayer Polysilicon Resonators", Sensors & Actuators, A43 (1994), pp. 351-356.

[2.48] D. J. Monk, D. S. Soane and R. T. Howe, "Hydrofluoric Acid Etching of Silicon Dioxide Sacrificial Layers .1. Experimental Observations", Journal of the Electrochemical Society, Vol. 141-1 (1994), pp. 264-269.

[2.49] F. Goodenough, "Airbag Boom When IC Accelerometer sees 50 g", Electronic Design, August 8 (1991).

[2.50] T. A. Core, W. K. Tsang and S. J. Sherman, "Fabrication Technology for an Integrated Surface-Micromachined Sensor", Solid State Technology, 36: 10 (1993), pp. 39-47.

[2.51] W. Kuehnel and S. Sherman, "A Surface Micromachined Silicon Accelerometer with On-Chip Detection Circuitry", Sensors & Actuators, A45 (1994), pp. 7-16.

[2.52] C. Linder, "Electromechanical Polysilicon Structures and Micromachining Processes for Sensor and Actuator Applications", Ph.D. Thesis, Institute of Microtechnology, University of Neuchâtel, Switzerland, 1993.

[2.53] V. P. Jaecklin, "Surface Micromachined Electrostatic Actuators", Ph.D. Thesis, Institute of Microtechnology, University of Neuchâtel, Switzerland, 1994.

[2.54] L. S. Tavrow, S. F. Bart, J. H. Lang and M. F. Schlecht, "A LOCOS Process for an Electrostatic Microfabricated Motor", Sensors & Actuators, A21-A23 (1990), pp. 893-898.

[2.55] T. J. Kamins, "Design Properties of Polycrystalline Silicon", Sensors & Actuators, A21-23 (1990), pp. 817-824.

[2.56] A. Benitez, J. Bausells, E. Cabruja, J. Esteve and J. Samitier, "Stress in Low Pressure Chemical Vapour Deposition Polycrystalline Silicon Thin Films Deposited Below 0.1 Torr", Sensors & Actuators, A37-38 (1993), pp. 723-726.

[2.57] P. J. French, B. P. van Drieënhuizen, D. Poenar, J. F. L. Goosen, R. Mallée, P. M. Sarro and R. F. Wolffenbuttel, "The Development of a Low-Stress Polysilicon Process Compatible with Standard Device Processing", Journal of Microelectromechanical Systems, Vol. 5-3 (1996), pp. 187-196.

[2.58] H. Guckel, D. W. Burns, H. A. C. Tilmans, D. W. de Roo and C. R. Rutigliano, "Mechanical Properties of Fine Grained Polysilicon The Repeatability Issue", Technical Digest of IEEE Solid-State Sensor and Actuator Workshop, Hilton Head Island, SC, June 1988, pp. 96-99.

[2.59] R. Legtenberg, H. A. C. Tilmans, J. Elders and M. Elwenspoek, "Stiction of Surface Micromachined Structures after Rinsing and Drying: Model and Investigation of Adhesion Mechanisms", Sensors & Actuators, A43 (1994), pp. 230-238.

[2.60] H.A.C. Tilmans, "Micro-Mechanical Sensors using Encapsulated Built-in Resonant Strain Gauges", Ph.D. Thesis, University of Twente, The Netherlands, 1993.

[2.61] A. Manz, N. Graber and H. M. Widmer, "Miniaturized total chemical analysis systems: a novel concept for chemical sensing", Sensors & Actuators, B1 (1990), pp. 244-248.

[2.62] P. Gravesen, J. Branebjerg and O. S. Jensen, "Microfluidics - A Review", Technical Digest of The 4th Workshop on Micromachining, Micromechanics and Microsystems, MME '93, Neuchâtel, Switzerland, September 1993, pp. 143-164.

[2.63] B. H. van der Schoot, E. M. J. Verpoorte, S. Jeanneret, A. Manz and N. F. de Rooij, ", "Microsystems for analysis in flowing solutions", Proceedings of Miniaturized Total Analysis Systems, μ-TAS94, Twente, The Netherlands, November 1994, pp. 181-190.

[2.64] D. J. Strike, P. Thiébaud, A. C. van der Sluis, M. Koudelka-Hep and N. F. de Rooij, "Glucose measurement using a micromachined open tubular heterogeneous enzyme reactor (MOTHER)", Microsystem Technologies, Vol.1 N°1 (1994), pp. 48-50.

[2.65] D. Sobek, S. D. Senturia and M. L. Gray, "Microfabricated fused silica flow chambers for flow cytometry", Technical Digest of IEEE Solid-State Sensor and Actuator Workshop, Hilton Head Island, SC, June 1994, pp. 260-263.

[2.66] W. Kaplan, H. Elderstig and C. Vieider, "A novel fabrication method of capillary tubes on quartz for chemical analysis applications", Proceedings of the 7th IEEE Workshop on Micro Electro Mechanical Systems, MEMS '94, Oiso, Japan, January 1994, pp. 63-68.

[2.67] Data sheet: Corning 7740 borosilicate Pyrex®, Corning Keramik GMBH & CO., Abraham-Lincoln Strasse 30, D-65189 Wiesbaden, Germany.

[2.68] D. Hülsenberg, A. Harnisch, H.-J. Horst, K. Schmidt and B. Straube, "New Glasses for Microsystem Technologies", Proceedings of the 4th International Conference on Micro Electro, Opto, Mechanic Systems and Components, Micro System Technologies 94, Berlin, Germany, October 1994, pp. 259-268.

[2.69] H. R. C. Strato, "Glass Technology", Master Thesis, Department of Electrical Engineering, TU Delft, the Netherlands, A94-09, August 1994.

[2.70] T. Tschan, "Simulation, design and characterization of a piezoresistive accelerometer fabricated by a bipolar-compatible industrial process", Ph.D. Thesis, Institute of Microtechnology, University of Neuchâtel, Switzerland, 1992.

[2.71] T. Diepold and E. Obermeier, "Smoothing of ultrasonically drilled holes in borosilicate glass by wet chemical etching", Technical Digest of The 6th Workshop on Micromachining, Micromechanics and Microsystems, MME '95, Copenhagen, Denmark, September 1995, pp. 35-38.

3. Polysilicon microrelays

3.1 Introduction:

Micromechanical relays are promising components for electronics as well as for microelectromechanical systems (MEMS), which require the ability to control and select a transmission path for an electrical signal. They have the same advantages as conventional mechanical relays over transistor-based switches, in that they exhibit a high off-state to on-state impedance ratio and have four-terminals with fully isolated input/output lines [3.1]. Thus it is an interesting component for signal switching applications [3.2]. The mechanical relays exhibit some advantages but the transistor based devices will remain better in term of lifetime and reliability, thus the choice of a mechanical or a transistor based relay will depend on the required application.

Different types of micromachined relays have been presented which use either electrostatic [3.1, 3.3, 3.4, 3.5, 3.6, 3.7, 3.8, 3.9, 3.10, 3.11, 3.12], electromagnetic [3.13, 3.14, 3.15, 3.16, 3.17] or thermal [3.18, 3.19, 3.20] actuation. The switching principle based on the deflection of a movable structure has also been used for transducer applications for example in pressure and acceleration switches [3.21, 3.22, 3.23, 3.24].

Just as with transistor based switches, it is possible to integrate arrays of micromechanical relays. These matrix of relays allow multiple switching which is very interesting for telecommunication applications [3.25].

This chapter describes the operation principle, the fabrication and the characterization of an IC compatible electrostatically driven microrelay, consisting of a polysilicon/silicon nitride/polysilicon beam fabricated with surface micromachining technology. It has become possible to build these polysilicon microrelays due to the progress made in the surface micromachining of multilayer structures [3.26, 3.27, 3.28, 3.29, 3.30, 3.31, 3.32].

3.2 Operation principle:

As indicated in the cross section (Figure 3.1), the electromechanical part of the microrelay consists of a polysilicon/silicon nitride/polysilicon microbridge. The different active polysilicon parts of the beam are insulated by a nitride layer [3.32]. On the right side of Figure 3.1, the actuation of the relay is performed by the electrostatic force between the upper thick polysilicon and the phosphorus doped n-type region in the substrate [3.33]. On the left side, the working circuit (contact) is formed by the lower polysilicon of the beam and a polysilicon lane on the substrate which goes underneath the micro-bridge.

When the switching voltage is applied to the actuation port, the beam is deflected downwards by the electrostatic force until it touches the substrate. The two polysilicon electrodes of the working circuit are electrically contacted: the relay is on. When the driving voltage is removed, the restoring spring force returns the beam to its free-standing position: the relay is off.

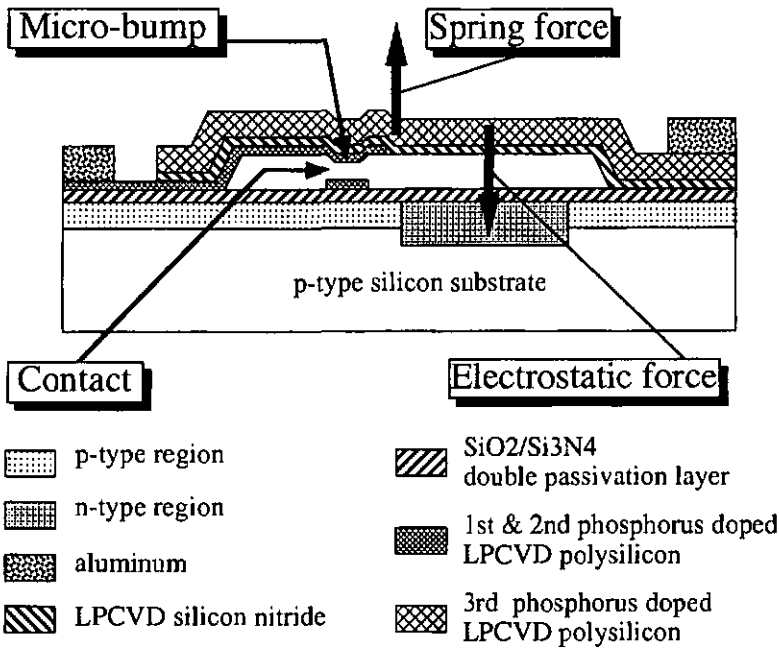

Figure 3.1: Cross section of the polysilicon microrelay with on the left side the working circuit (contact) and on the right side the actuation port.

3.3 Fabrication:

The polysilicon microrelays have been fabricated with an IC compatible surface micromachining process. The main processing steps explained in the following section are summarized in Figure 3.2. As the microrelays fabrication begins with the patterning of the actuation electrodes in the substrate, it has been necessary to define alignment marks with a first photoresist mask and the reactive ion etching of the silicon (4000Å). These small features are clearly visible with the mask-aligner even after several depositions.

The doping of the driving electrode has been performed by the diffusion of the impurities contained in a doped CVD silicon dioxide. First the deposition and the patterning of a boron doped silicon dioxide layer (doping of a channel stop region) is performed, and followed by the deposition of a phosphorus doped layer on the apertures defined in the latter to dope the driving electrodes. Each doped layer is about 1000Å thick and is covered by a 3000Å thick undoped layer to protect the furnace from back diffusion. Then an oxidation-diffusion step is performed at 1100 °C and the doping oxides are removed. This process has been developed for the realization of ion sensitive field effect transistors ISFETs at the IMT [34].

A silicon dioxide and a LPCVD silicon nitride are deposited to ensure the electrical passivation. These layers are open to contact the substrate and the diffusion driving electrodes.

The first polysilicon layer is deposited, doped, annealed and patterned, to obtain the first electrode of the working circuit. At this point of the process the drain and the source as well as the polysilicon gate electrode of the metal-oxide-semiconductor field effect transistors (MOSFET) which has been fabricated to show the IC compatibility of the process are formed. By opening windows in the silicon nitride, the underlying thermal oxide is used as gate insulator for the MOSFETs (Figure 3.3). The first polysilicon of the working circuit of the relay serves as gate electrode. As indicated in the cross section of the MOSFETs (Figure 3.3), the first polysilicon is also employed as interconnection layer for source and drain.

The subsequent processing steps concern the deposition and the patterning of the sacrificial layer which is 1.5 μm thick. A particular attention has been given to the patterning of the contact. Thus partial holes have been etched in the

- Substrate diffusions, silicon dioxide, 1st LPCVD silicon nitride and 1st LPCVD polysilicon

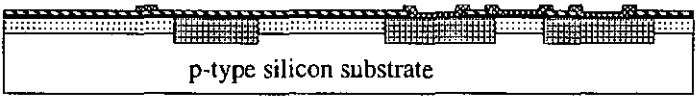

- Sacrificial silicon dioxide and 2nd LPCVD polysilicon

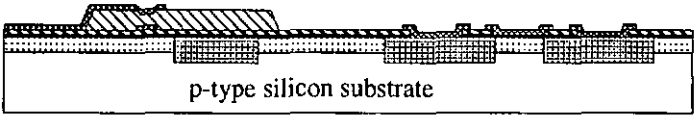

- 2nd LPCVD silicon nitride and 3rd LPCVD polysilicon

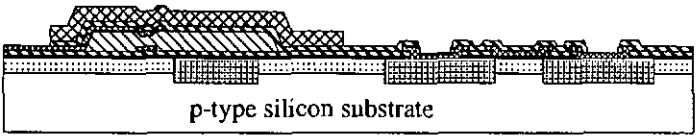

- Sacrificial layer etching / release of the microrelays

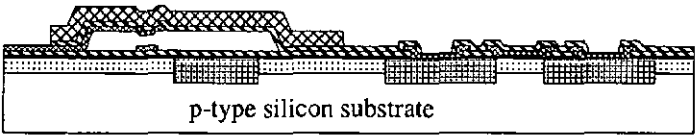

- Aluminium

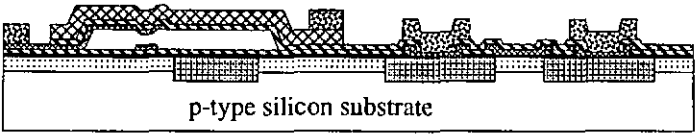

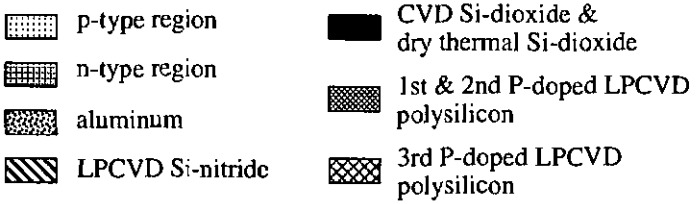

Figure 3.2: Main processing steps of the polysilicon microrelays fabrication. The IC compatibility is demonstrated by integrating MOSFETs together with the microrelays.

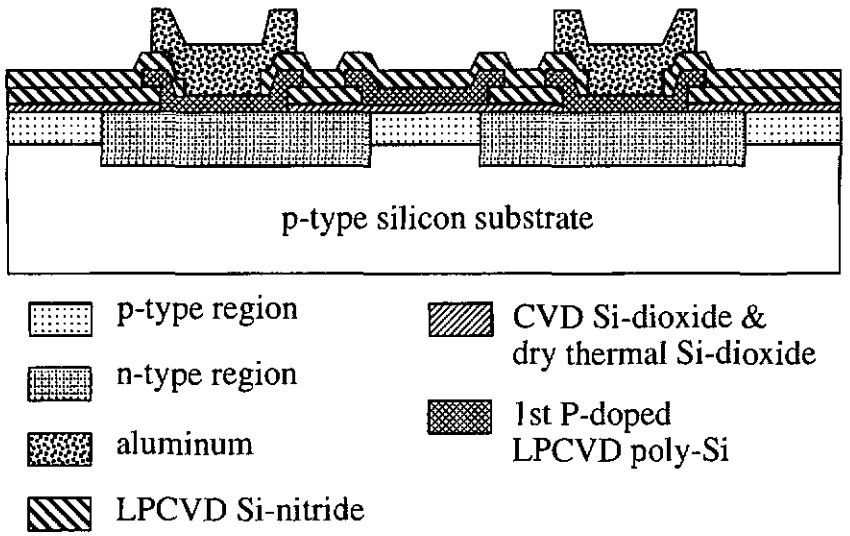

Figure 3.3: Cross section of the MOSFETs fabricated to prove the IC compatibility of the process.

sacrificial layer to define a micro-bump (Figure 3.1) providing a good contact between both conductors of the working circuit.

The layers of the micro-mechanical structure (Figure 3.2) are then deposited and patterned on top of the sacrificial layer. The first one is a 2500 Å thick doped polysilicon layer (second conductor of the working circuit) followed by a 2000 Å thick insulating silicon nitride layer and the main polysilicon layer (7500 Å thick). The whole mechanical structure is then released in BHF [7:1] and the final metallization is deposited and patterned the same way it has been explained in section 2.2.4. A thick aluminum layer (1.5 μm) is deposited and completely covers the free-standing microbridges. Thus it holds them during the subsequent photoresist spinning for its patterning.

Particular attention has to be given to the manipulation in liquids as well as to the rinsing of surface micromachined microstructures since the viscous forces in liquids are large compared to the other forces. For theses small structures, the forces are about equivalent to a man swimming in honey. Thus it is very important to slowly move the wafers in the etching solutions while releasing the structures otherwise they will break or undergo some plastic deformations. At this point of the process, it is also not yet possible to dry the wafers with the

nitrogen blow-gun. To ensure a through rinsing of the structures and to be sure that no acid remains under the structure, the wafers are rinsed in deionized water. The impedance of the bath is measured until it has decrease to that of deionized water. Then they are rinsed minimum one hour in isopropanol alcohol and dried 15 minutes in an air pulsed oven at 200 °C [2.27].

The dicing of a wafer containing free-standing structures was considered a major problem. A solution to this has been found by applying a thick sprayed resist, the micromechanical components are fairly well embedded in this resist layer and are therefore sufficiently protected to withstand IC sawing and in particular the water jet which cools the saw. Finally the resist is removed in acetone and again the chips are rinsed in isopropanol alcohol for 1 hour and dried 15 minutes in an air pulsed oven at 200 °C.

Figure 3.4 shows a schematic cross section of the final structure which is not symmetric (three layers on the working circuit side and two layers on the actuation port side). Scanning electron microscope (SEM) investigations have been performed to show some details of the microrelays. (Figure 3.5, Figure 3.6 and Figure 3.7). An optical micrograph of fabricated microrelays integrated together with MOSFETs is shown in Figure 3.8.

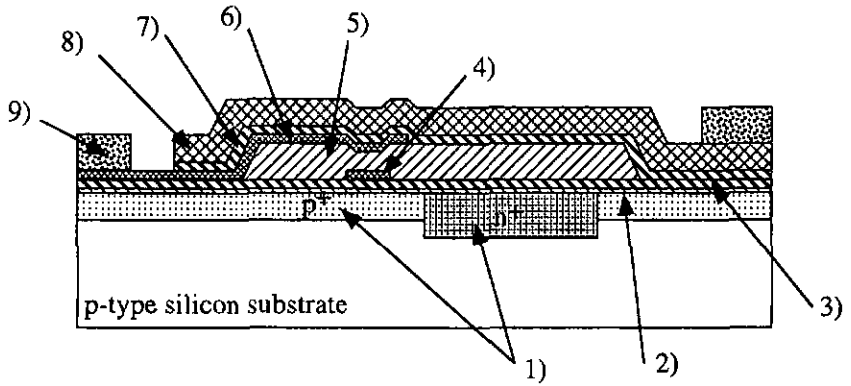

Figure 3.4: Cross section of the microrelay: 1) diffusion 2) SiO_2 (1000 Å), 3) Si_3N_4 (2000 Å), 4) polysilicon (2500 Å), 5) SiO_2 (1.6 μm): sacrificial layer which is underetched before the deposition of the aluminum (Al), 6) polysilicon (2500 Å), 7) Si_3N_4 (2000 Å), 8) polysilicon (7500 Å), 9) Al (1.5 μm).

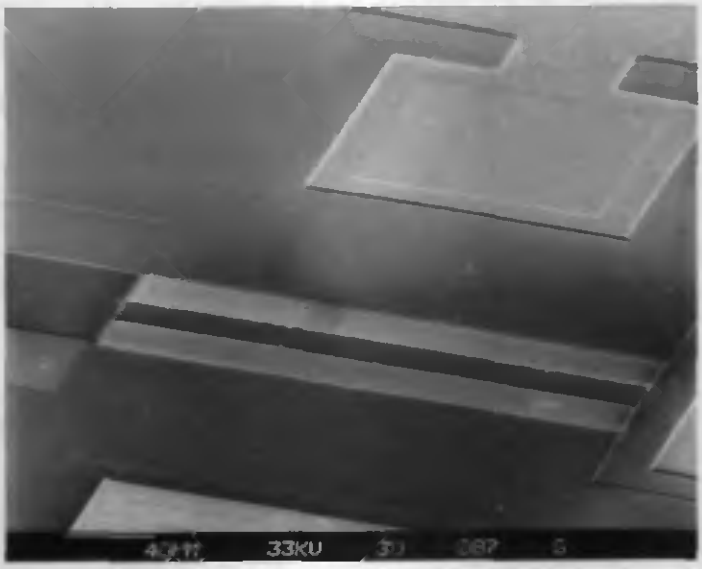

Figure 3.5: SEM of a 300 μm long polysilicon microrelay based on polysilicon/silicon nitride multilayer micro-bridge.

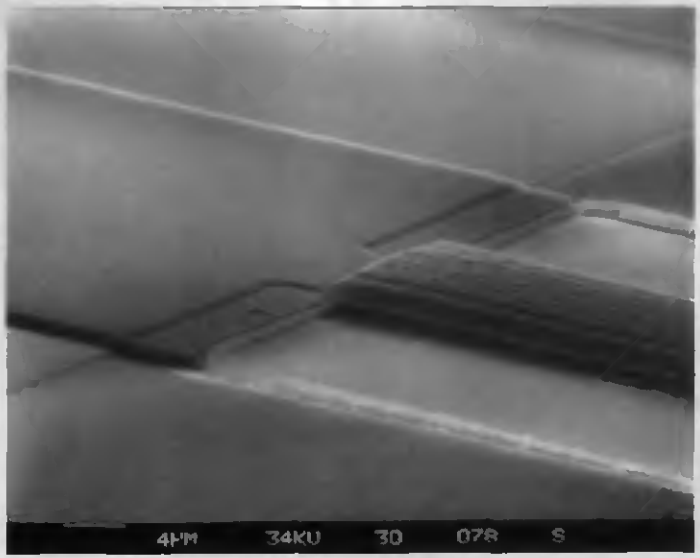

Figure 3.6: SEM of one end of the microrelay, note the three layers (polysillicon/silicon nitride/polysilicon).

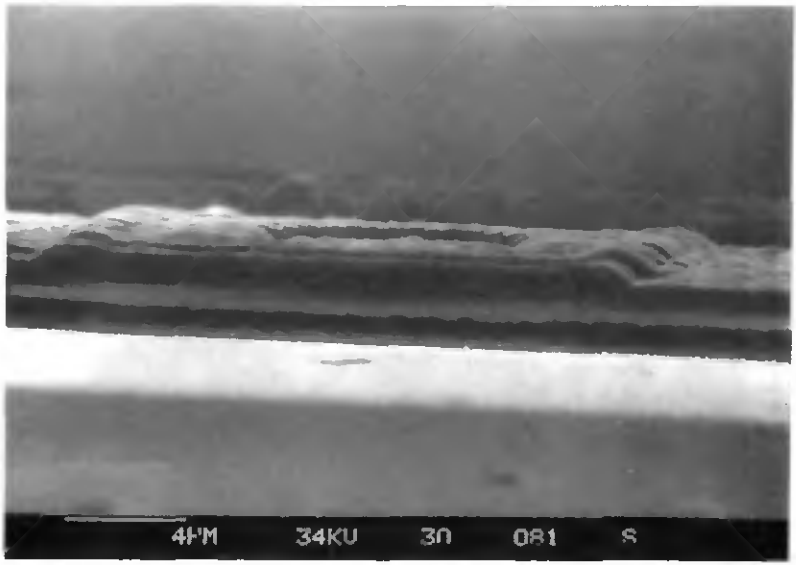

Figure 3.7: SEM of the micro-bump providing an improved electrical contact between both conductors of the working circuit.

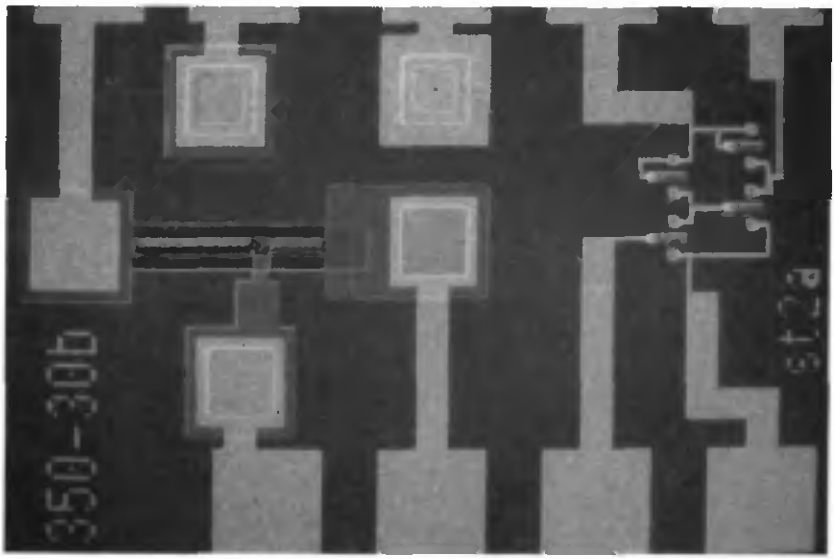

Figure 3.8: Optical micrograph of fabricated microrelays integrated together with MOSFETs.

3.4 Design considerations:

Several sizes of polysilicon microrelays have been fabricated. The length of the mechanical micro-bridges vary from 250 μm to 350 μm. The width is either 22 μm or 30 μm. As the working circuit is on one side of the relay beam, it has been necessary to integrate the actuation port on the other side. To get the maximum actuation strength, the driving electrode in the substrate has been designed to be a little bit longer than half of the beam length. Thus it overlaps slightly the middle of the beam and gives a reasonable pull-in voltage for the microrelays. The Figure 3.9 shows the mask set printout. It gives a good idea of the topology of the polysilicon microrelay as well as the optical micrograph of Figure 3.8. To reduce cross-talk phenomena, the actuation port and the working circuit have been placed on opposite chip sides. Thus the corresponding connections will also be on opposite sides of the dual-in-line IC socket, resulting in a maximum attenuation of this undesirable phenomena.

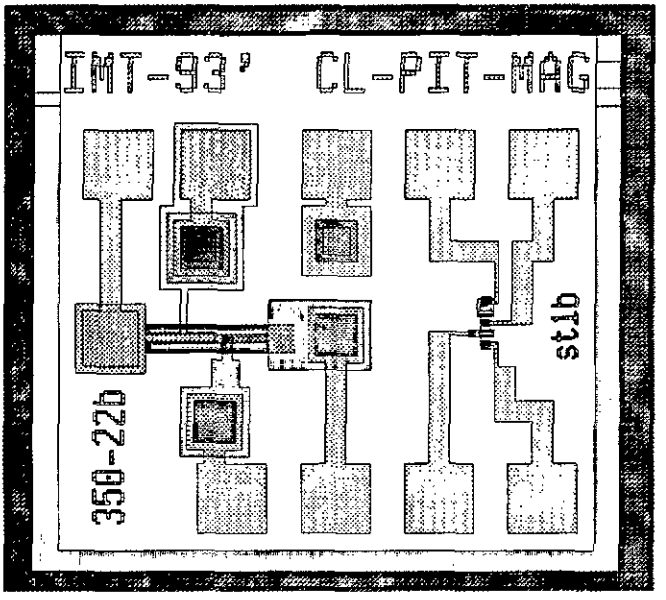

Figure 3.9: Printout of the mask set, each different pattern corresponds to one mask. The actuation and the working circuit are on opposite chip sides resulting in a high attenuation between both ports.

3.5 Measurements:

In this paragraph the characterization of the MOSFETs which have been integrated to show the IC compatibility as well as the measurements performed to characterize the polysilicon microrelays are presented.

The transistors have been characterized by measuring their output and transfer characteristics.

Initial measurements of the polysilicon microrelays have been performed in the air. The polysilicon electrodes of the contact were oxidized by the air oxygen resulting in contact wear. Thus it has been necessary to operate the microrelays in a nitrogen atmosphere. The latter has allowed to increase the switching speed of the polysilicon microrelays up to 100 kHz and to improve the life time of this device to more than 10^9 cycles. This demonstrates once more that polysilicon is a suitable and reliable material to be integrated in MEMS having relatively large displacements [3.26, 3.27, 3.35, 3.36].

3.5.1 MOSFETs characterization:

The measured output and transfer characteristics of the n-channel MOSFETs (NMOS transistors) shown in Figure 3.10 and Figure 3.11 correspond to typical transistor behavior [e.g. 3.37]. In the drain characteristics of Figure 3.10, no short channel effect is observed; this is due to the rather large gate dimensions of the MOSFETs having a length of 10 µm and a width of 30 µm. Furthermore, Figure 3.11 shows that the leakage current for Vgs=-0.5 V is about 75 pA being very low when considering the three polysilicon anneals that the p-n junctions in the substrate had to undergo.

The subthreshold slope (n), the gain (β) and the threshold voltage (V_t) are good ways to characterize the quality of MOSFETs [3.37]. This characterization was realized in the frame of a Diploma work at the IMT [3.38]. The results of this study are summarized in Table 3-1.

Table 3-1: Measurements and modeling of the MOSFETs [3.38]

	Measurements	Simulation	Errors
n	4.01	1.47	172%
β	88.1 10^{-6} A/V^2	72.4 10^{-6} A/V^2	21%
V_t	0.890 V	1.1 V	19%

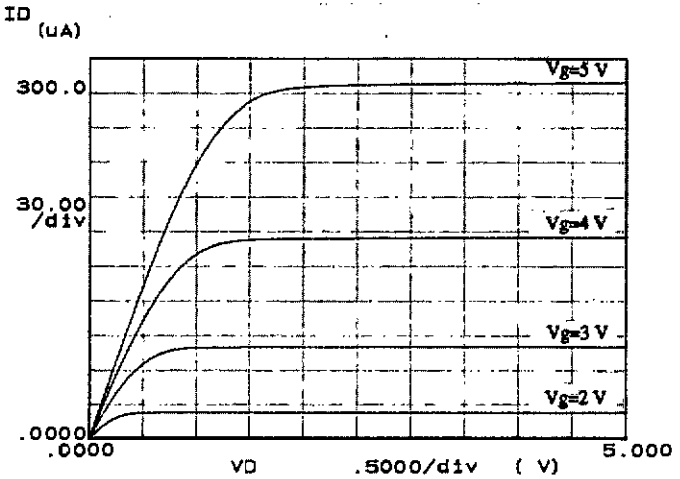

Figure 3.10: Output characteristics (I_d versus V_{ds} for different V_{gs}) of a MOSFET (W=30 μm / L=10 μm) integrated with the microrelays.

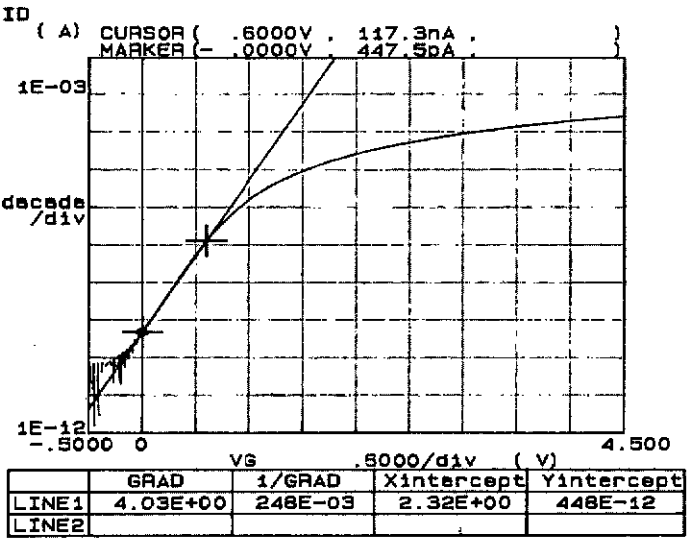

	GRAD	1/GRAD	Xintercept	Yintercept
LINE1	4.03E+00	248E-03	2.32E+00	448E-12
LINE2				

Figure 3.11: Transfer characteristics (I_d versus versus V_{gs}, with V_{ds}=5V) of a MOSFET (W=30 μm / L=10 μm) integrated with surface micromachined microrelays.

This example of integrating MOSFETs with the same technological steps as the MEMS highlights the limits of performing a coprocessing of electronics with a mechanical structure. The comparison of predicted values and measured values of Table 3-1, shows that the measured values are far away from the predicted ones. The subthreshold slope (n), is much too high. It should be around 1.5. This points out that these transistors are slower than equivalent ones built with an optimum MOS process [3.37]. Some trade-off where made in their design to ensure a minimal number of masks. The silicon nitride was etched to define windows over the gate oxide resulting in trapped charges in the gate oxide. Long high temperature thermal anneals were necessary to ensure the stability of the mechanical structures making the doping concentrations difficult to control. For all these reasons, the design of good transistors integrated with MEMS is a hard task, thus it may be often better to choose hybrid solutions and to connect two specialized chips with well defined characteristics together (e.g. sensor chip and it's front end electronics).

Nevertheless, these NMOS transistors have been used successfully by T. Akiyama et al. [3.39] to build a small inverter intended for the measurements of stress changes on cantilevers.

3.5.2 Electrical circuit:

To be able to describe the measurements which have been done with the microrelays, it is necessary to define the names of the different applied potentials. Figure 3.12 gives an electrical equivalent circuit of the microrelay. When it is compared to the technological cross-sections (Figure 3.1 and Figure 3.4) it shows how these potentials are applied to the different layers which form the structure.

For the working circuit, the potentials are:

V_{w1} : the voltage applied to the first polysilicon layer,

V_{w2} : the voltage applied to the second polysilicon layer,

and for the actuation port, the potentials are:

V_{am} : the voltage applied to the third polysilicon layer which forms the micro-bridge,

V_s : the substrate voltage,

V_{ad} : the voltage applied to the diffused area in the substrate.

These names will be used during the whole thesis also for the modeling of the microrelays which will be presented in the Chapter 4.

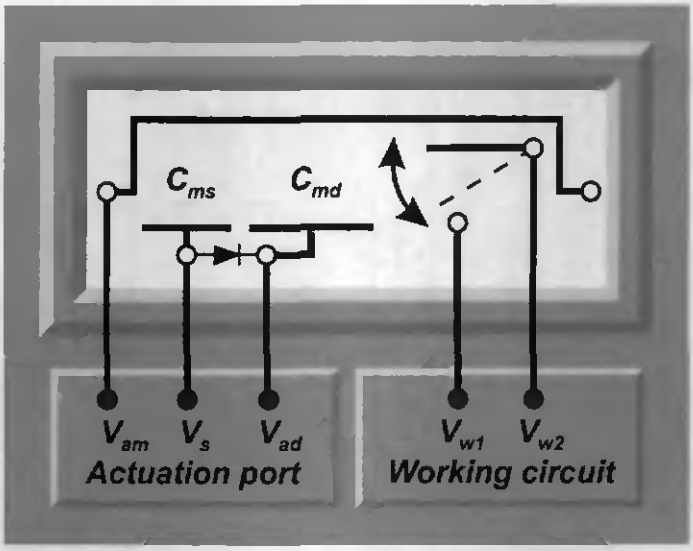

Figure 3.12: Electrical equivalent circuit of the microrelay. with the nomenclature of the different ports.

3.5.3 First measurements in air:

Initial measurements with the microrelay have been performed in air. The measurement setup is shown in Figure 3.13. The driving voltage has been applied to the third polysilicon layer (V_{am}) while the diffused area (V_{ad}) and the substrate (V_s) have been contacted to the ground. The output voltage has been measured over a load resistance of 100 kΩ, resulting in a rather low output current. The switched voltage (V_{w1}) was 10 V. As shown in Figure 3.14 a switching frequency of 1 kHz was reached. The low output current allows the microrelay to survive a several 10^3 operation cycles in air before noticeable contact degradation, mainly due to oxidation of the polysilicon electrodes, occured. This degradation can be noticed on Figure 3.14 where the level of the measured signal on the working circuit (Trace 2) is not constant. This can be avoided by using the microrelays in a nitrogen atmosphere. Thus it has been possible to increase the lifetime, the speed and the current capability of the polysilicon microrelay.

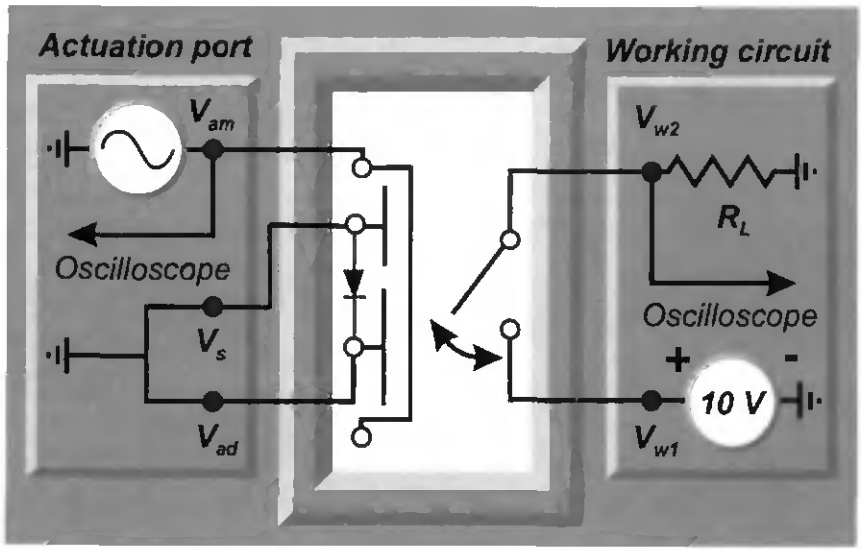

Figure 3.13: Measurement setup of the microrelay: for the first measurement in air and in nitrogen otmosphere, the driving voltage has been applied to the third polysilicon electrode (V_{am}).

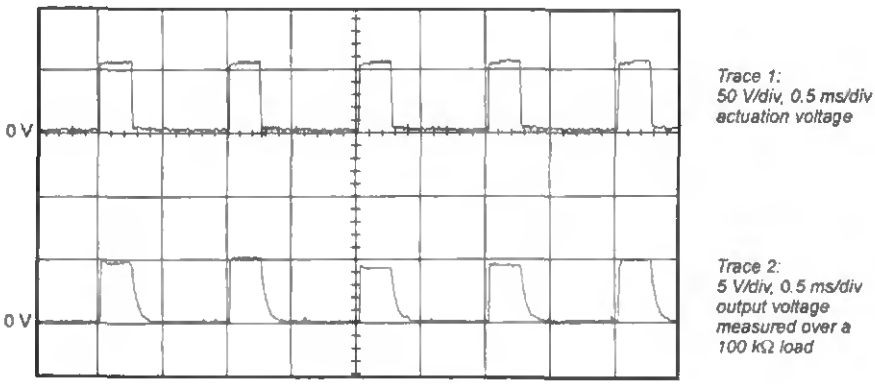

Figure 3.14: Switching behavior at 1 kHz of a 250 μm long microrelay measured in air

3.5.4 First measurements in nitrogen:

By operating the microbridge relays in a nitrogen atmosphere, it was possible to considerably increase the lifetime and to enhance the output current capability. An output current of 0.5 mA has been obtained, by taking a load resistance (R_L) of 1 kΩ and applying a DC bias of 10 V on the working circuit (V_{wl}). Moreover, the use of a small resistance load enabled higher switching speeds due to the shorter RC time constant. Figure 3.15 shows the output voltage of a microrelay at 20 kHz measured over such a 1 kΩ load. When the switching frequency is further increased, cross-talk between the actuation and the working circuit more and more influences the output signal. Figure 3.16 shows the output voltage at 75 kHz. This cross-talk is mainly due to the measurement setup. Figure 3.17 shows the signal on the working circuit due to the actuation voltage for a DIL socket without a microrelay. It reveals the importance of the capacitive coupling between the ports. Improved measurements will be presented in Chapter 4 (Section 4.4.3 Pull-in time simulation). They are realized with relays packaged on TO sockets where the connections are shorter, thus giving a much smaller cross-talk. In order to prevent the cross-talk phenomena appropriate shielding could also be used [3.31, 3.32].

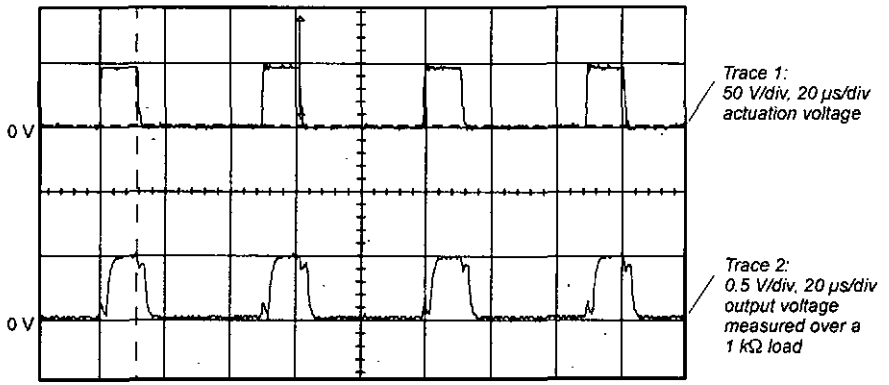

Figure 3.15: Switching behavior at 20 kHz of a 350 µm long microrelay measured in a nitrogen atmosphere

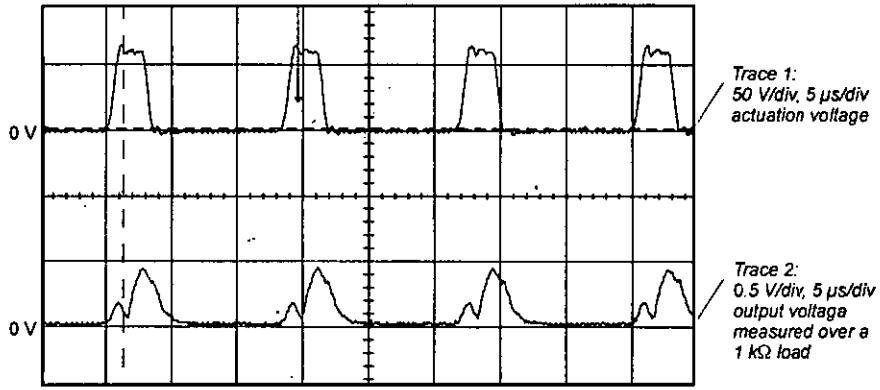

Figure 3.16: Switching behavior at 75 kHz of a 350 µm long microrelay measured in a nitrogen atmosphere.

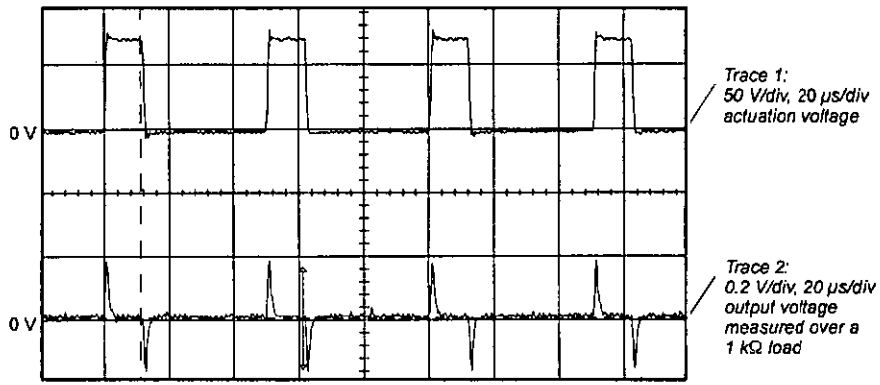

Figure 3.17: Cross-talk of the measurement setup. To perform this measurement, a DIL socket without a chip has been placed on the measurement setup while the voltages usually used to drive the relay have been applied.

3.5.5 Pull-in and Pull-out Voltages :

The pull-in $V_{p\text{-}in}$ and the pull-out voltage $V_{p\text{-}out}$ ($V_{p\text{-}in} > V_{p\text{-}out}$) are two important voltages for driving electromechanical microrelays. For voltages greater than $V_{p\text{-}in}$, the electrostatic driving force can no longer be balanced by the restoring spring force of the beam, i.e., there is no longer an equilibrium position. Therefore, the microbridge deflects downward until it touches the substrate and the relay goes to the on-state. When the driving voltage is subsequently diminished below $V_{p\text{-}out}$, the microbridge moves abruptly from the unstable equilibrium located at the downward-deflected position to the stable equilibrium which is close to the free-standing position; thus the relay switches from the on- to the off-state. So a special feature of these microrelays is the net switching voltage $V_{p\text{-}in}$-$V_{p\text{-}out}$ which allows the amplitude of the driving voltage to be significantly reduced. Table 3-2 shows measured values of $V_{p\text{-}in}$ and $V_{p\text{-}out}$ for microrelays with different lengths. In particular, it can be seen that low net switching voltages around 10 V have been achieved.

Table 3-2: Measured pull-in and pull-out

Microbridge length[μm]	Pull-in voltage [V]	Pull-out voltage [V]
250	54 ± 2	42 ± 1
300	45 ± 2	35 ± 1
350	41 ± 2	31 ± 1

3.5.6 Operate time and release time:

Two time constants are important in the microrelay characterization: the turn-on or operate time and the release time. Both limit the maximum speed at which the device can be operated. The operate time is measured from when power is applied to the driving port until the contact is settled. It gives particularly good information on the electromechanical coupling and allows the mechanical part of the relay to be characterized with a high accuracy (cf. Chapter 4). The release time gives an idea of the capability of the relay to open the contact. It is measured from the time when the power is removed on the driving port until the contact is open. It gives some information on whether the beam remains deflected on the substrate due to sticking phenomena. Figure 3.18 shows the operate time of a relay having a 250 μm long microbridge. It can be seen that the contact is made about 4 μs after the actuation voltage is applied, which is one order of magnitude faster than in [3.1], two orders than in [3.13] and three orders than in a conventional relay [e.g. 3.13]. As indicated in Figure 3.19, the opening time over a 1 kΩ load is about 1 μs. This shows the good behavior of these microrelays since clearly no sticking phenomena were observed.

Both curves show that no bounce was present for these polysilicon microrelays. Due to the hysteresis behavior of the beam capacitor, when the microrelay touches the substrate, the actuation force is high and does not allow the beam to bounce. Moreover, as these devices are operated at atmospheric pressure, their quality factor is very small due to air damping. This helps also to reduce bounce effects of these devices.

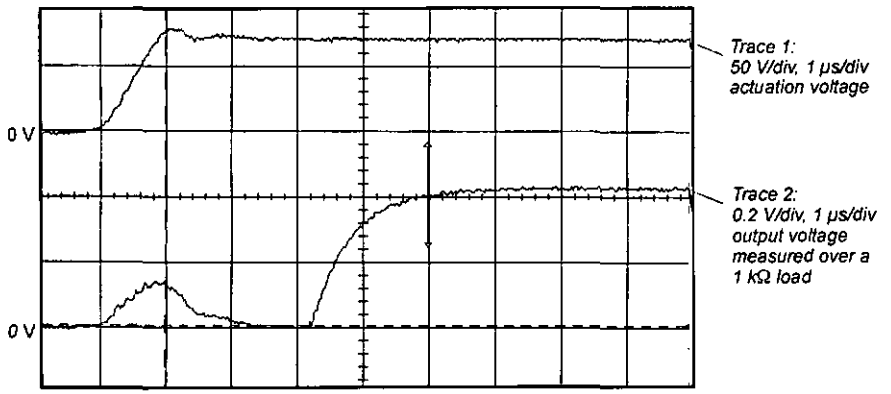

Figure 3.18: Switching behavior of a 250 µm long microrelay a few microseconds after the driving voltage has been applied to the actuation port. The operate time is about 4 µs.

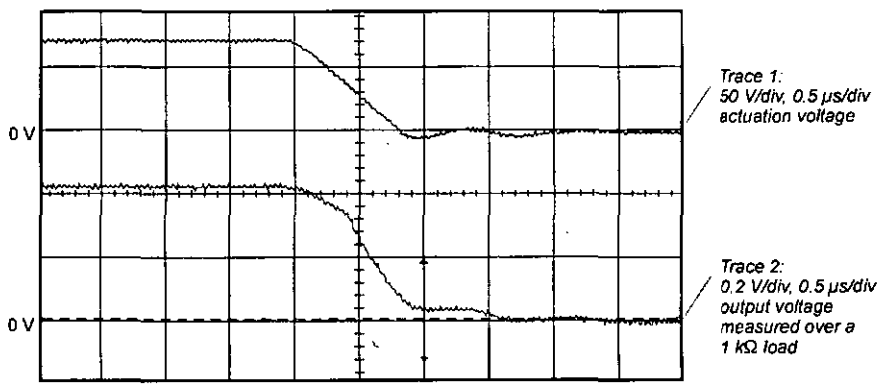

Figure 3.19: Opening of the microrelay contact, the release time is about 1 µs for this 250 µm long microrelay.

3.5.7 Life time tests:

Some life time tests have been performed with the microrelays. This characterization was made under nitrogen atmosphere. A 350 µm long microrelay has been operated at 20kHz, while the output voltage was measured over a 1 kΩ load. The relay has been operated $1.2 \cdot 10^9$ cycles before noticing critical changes in the signature of the output signal. Figure 3.20 shows the signal at the beginning of the test. Figure 3.21 shows the signal after $1.2 \cdot 10^9$ cycles (16h45 of operation) when the first signs of wear of the contact were observed. The test has been prolonged but after only $1 \cdot 10^8$ cycles the contact was definitively damaged and some soldering of the contact has been observed. The relay was closed and it was not yet possible to open it.

This test has pointed out that the critical part in a microrelay is the contact. No change has been observed in the mechanical structure where an actuation voltage of 70 V peek-to-peek was applied during the whole test.

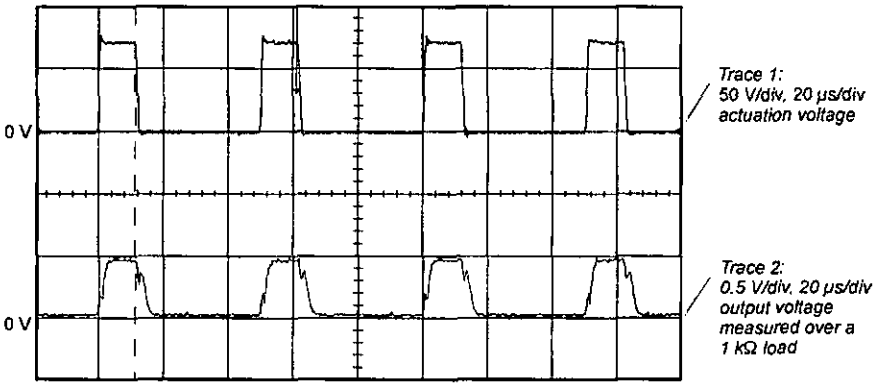

Figure 3.20: Switching behavior at 20 kHz of a 350 µm long microrelay measured in a nitrogen atmosphere, starting point of the life time tests.

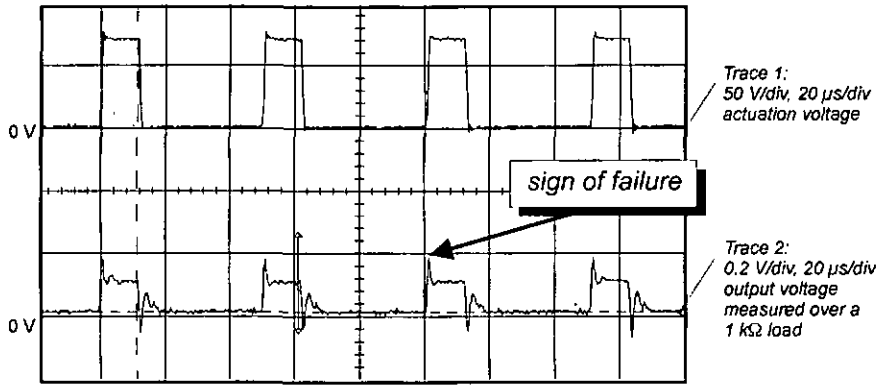

Figure 3.21: Switching behavior after $1.2 \cdot 10^9$ cycles, note the changes in the signature of the output voltage.

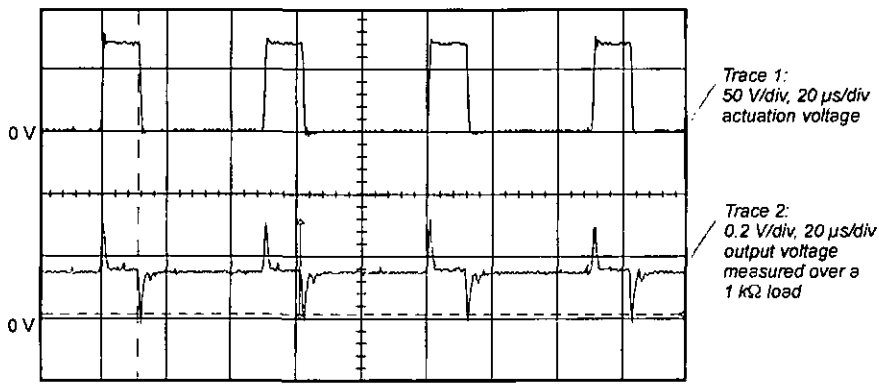

Figure 3.22: Sticking phenomena after $1.3 \cdot 10^9$ cycles when the first failure has been observed.

3.5.8 Maximum switching speed characterization:

Further experiments operating the relay in the AC mode have been carried out by driving the substrate electrode with an AC switching voltage with peak-to-peak in the range of $V_{p\text{-}in}$-$V_{p\text{-}out}$. A negative offset voltage V_{off} has been applied to the polysilicon drive electrode of the microbridge while the substrate was grounded.

Due to the negative offset voltage (V_{off}) the microrelay is slightly deflected and smaller driving signals are possible than the which ones presented in section 3.5.3 to 3.5.6. Thus it has been possible to use the driving electrodes diffused in the substrate. As the diodes between the driving electrodes and the substrate have to be polarized, the maximum voltage that can be applied to the driving electrode is about 18 V to 20 V, which corresponded to the reverse breakdown voltage of the diodes. The offset voltage remains in the 30 to 45 V which is still high for some applications and should be improved by a design update.

The output voltage has been measured over a resistance load, applying 5 V to the working port. Figure 3.23 shows a schematic of this measurement setup, which allows reduction of the transients of the driving signal and thus reduction of the cross talk between the excitation and the working port.

Several driving signals at different frequencies have been used to characterize the relays (Figure 3.24, Figure 3.25 and Figure 3.26). In particular, when driving the relays at high frequencies, as shown in Figure 3.26 for 100 kHz, the AC actuation voltages have to greatly exceed $V_{p\text{-}in}$-$V_{p\text{-}out}$, in order to overcome damping effects. In addition, cross-talk between the actuation and the working circuits as well as interference from the mechanical resonance frequency of the microbridges must be taken into account. The latter determines the cut-off frequency of these relays, which has been observed at about 200 kHz. For higher frequencies the relay is either on or off, since the mechanical structure is no longer able to follow the driving voltage. This also shows that the measured signal of Figure 3.26 is not cross-talk but the switched signal of the mechanical device. Due to their small masses, these relays offer a much larger frequency range than traditional mechanical relays.

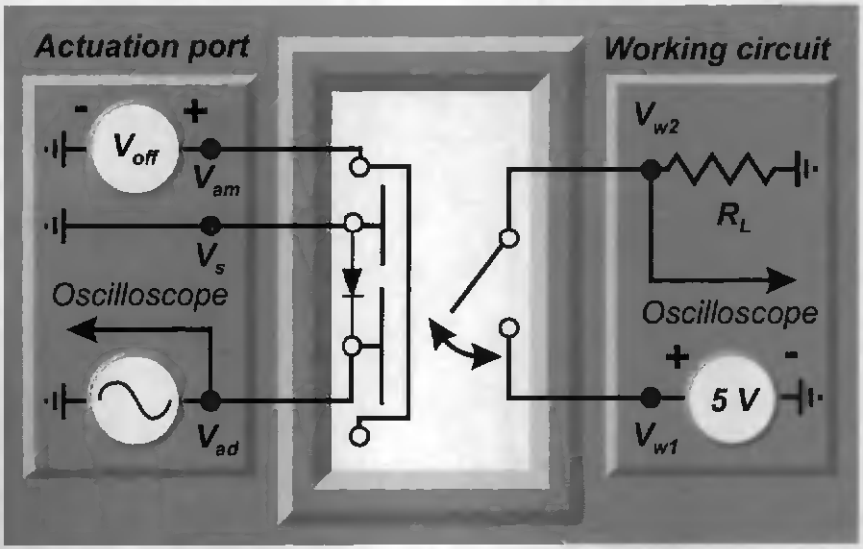

Figure 3.23: Measurement setup of the microrelay: for these cut-off frequency characterizations.

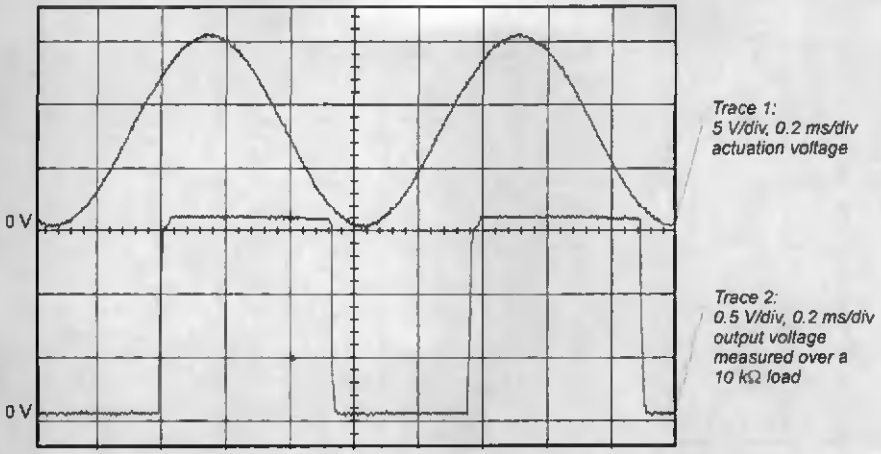

Figure 3.24: Switching behavior at 1 kHz for a 350 μm long microrelay where V_{off} is -32V.

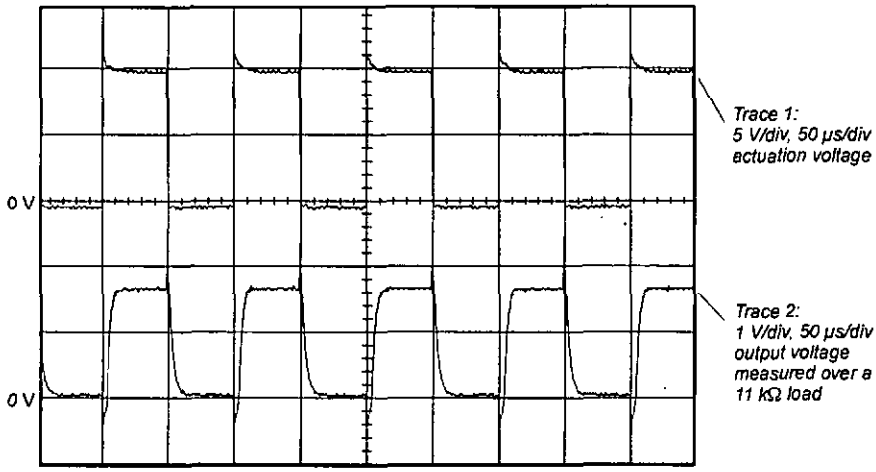

Figure 3.25: Switching behavior at 10 kHz for a 350 µm long microrelay where V_{off} is -33V.

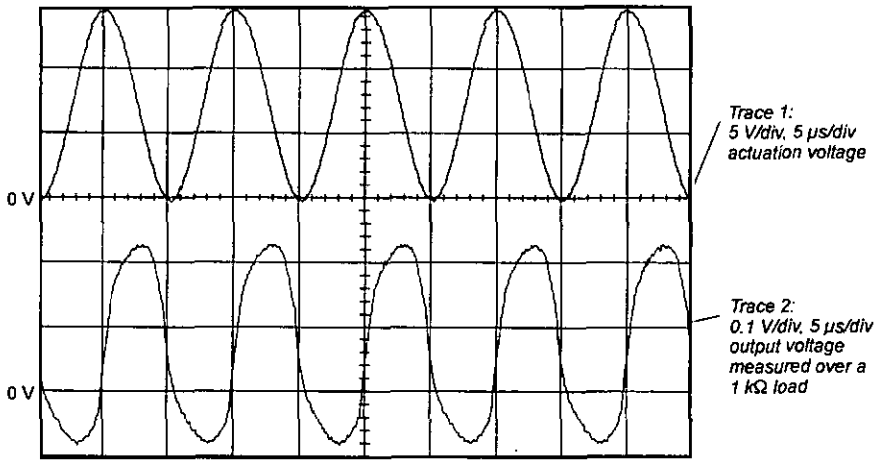

Figure 3.26: Switching behavior at 100 kHz for a 350 µm long microrelay where V_{off} is -33V.

3.5.9 The effect of the micro-bump:

By applying an offset voltage near $V_{p\text{-}in}$ and an AC-driving signal of about 1 V, a special behavior of the microrelay was observed. (Figure 3.27). This particularity consists in the fact that the relays could be operated with a signal smaller than the difference between the pull-in and pull-out voltages. The possibility to drive the relay with such a small net switching voltage is due to the microbump. When the voltage applied to the driving port just exceeds $V_{p\text{-}in}$, the beam is deflected until both electrodes of the working circuit touch and the beam may be held by the microbump, which provides an air gap between the driving electrodes. Therefore the dynamic pull-out voltage is much closer to the pull-in voltage. This interesting effect has been used by Zavracky et al [3.40] to determine an optimum size for the microbump and designing devices without hysteresis.

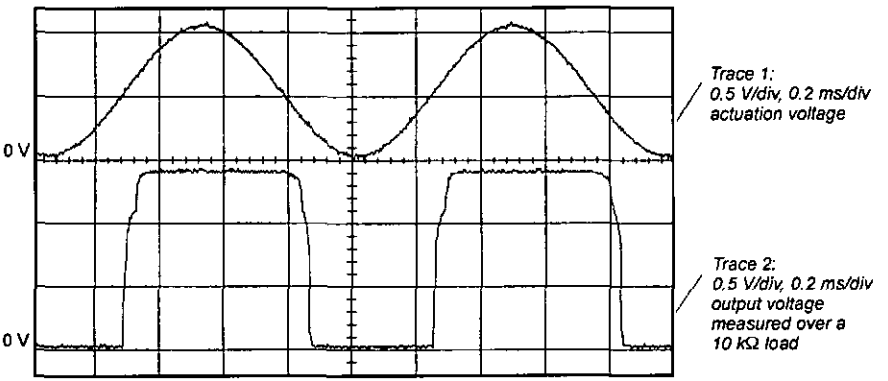

Figure 3.27: Switching behavior at 1 kHz for a 350 μm long microrelay where V_{off} is -41 V.

3.5.10 The contact resistance:

Table 3-3 gives an idea of the contact resistance of the polysilicon microrelays. It has been calculated from the different measurements presented in this chapter by using the following formula:

$$R_C = R_L\left(\cdot\frac{V_{W1}}{V_{W2}} - 1\right) \qquad (1)$$

This contact resistance is composed of both the resistance of the contact itself and the resistance of the two polysilicon lines of the working circuit. These lines are in the 20 kΩ range (estimation with the sheet resistance of doped polysilicon). However it is difficult to give a precise value and so it is difficult to give an estimation of the resistance of the contact itself. Nevertheless, for the measurements performed in the air, due to the oxidation of the contact it's resistance is very high and can be estimated to be 80 kΩ. When the contact is operated in nitrogen, the contact resistance is relatively constant. But for the special behavior of the microrelay with a low switching voltage, as the contact area is smaller, the contact resistance is a little bit higher.

The contact resistance is also dependent on the pressure applied between the two conductors of the contact [3.41], but unfortunately, it has not been possible to demonstrate this phenomena.

Table 3-3: Contact resistance of different polysilicon micro-relays

Figure Number	Relay length [µm]	Atmosphere	Driving voltage [V]	Contact resistance [kΩ]
Figure 3.14	250	AIR	55	100 ± 5
Figure 3.15	350	N_2	49	19.0 ± 1
Figure 3.16	350	N_2	60	21.2 ± 1
Figure 3.18	250	N_2	70	22.8 ± 1
Figure 3.19	250	N_2	70	22.8 ± 1
Figure 3.24	350	N_2	15	21.3 ± 1
Figure 3.25	350	N_2	10	21.4 ± 1
Figure 3.26	350	N_2	15	21.7 ± 1
Figure 3.27	350	N_2	1	25.7 ± 1

3.5.11 DC & AC isolation:

The DC isolation of mechanical microrelays is a key point of such devices. As shown in Figure 3.28 a leakage current of about 120 pA was measured when 10 Volts where applied to the working port of a 300 μm long polysilicon microrelay. This gives an impedance of 83 GΩ when the relay is open. For electromechanical devices 1 GΩ was reported in [3.2]. Compared to the contact resistance of 10 kΩ for the tested device, it makes an off-state to on-state impedance ratio of $8 \cdot 10^6$.

The maximum voltage which could be applied to the working port for a 350 μm long microrelay before noticing failure of the DC isolation was 60 V. This failure was due to the deflection of the microbeam. This value could be improved by an appropriate design update which would also be necessary in term of coupling capacitance.

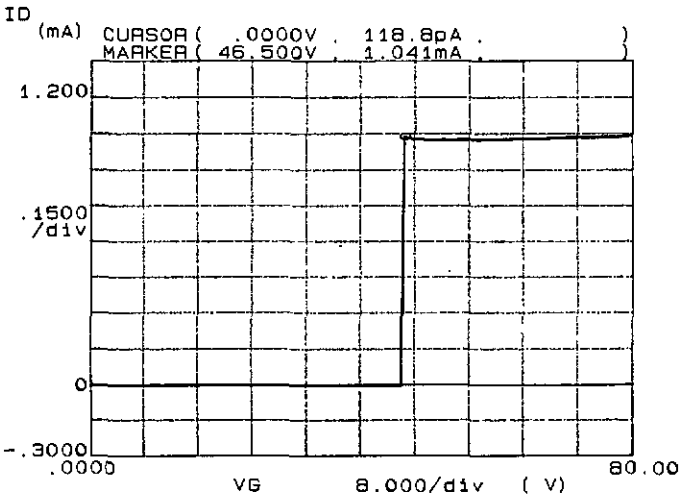

Figure 3.28: DC isolation of the microrelay. V_g corresponds to the voltage applied to the actuation port of the polysilicon microrelay, I_d corresponds to the current measured over the contact port of the microrelay. The off-state to on state impedance ratio of this device is $8 \cdot 10^6$.

With the design described in tbis chapter, an estimation gives a coupling capacitance of about 2.5 pF between the top polysilicon layer of the microrelay (driving electrode) and the lowest one (2nd layer of the working circuit). The overlap between both port has a surface of 9000 μm^2, while the gap defined by the nitride insulator is 0.2 μm (Figure 3.4). This feature could be improved by changing the configuration and having some crossing instead of overlapping of connectors as it is in the actual device, resulting in a coupling capacitance of 10 fF.

Figure 3.29 shows the design of a new polysilicon microrelay where the contact is made between two metallic conductors (for instance gold) post-processed after the realization of the polysilicon-nitride microbridge. This configuration offer some advantages compare to the previous one: larger actuation electrode, smaller coupling between the working circuit and the driving port, lower contact resistance due to the possibility of using metallic layer instead of polysilicon.

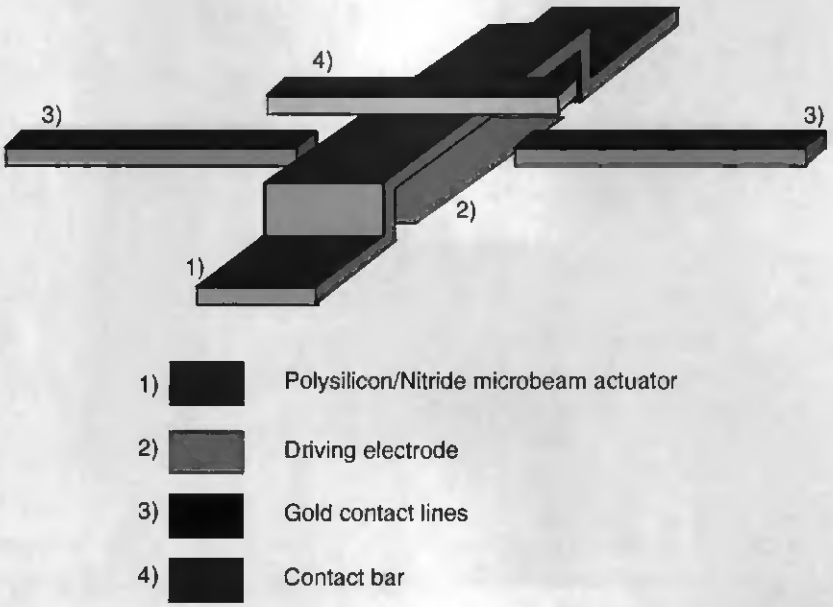

Figure 3.29: Design of an improved microrelay, the contact is performed when the contact bar (4) touches both lanes of the working circuit (3). A driving electrode is designed in the substrate and is larger than in the previous design.

3.6 Conclusions:

The fabrication of polysilicon/silicon nitride multilayer microbridge relays have been demonstrated using a fully IC compatible sacrificial layer technology. This prototype generation has been successfully tested and has shown rather promising features such as low net AC driving voltages in the 1 to 10 V range, an operation at frequencies up to 100 kHz and a lifetime of more than 10^9 cycles. These relays have an output current limitation of a few mA due to the relatively low conductivity of the polysilicon used for the working circuit. Moreover, their typical contact resistance which is about 22 kΩ is too high for switching applications. Thus it will be necessary to use other contact materials to improve this feature of the microrelays [3.42, 3.43].

The characterization presented here explains many features of the microrelay. Nevertheless, it has been found interesting to get a better understanding of these microrelays, by performing a special characterization of the non linear actuator. This work will be presented in chapter 4, with the simulation which has been performed at the Massachusetts Institute of Technology (MIT) in the group of Professor Stephen Senturia during a three month stay as a visiting scientist. Thus the reader will find more details about the resonance frequency as well as the pull-in time in the next chapter.

3.7 References:

[3.1] K. E. Petersen, "Micromechanical Membrane Switches on Silicon", IBM Journal of Research and Development, Vol. 23-4 (1979), pp. 376-385.

[3.2] "Switching Handbook", Keithley Instruments, Inc., Cleveland, 1995.

[3.3] M.-A. Grétillat, P. Thiébaud, N. F. de Rooij and C. Linder, "Electrostatic polysilicon microrelays integrated with MOSFETs", Proceedings of the 7th IEEE Workshop on Micro Electro Mechanical Systems, MEMS '94, Oiso, Japan, January 1994, pp. 97-101.

[3.4] M.-A. Grétillat, P. Thiébaud, C. Linder and N. F. de Rooij, "IC compatible electrostatic polysilicon microrelays", Journal of Micromechanics & Microengineering, 5 (1995), pp. 156-160.

[3.5] M. Sakata, "An Electrostatic Microactuator For Electro-Mechanical Relay", Proceedings of the 2nd IEEE Workshop on Micro Electro Mechanical Systems, MEMS '89, Salt Lake City, UT, February 1989, pp. 149-151.

[3.6] X. Q. Sun, Z. J. Li, X. Y. Zheng and L. T. Liu, "Study of Fabrication Process of a Micro-Electrostatic Switch and Its Application to a Micromechanical V-F Converter", Sensors & Actuators, A32 (1993), pp. 189-192.

[3.7] J. Schimkat, L. Kieswetter, H.-J. Gevatter, F. Arndt, A. Steckenborn and H. F. Schlaak, "Moving Wedge Actuator: An Electrostatic Actuator for Use in a Microrelay", Proceedings of the 4th International Conference on Micro Electro, Opto, Mechanic Systems and Components, Micro System Technologies 94, Berlin, Germany, October 1994, pp. 989-996.

[3.8] S. Roy and M. Mehregany, "Fabrication of Electrostatic Nickel Microrelays by Nickel Surface Micromachining", Proceedings of the 8th IEEE Workshop on Micro Electro Mechanical Systems, MEMS '95, Amsterdam, the Netherlands, January 1995, pp. 353-357.

[3.9] J. Drake, H. Jerman, B. Lutze and M. Stuber, "An Electrostatically Actuated Microrelay", Digest of Technical Papers of the 8th International Conference on Solide-State Sensors and Actuators, Transducers '95, Stockholm, Sweden, June 1995, vol.2: pp. 380-383.

[3.10] J. J. Yao and M. F. Chang, "A Surface Micromachined miniature Switch for Telecomunications Applications with Signal Frequencies from DC up to 4 GHz", Digest of Technical Papers of the 8th International Conference on Solide-State Sensors and Actuators, Transducers '95, Stockholm, Sweden, June 1995, vol.2: pp. 384-387.

[3.11] I. Schiele, J. Huber, C. Evers, B. Hillerich and F. Kozlowski, "Micromechanical Relay with Electrostatic Actuation", Digest of Technical Papers of the 9th International Conference on Solide-State Sensors and Actuators, Transducers '97, Chicago, IL, June 1997, pp. 1165-1168.

[3.12] S. Zhou, X. Sun and W. Carr, "A Micro Variable Inductor Chip Using MEMS Relays", Digest of Technical Papers of the 9th International Conference on Solide-State Sensors and Actuators, Transducers '97, Chicago, IL, June 1997, pp. 1137-1140.

[3.13] H. Hosaka, H. Kuwano and K. Yanagisawa, "Electromagnetic Microrelays: Concept and Fundamental Characteristics", Proceedings of the 6th IEEE Workshop on Micro Electro Mechanical Systems, MEMS '93, Fort Lauderdale, FL, February 1993, pp. 12-17.

[3.14] H. Hosaka, H. Kuwano and K. Yanagisawa, "Electromagnetic Microrelays: Concept and Fundamental Characteristics", Sensors & Actuators, A40 (1994), pp. 41-47.

[3.15] H. Ziad, D. Debruyker, J.-B. Chévrier, K. Baert, H. Löwe and H.A.C. Tilmans, "Toward Integrated Microrelays Using Electromagnetic Actuation", Proceedings of the 10th European Conference on Solide-State Transducers, Eurosensor X, Leuven, Belgium, September 1996, pp. 1193-1196.

[3.16] ASULAB SA. and CSEM SA., "A new Reed Microcontactor Fabricated by Multilevel UV-Lithography and Electrodeposition", M^2S^2 Intermediate report, 1994.

[3.17] W. P. Taylor and M. G. Allen, "Integrated Magnetic Microrelays: Normally Open, Normally Closed, and Multi-Pole Devices", Digest of Technical Papers of the 9th International Conference on Solide-State Sensors and Actuators, Transducers '97, Chicago, IL, June 1997, pp. 1149-1152.

[3.18] J. Simon, S. Saffer and C.-J. Kim, "A Micromechanical Relay with a Thermally-Driven Mercury Micro-Drop", Proceedings of the 9th IEEE Workshop on Micro Electro Mechanical Systems, MEMS '96, San Diego, CA, February 1996, pp. 515-520.

[3.19] M. Ashauer, A. Czarnowske, K. Hiltmann, W. Lang and H. Sandmaier, "Silicon Thermal Micro Relays with Multiple Switching States", Proceedings of the 10th European Conference on Solide-State Transducers, Eurosensor X, Leuven, Belgium, September 1996, pp. 1189-1192.

[3.20] T. Seki, M. Sakata, T. Nakajiama and M. Matsumoto, "Thermal Buckling Actuator For Microrelays", Digest of Technical Papers of the 9th International Conference on Solide-State Sensors and Actuators, Transducers '97, Chicago, IL, June 1997, pp. 1153-1156.

[3.21] H. V. Allen, "Silicon Based Micromechanical Switches for Industrial Applications", Proceedings of the IEEE Micro Robots and Teleoperators Workshop, Hyannis, MA, November 1987.

[3.22] K. E. Petersen, A. Sharteland N. F. Raley, "Micromechanical Accelerometers Integrated with MOS Detection Circuitry", IEEE Transactions on Electron Devices, Vol. 29-1 (1982), pp. 23-27.

[3.23] J. Fricke and E. Obermeier, "Cantilever Beam Accelerometer based on Surface Micromachining Technology", Journal of Micromechanics and Microengineering, 3 (1993), pp. 190-192.

[3.24] K. M. Hiltmann, B. Schmidt, H. Sandamaier and W. Lang, "Development of Micromachined Switches with Increased Reliability", Digest of Technical Papers of the 9th International Conference on Solide-State Sensors and Actuators, Transducers '97, Chicago, IL, June 1997, pp. 1157-1160.

[3.25] H. Hosaka and H. Kuwano, "Design and Fabrication of Miniature Relay Matrix and Investigation of Electromechanical Interference in Multi-Actuator Systems", Proceedings of the 7th IEEE Workshop on Micro Electro Mechanical Systems, MEMS '94, Oiso, Japan, January 1994, pp. 313-318.

[3.26] C. Linder, "Electromechanical Polysilicon Structures and Micromachining Processes for Sensor and Actuator Applications", Ph.D. Thesis, Institute of Microtechnology, University of Neuchâtel, Switzerland, 1993.

[3.27] V.P. Jaecklin, "Surface Micromachined Electrostatic Actuators", Ph.D. Thesis, Institute of Microtechnology, University of Neuchâtel, Switzerland, 1994.

[3.28] C. Linder, L. Paratte, M.-A. Grétillat, V. P. Jaecklin and N. F. de Rooij, "Surface micromachining", Journal of Micromechanics and Microengineering, Vol. 2 (1992), pp. 122-132.

[3.29] M.-A. Grétillat, "Réalisation de structures résonnantes-Méthodes d'excitation et de détection", MSc Thesis, Institute of Microtechnology, University of Neuchâtel, 1991.

[3.30] C. Linder; M.-A. Grétillat and N.F. de Rooij, "Realization of different polysilicon resonators with integrated excitation and detection elements", Microelectronic Engineering, 15 (1991), pp. 411-414.

[3.31] M.-A. Grétillat, C. Linder and N.F. de Rooij, "Multilayer polysilicon resonators including shielding for excitation and detection", Digest of Technical Papers of the 7th International Conference on Solide-State Sensors and Actuators, Transducers '93, Yokohama, Japan, June 1993, pp. 292-295.

[3.32] M.-A. Grétillat, C. Linder and N.F. de Rooij, "Integrated Shielding Lines on Multilayer Polysilicon Resonators", Sensors & Actuators, A43 (1994), pp. 351-356.

[3.33] C. Linder and N. F. de Rooij, "Investigation on Free-standing Polysilicon Beams in View of their Applications as Transducer's", Sensors & Actuators, A21-A23 (1990), pp. 1053-1059.

[3.34] H.-H. van den Vlekkert and N. F. de Rooij, "Design, fabrication and characterization of PH-sensitive ISFETs", Analusis, Vol. 16-2 (1988), pp. 110-119.

[3.35] C. Marxer, M.-A. Grétillat, R. Baettig, O. Anthamatten, B. Valk, P. Vogel and N. F. de Rooij, "Reliability Considerations for Electrostatic Polysilicon Actuators using as an Example the REMO-Component", Proceedings of the 10th European Conference on Solide-State Transducers, Eurosensor X, Leuven, Belgium, September 1996, pp. 1117-1121.

[3.36] C. Marxer, M.A Grétillat and N. F. de Rooij, "Breakdown Mechanisms of Electrostatic Polysilicon Actuators using as an Exemple the REMO Component", Digest of IEEE/LEOS 1996, Summer Topical Meeting, Optical MEMS and their Applications, Keystone, CO, August 1996, pp. 15-16.

[3.37] P.-E. Allen and D.-R. Holberg, "CMOS Analog Circuit Design", Holt, Rinehart and Winston, Inc., New York, 1987.

[3.38] J. D. Scherrer, "Mise en oeuvre d'une technologie CMOS dans la ligne de fabrication de capteurs de l'IMT", Diploma Work, Institute of Microtechnology, University of Neuchâtel, March 1994.

[3.39] T. Akiyama, N. Blanc and N. F. de Rooij, "A Force Sensor using a CMOS Inverter in view of its Application in Scanning Force Microscopy", Proceedings of the 9th IEEE Workshop on Micro Electro Mechanical Systems, MEMS '96, San Diego, CA, February 1996, pp. 447-450

[3.40] P. Zavracky, S. Majumder and N. E. McGruer, "Micromechanical Switches Fabricated Using Nickel Surface Micromachining", Journal of Microelectromechanical Systems, Vol. 6-1 (1997), pp. 3-9.

[3.41] S. Majumder, N. E. Mc Gruer, P. M. Svaracky, G. G. Adams, R. H. Morrison and J. Krim, "Measurement and Modeling of Surface Micromachined, Electrostatically Actuated Microswitches", Digest of Technical Papers of the 9th International Conference on Solide-State Sensors and Actuators, Transducers '97, Chicago, IL, June 1997, pp. 1145-1148.

[3.42] S. Hannoe and H. Hosaka, "Characteristics of Electrical Contacts used for Microrelays-Developpment of Measurement apparatus and Resistance Measurement of Ultra Low Force Contacts", Proceedings of the International Symposium on Microsystems, Intelligent Materials and Robots, Sendai, Japan, September 1995, pp. 173-176.

[3.43] J. Schimkat, H.-J. Gevatter and L. Kieswetter, "Gold-Nickel als Kontaktwerkstoff für ein Silizium-Mikrorelais", Feinwerktechnik & Messtechnik, 104/7-8 (1996), pp. 515-518.

4. Characterization and modeling of a non linear actuator

4.1 Introduction:

This Chapter describes simulation performed at the Massachusetts Institute of Technology (MIT), in the group of Professor Stephen Senturia to whom I am grateful for giving me the opportunity to be a visiting scientist in his laboratory over three months during the Summer 1996. The measurements described here have been made with the microrelays presented in Chapter 3. They have been performed at the Institute of Microtechnology (IMT)

The simulation of the nonlinear electromechanical behavior of an electrostatically actuated microbeam, fabricated as the moving part of the polysilicon microrelay will be reported. The electrical performance of the relay has been presented in Chapter 3 as well as in [4.1, 4.2]. This Chapter emphasizes a comparison between the basic measured properties (the pull-in voltage, the resonance frequency, the quality factor, the switching speed and the electrostatic spring softening). It presents simulations obtained with the corresponding quasi-static and dynamic models. The combination of different simulation tools (MEMCAD [4.3], Abaqus™ and MIT's macro-models [4.4, 4.5, 4.6, 4.7]) offer good insights into the behavior of the polysilicon microrelay, including the squeeze-film effects due to the air under the beam [4.8, 4.9, 4.10, 4.11, 4.12].

This work was presented at Transducers '97 in Chicago in two different papers. One paper discusses the details of the squeeze film damping simulation using macro-models [4.7] while the other presents the behavior of the nonlinear actuator [4.13].

4.2 Mechanical device:

As explained in Chapter 3, the mechanical part of the microrelay consists of a polysilicon/ silicon-nitride/ polysilicon microbridge realized by sacrificial-layer technology. Figure 4.1 shows a schematic cross section of the microrelay. The actuation circuit is formed between the polysilicon layer of the microbridge (3^{rd} polysilicon electrode) and the n-doped region in the substrate (counter electrode). The working circuit consists of two polysilicon layers: the first one is on the substrate (1^{st} polysilicon) and the second one is under the beam (2^{nd} polysilicon). Figure 4.2 shows a SEM of a 350 µm long microrelay. More details about the realization and first characterization of these microrelays are given in Chapter 3 and in [4.1, 4.2].

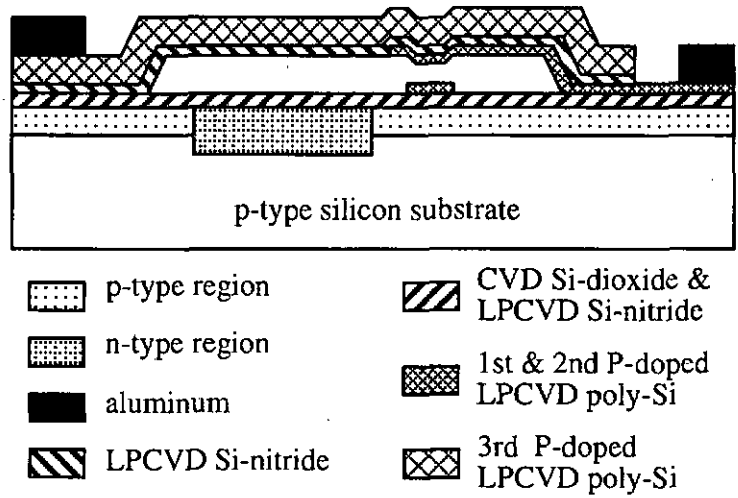

Figure 4.1:Cross section of the polysilicon microrelay with the working circuit on the right side and the actuation port on the left side.

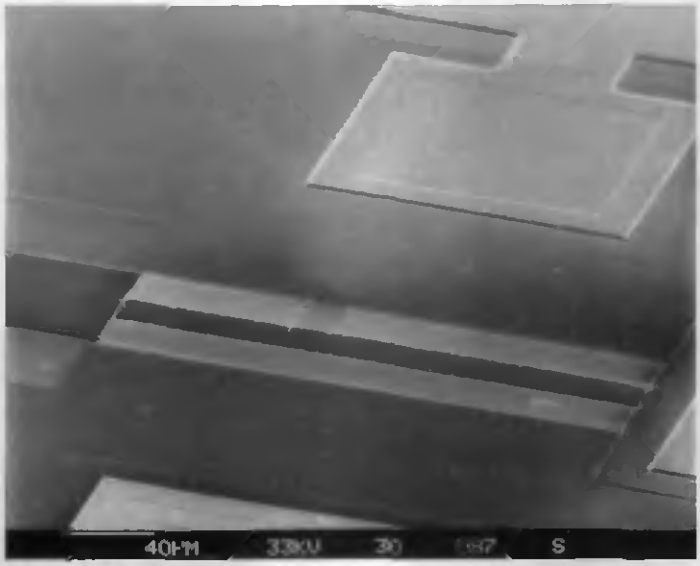

Figure 4.2: SEM of a 350 μm long microrelay.

4.3 Quasi static modeling:

4.3.1 What is MEMCAD:

MEMCAD is a software system for quasi-static analysis of coupled electromechanical devices. A Schematic view of the different modules which compose MEMCAD is given in Figure 4.3.

Every Finite Element Modeling (FEM) program requires the user to enter the structure in the software. Many of them discourage people due to their user interface which is very hard to learn. For MEMCAD the procedure is slightly different. The user starts the simulation by editing a fabrication process in a process editor. The different layers used in the technology are given by their thickness and the shape of the step covering.

A masks set is used to define the areas where the layers are etched or not as in the real process. These masks can be designed with a process editor included in MEMCAD or by importing CIF format files from an other Computer Aided Design (CAD) tool.

The next operations are realized with a commercially available product (Ideas™). The Membuilder module reads the data which have been introduced

in the process editor and builds the model. At this point a particularly important task has to be done: the mesh of the model. This work takes a certain time, because the mesh needs to be optimized. A too fine mesh will slow down the computation time and thus penalize the model. A too rough mesh can be far away from the physical reality and thus will give wrong results. A solution to control the quality of the mesh is to use the Finite Element Modeling (FEM) software (in MEMCAD it is Abaqus™) and to follow the evolution of the resonance frequency. The resonance frequency is calculated for a particular mesh and for another one where the number of elements is divided by two. If both resonance frequencies match together, either mesh can be used. In case the mismatch is too big, a finer mesh has to be investigated and tested with the same method. Only the mechanical part of the device and the electrodes in the substrate are meshed.

The inter-electrode capacitance is calculated with Fastcap. This module finds the charge distribution to match the applied potentials. At this point of the modeling it is also important to use different meshes to look if the aspect ratio of the panels doesn't generate numerical errors.

The coupled electro-mechanical simulation at this point is controlled by CoSolve. This module evaluates the convergence of the solution. While it considers it has not yet converged with a certain accuracy, it continues to switch between Fastcap, which calculates the charges and the corresponding forces, and Abaqus™, which calculates the mechanical solution.

MEMCAD allows evaluation of several points for a defined variable. For example the applied voltage between the microbridge and the substrate electrode can be varied. Thus it is possible to get a quasi-static modeling of the pull-in voltage of the microelectromechanical device. Moreover it allows changes in the size of the device by enlarging the element size providing results for different sizes of devices, without having to mesh it again.

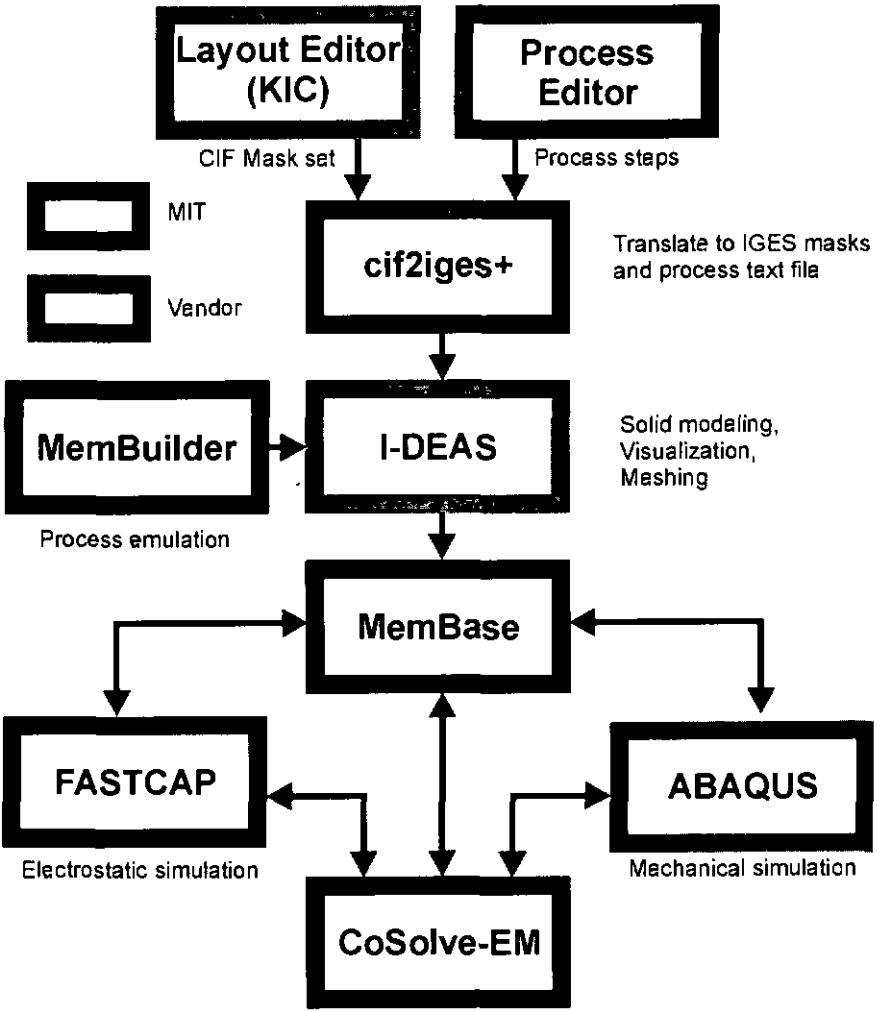

Figure 4.3: Schematic of the different modules of MEMCAD 2.0 [4.14, 4.15]; note that a new version of MEMCAD is now available [4.16]

4.3.2 Pull-in voltage simulation:

The pull-in voltage is measured with a reverse bias on the p-n junction, and a steady bias between the polysilicon beam and the p^+ substrate (-33V for the 300 μm and -27 V for the 350 μm long relays). In the presence of this bias, the potential on the counter electrode (n-doped region) is increased until the device pulls in. The result is 48.7 V for a 300 μm long relay and 42.8 V for a 350 μm relay (Figure 4.4).

Simulation of the pull-in voltage has been done by building a model (Figure 4.5) with MIT's MEMCAD system [4.3]. Because of the p-n junction bias and because the polysilicon of the working circuit under the beam is at the same potential as the substrate and hence screens the field of the upper polysilicon electrode in that region, pull-in was modeled with different potentials in the different regions of the structure.

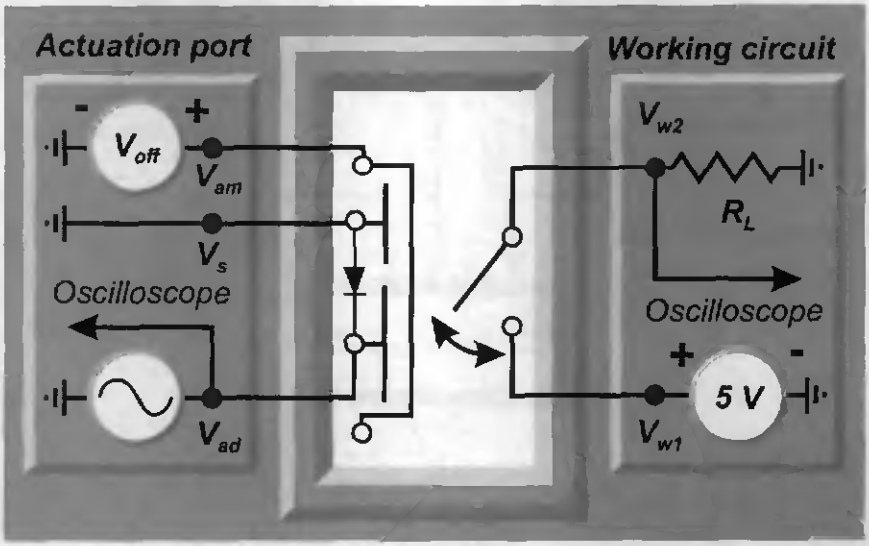

Figure 4.4: Schematic of the electrical circuit used for the pull-in measurements.

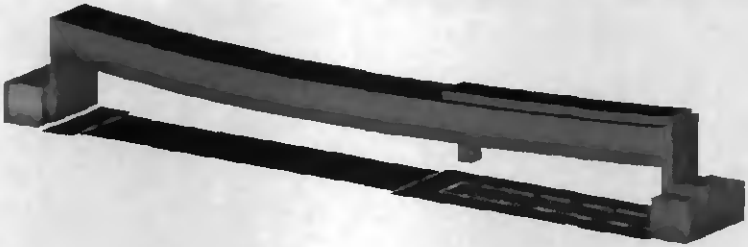

Figure 4.5: View of the model realized with MEMCAD for a 350 μm long microrelay with 36 V applied to the counter electrode. Note the different parts under the beam which correspond to the driving electrode in the substrate and the 2nd polysilicon under the beam. Vertical scale was enlarged 20 time on the visualizer to get a better readout of the view.

An equivalent Young's modulus (E) of 200 GPa was used to simulate the multilayer beam. A volume average of the different materials [4.17] was used to estimate this equivalent Young's modulus from values for the nitride (330 GPa [4. 18, 4. 19]) and polysilicon (170 GPa [4.20]). For the beam ends, both stepped-up and fully clamped boundary conditions (BCs) were investigated. Figure 4.6 shows the importance of such investigation in the modeling of free standing beams for the case of a residual stress σ_r=130 MPa. The effect of the boundary conditions is more than 10 % on the pull-in voltage.

Thus it has been decided to use the stepped-up support. The residual stress value was adjusted to 145 Mpa to match the pull-in voltage of a 300 μm long device, giving an error of 4.9% for the resonance frequency. Figure 4.7 shows the simulated displacement of two microrelays of different lengths for different applied voltages. These curves are given by MEMCAD, which also gives the shape of the microrelay for each applied voltage (Figure 4.8). The simulated pull-in voltages are 48.5 V for the 300 μm relays and 41 V for the 350 μm relays which agree with experiment within 4.5%. A summary of these simulation results is given in Table 4-1.

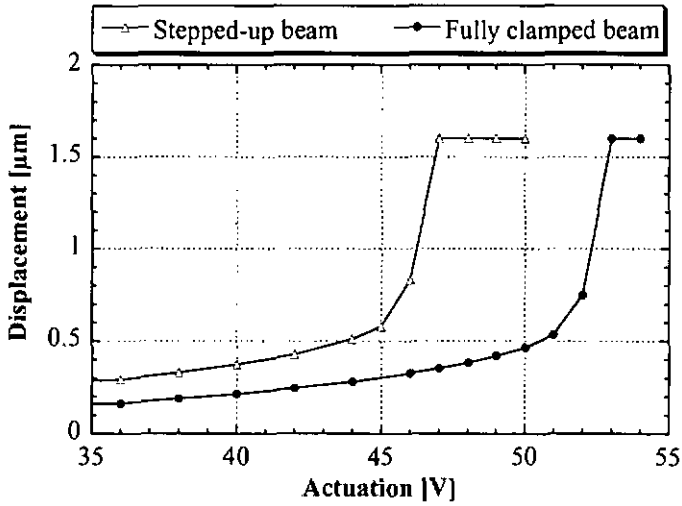

Figure 4.6: Comparison of the effect of the boundary conditions on the pull-in voltage (E = 200 GPa and σ_r = 130 MPa)

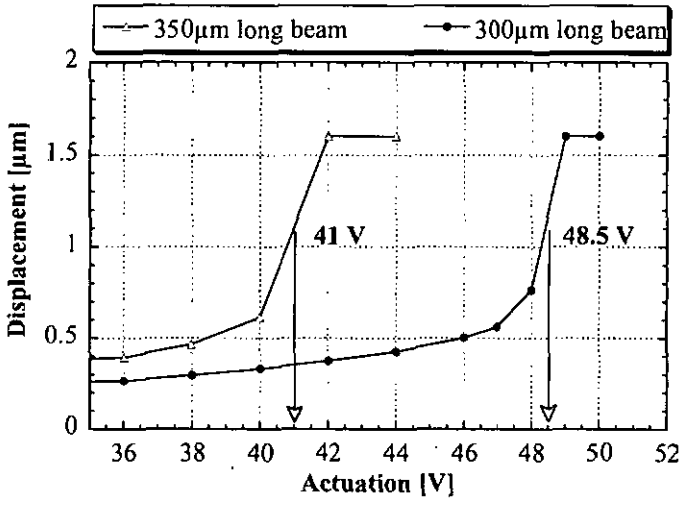

Figure 4.7: Simulation of the pull-in voltage. The values are close to the measured values of 48.7 V for the 300 µm long relay and 42.8 V for the 350 µm long relay (E = 200 GPa and σ_r = 145 MPa).

Using the same mechanical properties as in the pull-in voltage simulation, a modal analysis was performed with Abaqus™ to get the resonance frequencies as well as the shapes of the five first modes. An error smaller than 5% has been obtained for the first resonance frequency. The five first modes are shown in Figure 4.9.

This pull-in voltage simulation shows that the measurement of this value allows to get an approximately consistent set of constitutive material properties of the multilayer electromechanical device [4.21, 4.22, 4.23]. Nevertheless, some details like the boundary conditions of the supports as well as the geometry of the devices must be considered with a particular attention.

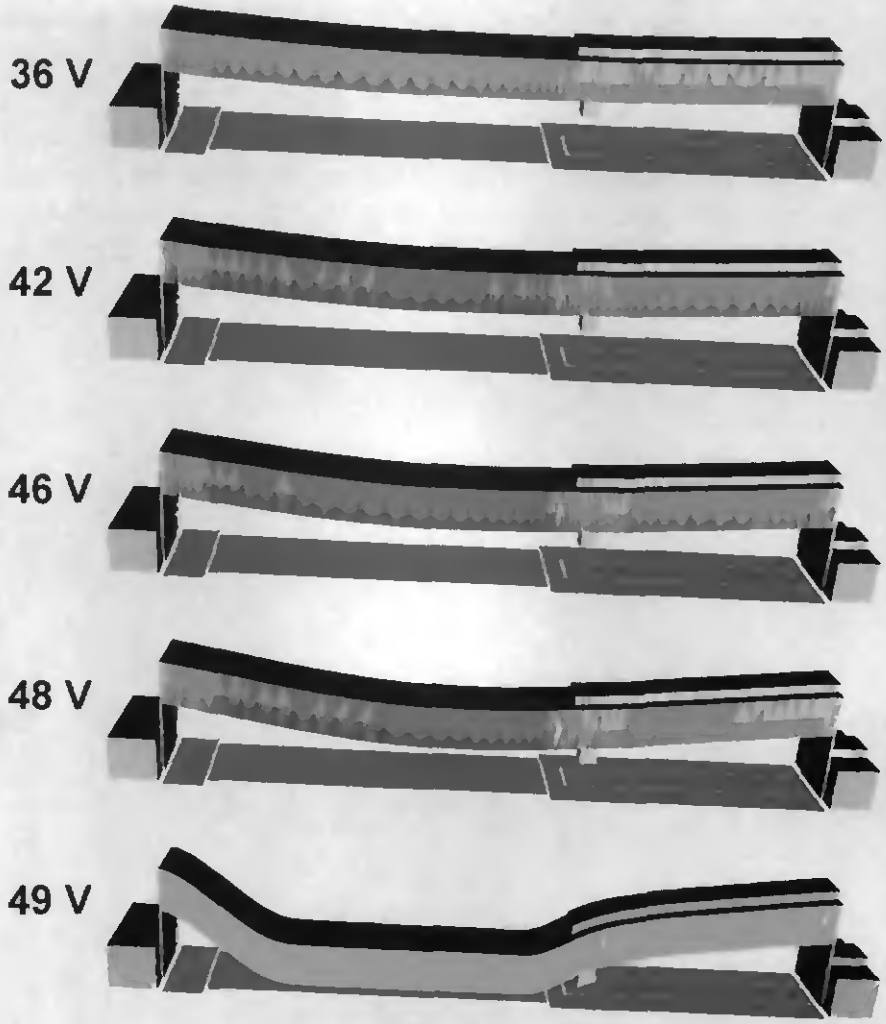

Figure 4.8: MEMCAD plots of five applied voltages for a 300 μm long relay. This kind of simulation allows the pull-in voltage of the device, here a multilayer polysilicon/nitride/polysilicon microrelay to be obtained. Vertical scale was enlarged 20 time on the visualizer to get a better reodout of the view.

Table 4-1: Summary of the simulation results

	Pull-in		Resonance frequency	
Length	300 µm	350 µm	300 µm	350 µm
Measured	48.7 V	42.8 V	360 kHz	316 kHz
Simulated	48.5 V	41.0 V	378.5 kHz	320.6 kHz
Errors	<1%	<4.5%	4.9 %	1.4 %

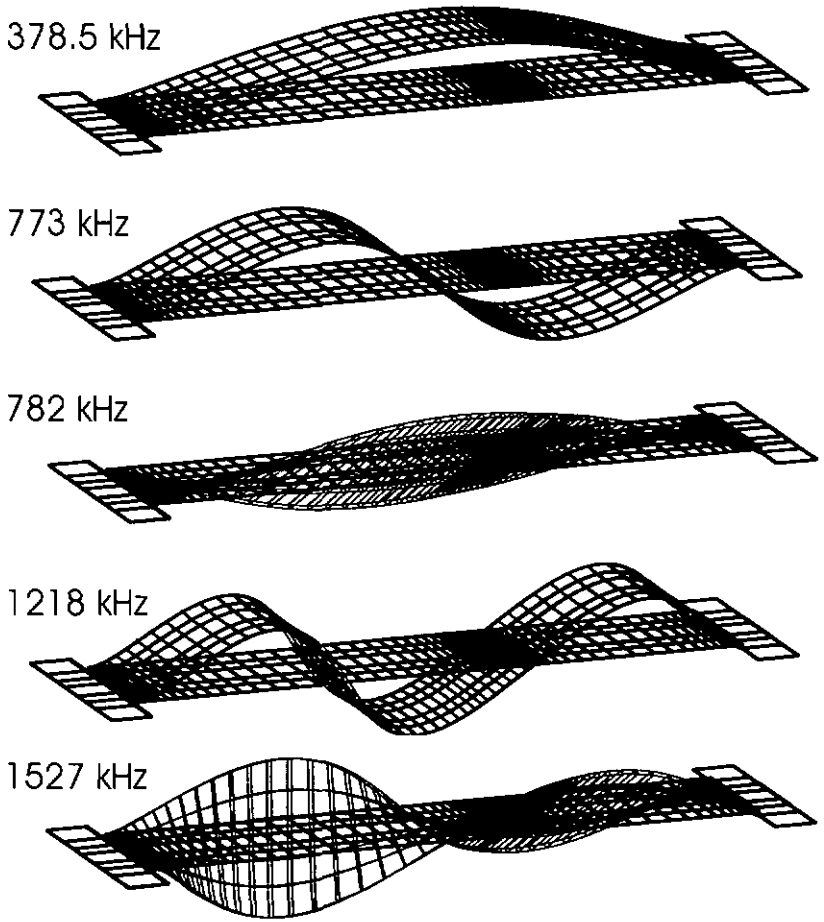

Figure 4.9: Abaqus™ plots of the five first modes with their frequency. This kind of simulation is very useful to realize a dynamic macro model [4.6, 4.7].

4.4 Dynamic modeling:

The dynamic behavior of these devices has also been simulated, but because of various approximations, the dynamic models are less accurate than the quasi-static models used for the pull-in and resonance frequency. Two different models have been investigated [4.4, 4.5]. They differ only in the numerical treatment of the beam mechanics. Both include squeeze-film air damping by solving the Reynolds (4.1) equation using finite difference methods.

The Reynolds equation is given by:

$$\frac{\partial(hP_D)}{\partial t} = \frac{\nabla(P_D h^3 \nabla P_D)}{12\mu} \tag{4.1}$$

Where

- h is the gap between the beam and the substrate
- P_D is the pressure due to the damping
- t is the time
- μ is the air viscosity: 1.82 ×·10-5 kg/(m·s)

4.4.1 Macro-model based on modal analysis [4.6]:

The first simulation for the pull-in time uses a modal analysis which includes the step boundary conditions but not the stress-stiffening in large deflection [4.6].

The modal analysis start from the Newton equation:

$$[M]\{\ddot{x}\} + [K]\{x\} = F_D(\{x\},\{\ddot{x}\}) + F_E(\{x\}) \tag{4.2}$$

Where

- [M] is the matrix of the mass for each coordinate
- [K] is the spring constant matrix
- $\{x\}$ is the position vector and $\{\ddot{x}\}$ the acceleration vector
- F_D is the term for the damping forces and
- F_E for the electrical forces.

By changing from the normal $\{x\}$ to the modal $\{q\}$ coordinates:

$$\{x\} = [S]\{q\} \tag{4.3}$$

(4.2) becomes (4.4):

$$[M][S]\{\ddot{q}\}+[K][S]\{q\}=F_D([S]\{q\},[S]\{\ddot{q}\})+F_E([S]\{q\}) \quad (4.4)$$

Where [S] is a matrix whose columns are mode shape vectors.

By applying $[S]^T$ to the whole equation we get:

$$[S]^T[M][S]\{\ddot{q}\}+[S]^T[K][S]\{q\}=[S]^T(F_D([S]\{q\},[S]\{\ddot{q}\})+F_E([S]\{q\})) \quad (4.5)$$

This results in a system of equations that is completely uncoupled on the left hand side of the equation because $[S]^T[M][S]$ and $[S]^T[K][S]$ are diagonal matrixes.

Thus this equation becomes:

$$\boxed{[M_G]\{\ddot{q}\}+[K_G]\{q\}=[S]^T(F_D([S]\{q\},[S]\{\ddot{q}\})+F_E([S]\{q\}))} \quad (4.6)$$

Where $[M_G]$ and $[K_G]$ are generalized matrixes for mass and stiffness with the eigenvalues in the diagonal.

4.4.1.1 Approximations used in the model based on modal analysis:

1) Under the assumption that the higher modes have negligible effect on the system, the first three mode shapes were derived from Abaqus™ modal analysis with residual stress and the stepped-up beam ends.
2) Electrostatic force is given by the parallel-plate approximation.
3) Finite difference for Reynold's Equation (26 × 11 nodes) with slip flow model which is the same as the model used for small amplitude oscillation simulation [4.7]
4) No stress-stiffening effect.
5) The stiffness was choosen for the model parametric adjustment.

4.4.2 Macro-model based on the Euler wide beam [4.5]:

The second model solves the two-dimensional (2D) finite-difference equation of motion for a uniformly-flat Euler wide-beam (4.7) with stress stiffening, but with fully clamped beam ends [4.5].

$$\frac{Et'^3}{(1-\upsilon^2)12}\nabla^4 h + \sigma_s(h)\nabla^2 h = P_E(h) + P_D(h,\dot{h}) - \rho_s \frac{\partial^2 h}{\partial t^2} \quad (4.7)$$

Where

- E is the Young's modulus and ν is the Poisson's ratio (ν=0.3).
- t′ is the beam thickness.
- h is the gap between the beam and the substrate.
- $\sigma_s(h)/t'$ is the gap dependent stress.
- P_E is approximated by the nonlinear electrostatic pressure due to a parallel-plate.
- P_D is the pressure due to the damping.
- t is the time.
- ρ_s/t' is the density of the beam: 2300 kg/m^3.

4.4.2.1 Approximations used in the Euler wide beam madel:

1) The beam has been discretized into 2D grid (50 × 50 nodes)
2) Electrostatic force is the parallel-plate approximation.
3) Damping pressure from compressible Reynold's Equation (no slip flow)
4) $\sigma_s(h)/t'$ includes the stress-stiffening effect and residual stress for h equal to the nominal gap between the beam and the substrate.
5) The residual stress has been chosen as the parametric adjustment.

4.4.3 Pull-in time simulation:

As described in Section 3.5.4, it has been necessary to perform improved measurement with devices packaged on TO sockets to get useful data for the pull-in time simulation. These data are given in Figure 4.10. Compare to previous operate time presented in Section 3.5.6, the cross talk between actuation and working circuit was considerably reduced. On this Figure, an arrow shows how the pull-in time was measured. It is measured from when power is applied to the driving port until the output voltage start to increase. Thus it is not exactly the same as the operate time which would be measured from when power is applied to the driving port until the contact is settled.

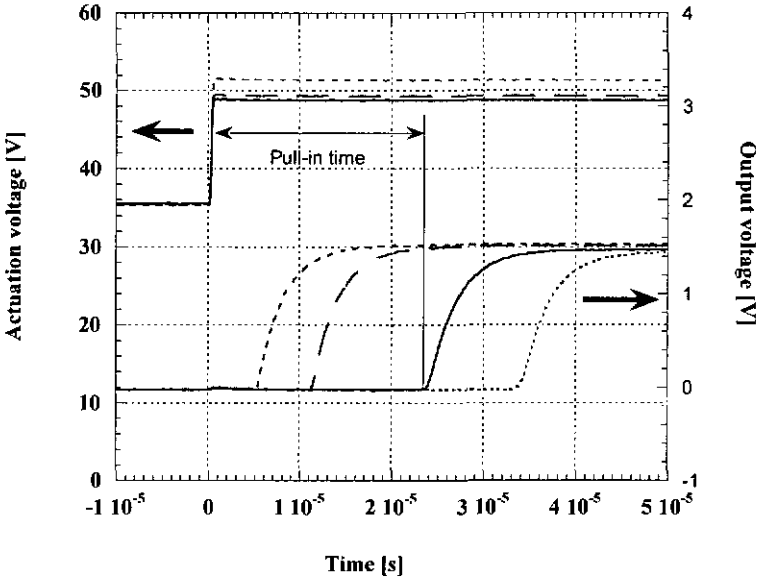

Figure 4.10: Data for the switching time versus voltage characterization (300 μm long microrelay). The actuation voltage is the voltage between the driving electrode in the substrate and the polysilicon microrelay. The resistance load was 10 kΩ

Both models (cf. § 4.4.1 and § 4.4.2) required parametric adjustment to fit the pull-in voltage. The stiffness was selected for the first model adjustment, while the residual stress was selected for the second one. Figure 4.11 shows the experimental switching time versus actuation voltage for a 300 µm long relay, together with several simulations. Once the pull-in voltage is matched by adjusting respectively the stiffness or the residual stress, the curves fit the measured variation of pull-in time with voltage very well. It should be emphasized that the residual stress and the stiffness adjustment used here is to provide compensation for the unmodeled effects in the two models, and does not mean that the physical values have changed from the previous values.

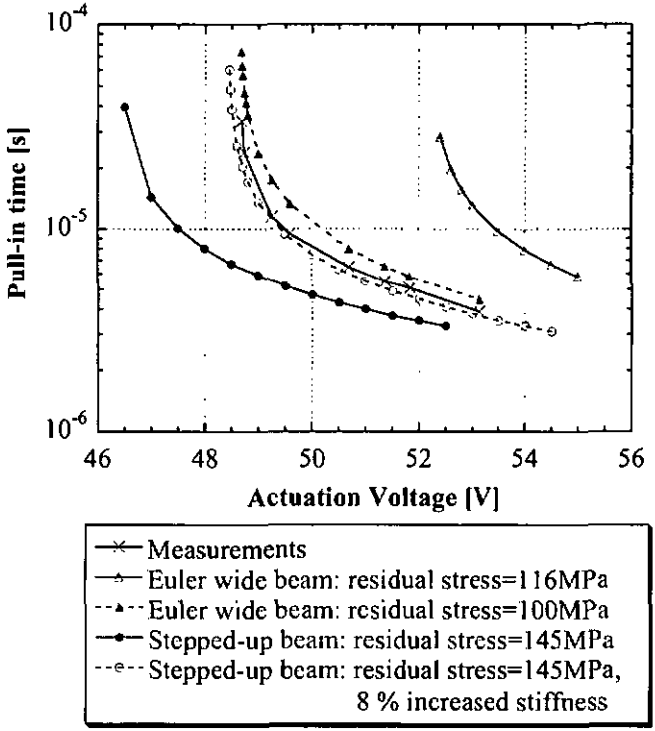

Figure 4.11: Switching time versus voltage for a 300 µm long microrelay. Two different models have been used to simulate the behavior of this device. The residual stress has been adjusted to match the pull-in voltage as explained in the text.

4.4.4 Quality factor modeling:

The quality factor and the frequency shift have been extracted from the transfer function of the microrelay for different ambient pressures. This measurement has been realized with a laser interferometer in a vacuum chamber. The pressure has been measured with a Pirani gauge. The quality factor is defined as:

$$Q = \frac{f_0}{\Delta f_{-3dB}} \tag{4.8}$$

Where

- f_0 is the value of the resonance frequency.
- Δf_{-3dB} is the bandwidth measure at -3 dB from the maximum of the curve.

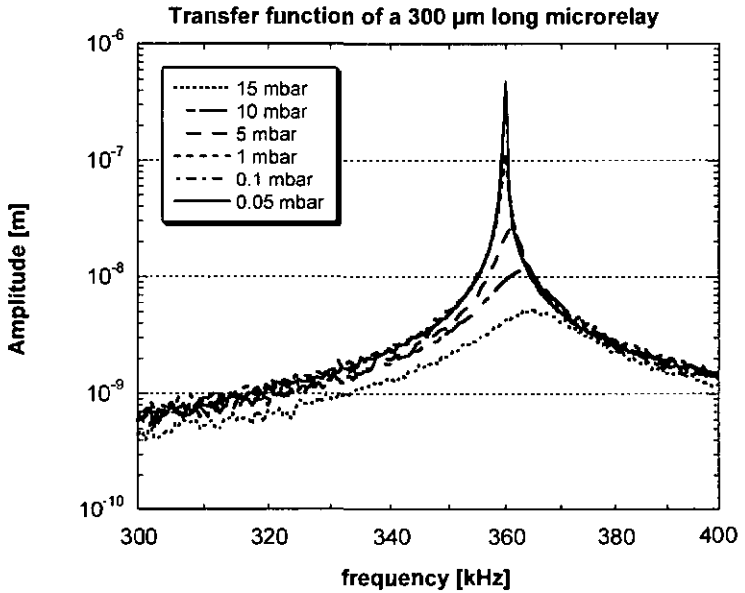

Figure 4.12: Optically measured transfer function of a 300 µm long microrelay. These measurements have allowed extraction of the resonance frequency shift and the quality factor versus the ambient pressure.

The simulation of these measurements has been performed with the macro model approach based on modal analysis which is described in § 4.4.1. Thus it has been possible to simulate the effect of air pressure on the resonance frequency and the quality factor. These simulations have been presented in detail in [4.7]. Figure 4.13 shows the measured and simulated data for a 300 µm long microrelay. Such simulation has also been realized for a 350 µm long microrelay (Figure 4.14). By using the material properties used in the pull-in and resonance frequency modeling presented in § 4.3.2 an error within about 5% has been obtained. In order to demonstrate the perturbation of the resonance by the air damping spring force, the modal stiffness in the simulation was arbitrarily reduced slightly so that the low pressure resonance frequency agreed with the experiment value.

This simulation has pointed out the possibility to get a model for relatively complex systems where the external forces are dependent on the position of the mechanical structure.

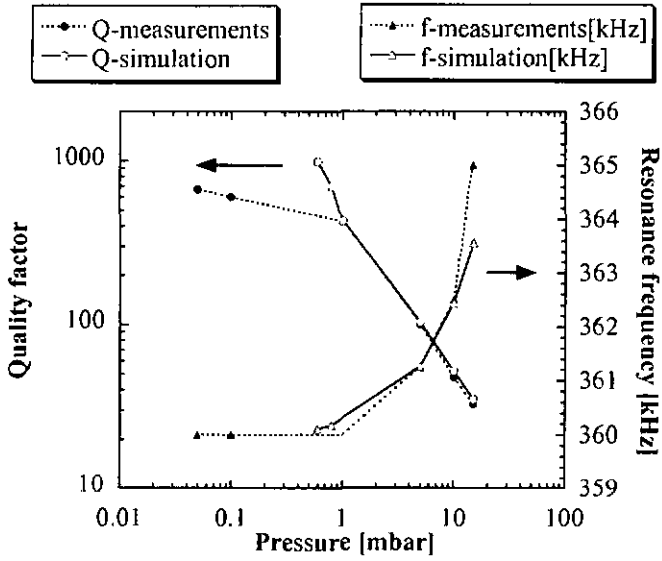

Figure 4.13: Small amplitude simulation of the effect of air damping for a 300 µm long microrelay [4.7] Because no intrinsic mechanical damping was included in the modeling, the quality factor measurements and the simulation diverge for pressures less than 1 mbar.

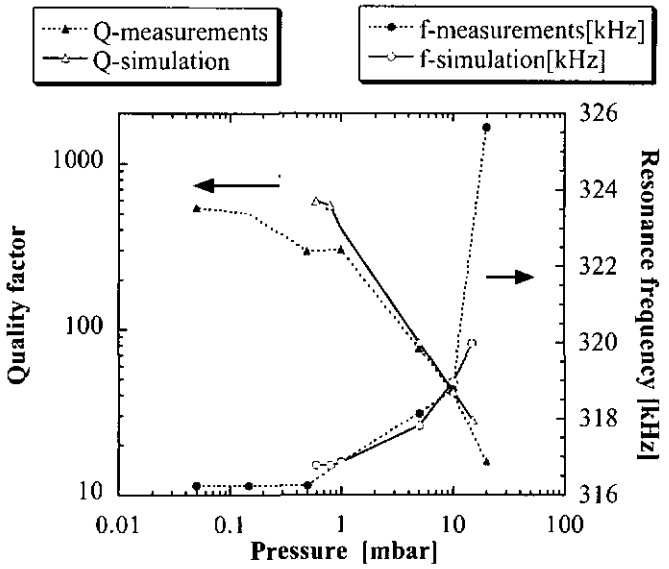

Figure 4.14: Small amplitude simulation of the effect of air damping for a 350 μm long microrelay [4.7] Because no intrinsic mechanical damping was included in the modeling, the quality factor measurements and the simulation diverge for pressures less than 1 mbar.

4.4.5 Spring softening effect:

The model presented in § 4.4.4 also includes the spring softening effect. This effect occurs when an external nonlinear force is applied to a resonator. The external force modifies the spring constant of the whole system and thus a change of the resonance frequency is visible. In our case the nonlinear force is due to the applied voltage between the relay and the substrate. When this voltage is increased, the resonance frequency decreases and would be zero at the pull-in voltage of the microrelay beam. This small paragraph is here to show this effect separately from the squeeze film damping. The spring softening effect shown in Figure 4.15 is given for a 300 µm long microrelay. A change of about 2% has been observed for 15V applied to the beam [4.24].

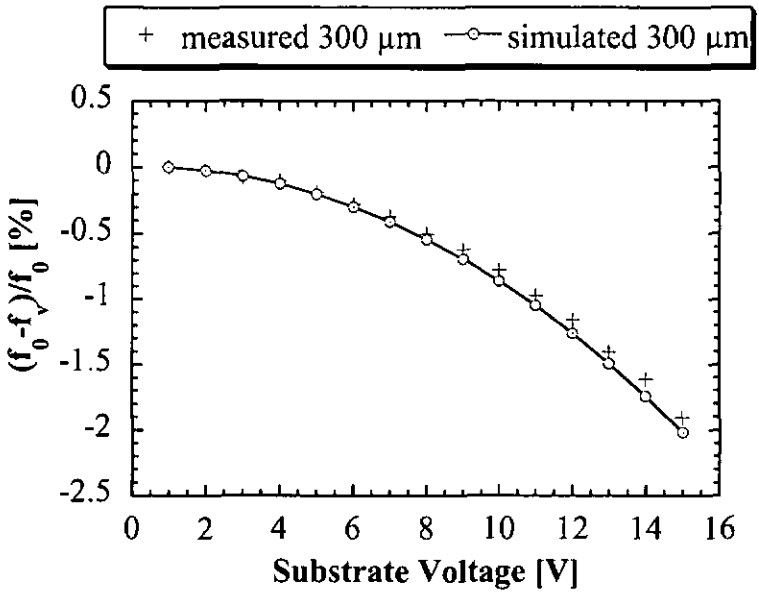

Figure 4.15: Spring softening effect: measurements and simulation for the 300 µm long microrelay.

4.5 Conclusions:

Thanks to Professor Stephen Senturia who invited me in his laboratory and to Professor Nico de Rooij who let me go to Boston for three months, I was able to simulate these polysilicon electrostatic microrelays.

Thanks to this stay, full modeling of the nonlinear dynamic behavior of an electrostatic microrelay has been demonstrated. The pull-in voltage, the switching time, the resonance frequency and the quality factor of such compliant structures have been simulated. Squeeze-film damping has been included for the dynamic simulations. This modeling illustrates the potential for predicting the behavior of such micro electromechanical systems with good accuracy.

Some particularly interesting aspects of such modeling have to be emphasized. The first one is the potential of the simulation to find an equivalent set of mechanical properties for these multilayer microrelays. The second one is the possibility to simulate the dynamics of a nonlinear device with a good accuracy (less than 5% error). The latter allows to get a good insight in the external forces applied on the device, which can be produced by the damping and the squeeze film damping due to the air under the beam [4.7].

Such modeling approach has to be developed in the sensors, actuators and microsystems field to get smarter devices in a shorter time. It will also shorter the time to push new prototypes on the market, with better controlled specifications.

4.6 References

[4.1] M.-A. Grétillat, P. Thiébaud, N. F. de Rooij and C. Linder, "Electrostatic polysilicon microrelays integrated with MOSFETs", Proceedings of the 7th IEEE Workshop on Micro Electro Mechanical Systems, MEMS '94, Oiso, Japan, January 1994, pp. 97-101.

[4.2] M.-A. Grétillat, P. Thiébaud, C. Linder and N. F. de Rooij, "IC compatible electrostatic polysilicon microrelays", Journal of Micromechanics & Microengineering, 5 (1995), pp. 156-160.

[4.3] J. R. Gilbert, R. Legtenberg and S. D. Senturia, "3D Coupled Electro-mechanics for MEMS: Applications of CoSolve-EM", Proceedings of the 8th IEEE Workshop on Micro Electro Mechanical Systems, MEMS '95, Amsterdam, the Netherlands, January 1995, pp. 122-127.

[4.4] Y. J. Yang and S. D. Senturia, "Numerical Simulation of Compressible Squeezed-Film Damping", Technical Digest of IEEE Solid-State Sensor and Actuator Workshop, Hilton Head Island, SC, June 1996, pp. 76-79.

[4.5] R. K. Gupta, E. S. Hung, Y. J. Yang, G. K. Ananthasuresh and S. D. Senturia, "Pull-in Dynamics of Electrostatically-actuated Beams", Technical Digest of IEEE Solid-State Sensor and Actuator Workshop, Late news paper, Hilton Head Island, SC, June 1996, pp. 1-2.

[4.6] G. K. Ananthasuresh, R. K. Gupta and S. D. Senturia, "An Approach to Macromodeling of MEMS for Nonlinear Dynamic Simulation", Proceedings of the ASME International Mechanical Engineering Congress and Exposition, Symposium on MEMS, Atlanta, GA, November 1996, pp. 18-22.

[4.7] Y. J. Yang, M.-A. Grétillat and S. D. Senturia, "Effect of Air Damping on the Dynamics of Nonuniform Deformations of Microstructures", Digest of Technical Papers of the 9th International Conference on Solide-State Sensors and Actuators, Transducers '97, Chicago, IL, June 1997.

[4.8] W. W. Langlois, "Isothermal Squeeze Films", Quarterly of Applied Mathematics, Vol. 20-2 (1962), pp. 131-150.

[4.9] J. J. Blech, "On Isothermal Squeeze Films", Journal of Lubrification Technology, Vol. 105 (1983), pp. 615-620.

[4.10] M. Andrews, I. Harris and G. Turner, "A comparison of Squeeze-Film Theory with Measurements on a Microstructure", Sensors & Actuators, A36 (1993), pp. 79-87.

[4.11] M. K. Andrews, G. Turner, P. D. Harris and I. M. Harris, "A Resonant Pressure Sensor Based on a Squeezed Film of Gas", Sensors & Actuators, A36 (1993), pp. 219-226.

[4.12] T. Veijola, H. Kuisma, J. Lahdenperä and T. Ryhänen, "Equivalent-circuit Model of the Squeezed Gas Film in a Silicon Accelerometer", Sensors & Actuators, A48 (1995), pp. 239-248.

[4.13] M.-A. Grétillat, Y. J. Yang, E. S. Hung, V. Rabinovich, G. K. Anathasuresh, N. F. de Rooij and S. D. Senturia, "Nonlinear Electromechanical Behavior of an Electrostatic Microrelay", Digest of Technical Papers of the 9th International Conference on Solide-State Sensors and Actuators, Transducers '97, Chicago, IL, June 1997.

[4.14] S. D. Senturia, "CAD for Microelectromechanical Systems", Digest of Technical Papers of the 8th International Conference on Solide-State Sensors and Actuators, Transducers '95, Stockholm, Sweden, June 1995, vol. 2: pp. 5-8.

[4.15] P. M. Osterberg and S. D. Senturia, ""MemBuilder": An Automated 3D Solid Model Construction Program for Microelectromechanical Structures", Digest of Technical Papers of the 8th International Conference on Solide-State Sensors and Actuators, Transducers '95, Stockholm, Sweden, June 1995, vol. 2: pp. 21-24.

[4.16] MICROCOSM, Software solutions for MEMS design, 201 Willesden Drive, Cary, NC 27513, davec@memcad.com.

[4.17] O. Tabata, K. Kawahata, S. Sugiyama and I. Igarashi, "Mechanical Property Measurements of Thin Films Using Load-Deflection of Composite Rectangular Membranes", Sensors & Actuators, 20 (1989), pp. 135-141.

[4.18] D. Maier-Schneider, J. Maibach and E. Obermeier, "Computer-Aided Characteristization of Elastic Properties of Thin Films", Journal of Micromechanics & Microengineering, 2 (1992), pp. 173-175.

[4.19] E. Obermeier, "Material Property Data-A Key Issue for the Design of Microsystems", Proceedings of the International Symposium on Microsystems, Intelligent Materials and Robots, Sendai, Japan, September 1995, pp. 110-113.

[4.20] H. Guckel, D. W. Burns, H. A. C. Tilmans, D. W. de Roo and C. R. Rutigliano, "Mechanical Properties of Fine Grained Polysilicon The Repeatability Issue", Technical Digest of IEEE Solid-State Sensor and Actuator Workshop, Hilton Head Island, SC, June 1988, pp. 96-99.

[4.21] P. Osterberg, R. K. Gupta, J. R. Gilbert and S. D. Senturia, "Quantitative Models for the Measurement of Residual Stress, Poisson Ratio and Young's Modulus Using Electrostatic Pull-in of Beams and Diaphragms", Technical Digest of IEEE Solid-State Sensor and Actuator Workshop, Hilton Head Island, SC, June 1994, pp. 184-188.

[4.22] R. K. Gupta, P. Osterberg and S. D. Senturia, "Material Property Measurement of Micromechanical Polysilicon Beams", Proceedings of the SPIE 1996 Conference: Microlithography and Metrology in Micromachining II, Austin, TX, October 1996, pp. 39-45.

[4.23] P. M. Osterberg and S. D. Senturia, "M-Test: A Test Chip of MEMS Material Property Measurement using Electrostatic Actuated Test Structures", Journal of Microelectromechanical Systems, Vol. 6-N°2 (1997), pp. 107-118.

[4.24] H.A.C. Tilmans, "Micro-Mechanical Sensors using Encapsulated Built-in Resonant Strain Gauges", Ph.D. Thesis, University of Twente, The Netherlands, 1993.

5. Conclusion and outlook

5.1 Technology and microrelays:

This conclusion will emphasizes the work which was done from 1993 to 1997 during my Ph.D. Thesis, focusing on the realization, the characterization and the modeling of microrelays. A comparison of the main publications related to micromechanical microrelays is given in Table 5-1 and Table 5-2. Their main characteristics are compared with the IMT microrelays described in this Ph.D. Thesis.

Chapter 2 gives a summary of the surface micromachining technology which was used for the realization of these polysilicon based microrelays. It describes also some aspects of the packaging. The surface encapsulation and the glass micromachining are detailed. The example of the packaging of a silicon vibrating gyroscope illustrates the use of glass micromachining.

The increase of the number of laboratories working on microrelays can be seen on Table 5-1 and Table 5-2. The work of Petersen et al. [5.1] published in 1979 remains as the main reference of this field of activity. Nevertheless, the different approaches presented since that first contribution are interesting. Different points have to be highlighted. The electrostatic actuation is often too high to integrate these microrelays with standard electronics circuits available on the market. There is one contribution from Schimkat et al. [5.4] which obtains a relatively low pull-in voltage of 15 V. The configuration used in this paper (wedge actuator) is of interest but does not allow fast switching (maximum 35 Hz). The IMT contribution exhibits a switching voltage of 40 V to 55 V. The DC switching voltage could be reduced by applying a constant offset voltage on the microrelays but the latter remains in the 30 V to 40 V range. A trade-off has to be found which would keep relatively high restoring spring force with low switching voltage. As explained in section 3.5.11 a better design could improve this feature.

Table 5-1:Switching characteristic of some micromachined relays:

	[5.1]	[5.2]	[5.3]	[5.4]	[5.5]	[5.6]	**1MT**	*Units*
Year	'79	'89	'93	'94	'95	'96	**'94**	*Year*
Actuation principle	Es	Es	Em	Es	Es	Es	**Es**	
Pull-in voltage	60	100	3	15	35 - 150	50 - 100	**40 - 55**	*[V]*
Switching time	40µ	60µ	200µ	NA	NA	20µ	**3µ - 70µ**	*[s]*
Switching speed	10k	NA	1k	35	5k - 40k	NA	**100k**	*[Hz]*
Gap	5 - 7	10	NA	6 - 14	2	1 - 2	**1.6**	*[µm]*
Maximum lifetime of actuator	$1{\cdot}10^{10}$	NA	NA	$20{\cdot}10^{6}$	NA	$1{\cdot}10^{8}$	$\mathbf{1{\cdot}10^{9}}$	*Nb*
Lifetime of contact	$2{\cdot}10^{6}$	NA	NA	NA	NA	$1{\cdot}10^{8}$	$\mathbf{1{\cdot}10^{9}}$	*Nb*
Maximum current	1	0.1	0.1	NA	150m	100µ	**1m**	*[A]*
Contact Resistance	5	NA	2	NA	5-20	3	**20k**	*Ω*

NA: Non available
Em: Electromagnetic
k: kilo
µ: micro
Es: Electrostatic
Th: Thermal
m: milli

Table 5-2:Switching characteristic of some micromachined relays:

	[5.7]	[5.8]	[5.9]	[5.10]	[5.11]	IMT	*Units*
Year	'96	'97	'97	'97	'97	'94	*Year*
Actuation principle	Es	Es	Th+Es	Es	Em	Es	
Pull-in voltage	28	20 - 90	8mW* + 20	30 - 400	0.18 - 0.53	40 - 55	*[V]*
Switching time	30µ	2.6µ - 20µ	12µ	10µ - 10m	1m - 2.5m	3µ - 70µ	*[s]*
Switching speed	1k	2k	NA	150k	NA	100k	*[Hz]*
Gap	2	4 - 55	1.5	1.5	NA	1.6	*[µm]*
Maximum lifetime of actuator	$6 \cdot 10^{10}$	$1 \cdot 10^{6}$	NA	$1 \cdot 10^{9}$	$3 \cdot 10^{6}$	$1 \cdot 10^{9}$	*Nb*
Lifetime of contact	NA	7k	NA	$5 \cdot 10^{8}$	$3 \cdot 10^{6}$	$1 \cdot 10^{9}$	*Nb*
Maximum current	0.2	1m	NA	10m	1.2	1m	*[A]*
Contact Resistance	0.22	12 - 80	0.6 - 0.8	20	0.85 - 3	20k	*Ω*

NA: Non available
Em: Electromagnetic
k: kilo
µ: micro
Es: Electrostatic
Th: Thermal,
m: milli
*: Thermal power

For the electromagnetic actuation the driving voltage is smaller but the power consumption is still high. A power consumption of 33mW to 350mW was reported in [5.11], thus this solution is not the best for low power applications.

The switching time is relatively fast for all the relays mentioned here. It vary from 2.6 µs to 2.5 ms. For electromechanical, dry reed and mercury wetted devices it is in the 0.1 ms to 100 ms range [5.12]. This points out the interest of the miniaturization of mechanical relays. It is the same for the frequency which is also relatively high, the IMT relay being one of the fastest with 100 kHz switching frequency.

These miniature microrelays have the same problem as traditional ones in that their lifetime is limited by the contact wear. The miniaturization of these devices induces also a limited current capability. There will certainly be a trade-off between the size, the speed and the current capability of micromechanical relays.

The modeling presented in Chapter 4 was of great interest. It has allowed to understand some features of these microelectromechanical devices. It has been possible to simulate the microrelays pull-in voltage, pull-in time and resonance frequency with a good accuracy (less than 5 % error). The geometry of this microrelay was enough complex to be a good test for these emerging simulation tools which offer new possibilities in the development of MEMS.

As a final conclusion, I would say that this Ph.D. Thesis is complementary to the other contributions in the world. It has demonstrated the use of polysilicon layers for the mechanical part of such a device. Some interesting behavior could be measured and simulated such as the dependence of the switching time in function of the actuation voltage.

5.2 Outlook-future of MEMS:

I think that the future of microelectromechanical systems will be the integration and the combination of more and more sophisticated devices. Thus the modeling will take a big place in the development of these new devices which will have to fulfill certain requirements. This modeling will not only concern the design of the new devices but will also be a complement for the characterization of the technologies. I think that every laboratories and foundries working in this field of activity should create lists of the physical

properties of the layers they are able to deposit with the tolerances they can achieve. Thus people who are developing prototypes could design them by knowing theses specifications and could shorten the time necessary to the industrialization of the prototypes. This aspect is very important and will be the only way to realize accurate modeling of MEMS and thus to improve their behavior. This effort of processing steps qualification has been done for the IC technology, why not for MEMS technology? This approach should improve globally the quality of the devices as well as their reproducibility which is the only way to interest industrial partners to integrate MEMS in their products [5.13].

The silicon micromachining offers certain advantages like the precision of the layer patterning which allows a certain level of miniaturization. Nevertheless the product and its market have to be chosen properly. First the number of pieces has to be evaluated. This number is often in the 1000 to 10'000 and rarely in the 100'000 pieces per Year. Compare to the ICs it is relatively low and thus the price of each device will never be comparable to electron devices. Successful devices will be those which take advantages from the IC compatibility of the technology as well as from its precision. Thanks to the effort which is done in this field of activities since 35 Years, I hope more and more devices will pass from the prototype level to industrial products.

5.3 References:

[5.1] K. E. Petersen, "Micromechanical Membrane Switches on Silicon", IBM Journal of Research and Development, Vol. 23-4 (1979), pp. 376-385.

[5.2] M. Sakata, "An Electrostatic Microactuator For Electro-Mechanical Relay", Proceedings of the 2nd IEEE Workshop on Micro Electro Mechanical Systems, MEMS '89, Salt Lake City, UT, February 1989, pp. 149-151.

[5.3] H. Hosaka, H. Kuwano and K. Yanagisawa, "Electromagnetic Microrelays: Concept and Fundamental Characteristics", Proceedings of the 6th IEEE Workshop on Micro Electro Mechanical Systems, MEMS '93, Fort Lauderdale, FL, February 1993, pp. 12-17.

[5.4] J. Schimkat, L. Kieswetter, H.-J. Gevatter, F. Arndt, A. Steckenborn and H. F. Schlaak, "Moving Wedge Actuator: An Electrostatic Actuator for Use in a Microrelay", Proceedings of the 4th International Conference on Micro Electro, Opto, Mechanic Systems and Components, Micro System Technologies 94, Berlin, Germany, October 1994, pp. 989-996.

[5.5] S. Roy and M. Mehregany, "Fabrication of Electrostatic Nickel Microrelays by Nickel Surface Micromachining", Proceedings of the 8th IEEE Workshop on Micro Electro Mechanical Systems, MEMS '95, Amsterdam, the Netherlands, January 1995, pp. 353-357.

[5.6] J. Drake, H. Jerman, B. Lutze and M. Stuber, "An Electrostatically Actuated Microrelay", Digest of Technical Papers of the 8th International Conference on Solide-State Sensors and Actuators, Transducers '95, Stoekholm, Sweden, June 1995, vol.2: pp. 380-383.

[5.7] J. J. Yao and M. F. Chang, "A Surface Micromachined miniature Switch for Telecomunications Applications with Signal Frequencies from DC up to 4 GHz", Digest of Technical Papers of the 8th International Conference on Solide-State Sensors and Actuators, Transducers '95, Stockholm, Sweden, June 1995, vol.2: pp. 384-387.

[5.8] I. Schiele, J. Huber, C. Evers, B. Hillerich and F. Kozlowski, "Micromechanical Relay with Electrostatic Actuation", Digest of Technical Papers of the 9th International Conference on Solide-State Sensors and Actuators, Transducers '97, Chicago, IL, June 1997, pp. 1165-1168.

[5.9] S. Zhou, X. Sun and W. Carr, "A Micro Variable Inductor Chip Using MEMS Relays", Digest of Technical Papers of the 9th International Conference on Solide-State Sensors and Actuators, Transducers '97, Chicago, IL, June 1997, pp. 1137-1140.

[5.10] P. Zavracky, S. Majumder and N. E. McGruer, "Micromechanical Switches Fabricated Using Nickel Surface Micromachining", Journal of Microelectromechanical Systems, Vol. 6-1 (1997), pp. 3-9.

[5.11] W. P. Taylor and M. G. Allen, "Integrated Magnetic Microrelays: Normally Open, Normally Closed, and Multi-Pole Devices", Digest of Technical Papers of the 9th International Conference on Solide-State Sensors and Actuators, Transducers '97, Chicago, IL, June 1997, pp. 1149-1152.

[5.12] "Switching Handbook", Keithley Instruments, Inc., Cleveland, 1995.

[5.13] P. M. Osterberg and S. D. Senturia, "M-Test: A Test Chip of MEMS Material Property Measurement using Electrostatic Actuated Test Structures", Journal of Microelectromechanical Systems, Vol. 6-N°2 (1997), pp. 107-118.

Acknowledgments

First of all I would like to thank Professor Nico de Rooij who gave me the opportunity to do this Ph.D. Thesis and for the interest he gave to my different projects. I would also thank him for the powerful team he has constituted. It is a great pleasure to work in such an environment.

I would also particularly thank Dr. Christian Linder who was my Senior assistant when I started my work at IMT. He has been a very attentive supervisor and his advises were always useful for the progression of my work.

I would also thank the different people who have shared my office during the whole period of my thesis. The ambiance was often stimulating allowing new ideas to emerge. These persons are Dr. Teru Akiyama, Dr. Jurgen Brugger, Dr. Giovanni-Carlo Fiaecabrino, Dr. Volker Gass, Dr. Ben Kloeck, Dr. Thomas Tschan and Dr. David Strike. Thank you David for giving me the desire to learn Shakespeare's mother tongue and for correcting me when I was making big mistakes. Thank you also for reviewing this thesis.

Some internal collaborations have allowed us to design good devices like the gyroscopes, the surface acoustic wave devices, the optical microelectromechanical devices and the glass capillary tubes. I would like to acknowledge Prof. Milena Koudelka, Mr. Olivier Guenat, Mr. Philippe Luginbuhl, Dr. Cornel Marxer, Mr. Sylvain Roth and Mr. Pierre Thiébaud, for the passionate discussions and their enthusiast to believe that we would be successful in these projects. One of these projects was the angular rate sensor which is particular because it started with Ms. Florence Paoletti and will continue with Mrs. Florence Grétillat. Indeed, Florence became my wife on August 16^{teen} 1997. I would like to thank her for her support since 1994.

I wish to express my gratitude to the technical team, Mrs. Sabina Jenny, Ms. Sylviane Pochon, Mr. Pierre-André Clerc and Mr. Sylvain Jeanneret, who work hard to deposit thin and thicker layers on our wafers and who help us to etch them. Their input in this work is considerable.

I would also thank the persons who took part in the great adventure of the research laboratory of Prof. Nico de Rooij: Ms. Cynthia Beuret, Mrs. Antoinette

Goumaz-Rebetez, Ms. Margrit Rüegg, Dr. Sabeth Verpoorte, Dr. Philippe Arquint, Dr. Nicolas Blanc, Mr. Marc Boillat, Dr. Rudi Buser, Mr. Bas de Heij, Mr. Laurent Dellmann, Mr. Bastien Droz, Dr. Karl Fluri, Mr. Benedikt Guldimann, Mr. Pierre-François Indermühle, Dr. Victor Jaecklin, Dr. Werner Morf, Mr. Marco Meijerink, Dr. Lionel Paratte, Dr. Georges-André Racine, Mr. Mathias Schulze, Mr. Grégor Schürmann, Dr. Urs Staufer, Dr. Albert van den Berg, Dr. Bart van der Schoot, Dr. Appo van der Wiel, Dr. Peter van der Wal, and all the others. I thank them for the great ambiance as well as the friendship which has allowed me to work with a lot of pleasure during all these years.

I also express my gratitude to Professor Stephen Senturia at the Massachusetts Institute of Technology who gave me the opportunity to be a visiting scientist during three months in this famous North American Institute. I would thank him for his kind hospitality as well as his coworkers, Mrs. Scottie Fuller, Dr. G. K. Anantasuresh, Dr. Raj Gupta, Mr. Elmer Hung, Mr. Joseph Yang, Dr. Vladimir Rabinovich, Dr. Daniel Sobeck and Mr. Matthew Varghese The party of 4th July as well as the trips to Newport and Martha's Vineyard will remain in my mind as great moments of this Summer 1996.

Furthermore, I would like to thank Professor Stephen Senturia, Dr. Harrie Tilmans and Dr. Hans-Peter Herzig who kindly accepted to be co-examiners of my work as well as "la Fondation Suisse pour la Recherche en Microtechnique" (FSRM) for the financial support on the microrelays project.

Finally, I would give particular thanks to my beloved who have supported me during this great advanture.

Merci à vous tous qui m'avez soutenus pendant ce travail passionnant et astreignant: Merci à mes grands parents, à Popili trop tôt disparu, qui m'ont souvent demandé des nouvelles de ma thèse. Merci à mon frère et à sa femme ainsi qu'à Fonny et à Loïc, leurs charmants petits enfants, pour les magnifiques moments que nous passons ensemble. Merci à mes chers parents qui m'ont donné le goût des études et qui m'ont permis de faire des études en électronique-physique à l'Université de Neuchâtel. Merci à vous qui m'avez toujours encouragés à exploiter mes possibilités dans les branches scientifiques, qui m'avez transmis deux passions: mon travail et la voile. Enfin merci à Florence qui en compagne attentive a su m'encourager pendant tous ces longs mois d'écriture. Grâce à Dieu nos routes se sont croisées, nos thèses nous ont réunis, à toi et à tous ceux qui nous aiment, je souhaite bon vent...

Biography

Marc-Alexis Grétillat was born on October 6, 1967 in Bern, Switzerland. He received his M.Sc. degree in physical electronics from the University of Neuchâtel, Switzerland, in July 1991. In September 1991, he joined the Institute of Microtechnology (IMT) at the University of Neuchâtel, as a research and teaching assistant. His research interests include investigations on resonators and actuators, realized by IC-compatible processes, in view of their application in integrated microsystems. Since spring 1994 he has been involved as a senior assistant in the development of silicon micromachined angular rate sensors, polysilicon optical modulators, optical microswitches, glass capillary tubes and flexural plate wave devices. From June to August 1996, he was a visiting scientist at the Massachusetts Institute of Technology (MIT) in the group of Professor Stephen Senturia.

Bibliography

Refereed Articles:

- C. Linder, L. Paratte, M.-A. Grétillat, V. P. Jaecklin and N. F. de Rooij, "Surface micromachining", Journal of Micromechanics and Microengineering, 2 (1992), pp. 122-132.
- M.-A. Grétillat, C. Linder and N.F. de Rooij, "Integrated Shielding Lines on Multilayer Polysilicon Resonators", Sensors & Actuators, A43 (1994), pp. 351-356.
- M.-A. Grétillat, P. Thiébaud, C. Linder and N. F. de Rooij, "Integrated Circuit Compatible Electrostatic Polysilicon Microrelays", Journal of Micromechanics & Microengineering, 5 (1995), pp. 156-160.
- C. Marxer, M.-A. Grétillat, V. P. Jaecklin, R. Baettig, O. Anthamatten, P. Vogel and N. F. de Rooij, "MHz Opto-mechanical Modulator", Sensors & Actuators, A52 (1996), pp. 46-50.
- C. Marxer, M.-A. Grétillat, R. Baettig, O. Anthamatten, B. Valk, P. Vogel and N. F. de Rooij, "Reliability Considerations for Electrostatic Polysilicon Actuators using as an Example the REMO-Component", Sensors & Actuators, A61 (1997), pp. 449-454.
- M.-A Grétillat, F. Paoletti, P. Thiébaud, S. Roth, M. Koudelka-Hep and N.F. de Rooij, "A New Fabrication Method for Borosilicate Glass Capillary Tubes with Lateral Inlets and Outlets", Sensors & Actuators, A60 (1997), pp. 219-222.
- C. Marxer, M.-A Grétillat, O. Anthamatten, R. Baettig, B. Valk, P. Vogel and N. F. de Rooij, "Vertical Mirrors Fabricated By Deep Reactive Ion Etching For Fiber Optic Switching Applications", Journal of Microelectromechanical Systems, Vol.6 N°3 (1997), pp. 277-285.

- Ph. Luginbuhl, S. D. Collins, G.-A. Racine, M.-A. Grétillat, N. F. de Rooij, K. G. Brooks and N. Setter, "Microfabricated Lamb Wave Device Based on PZT Sol-Gel Thin Film for Mechanical transport of Solid Particles and Liquids", Journal of Microelectromechanical Systems, Vol.06-N°4 (1997), pp. 337-346.
- Ph. Luginbuhl, S. D. Collins, G.-A. Racine, M.-A. Grétillat, N. F. de Rooij, K. G. Brooks and N. Setter, "Ultrasonic Flexural Lamb Wave Actuators based on PZT Thin Film", Sensors & Actuators, A64 (1998), pp. 41-49.

Conference and Workshop Papers

- C. Linder, M.-A. Grétillat and N.F. de Rooij, "Realization of different polysilicon resonators with integrated excitation and detection elements", Microelectronic Engineering, 15 (1991), pp. 411-414.
- C. Linder, L. Paratte, M.-A. Grétillat, V. P. Jaecklin and N. F. de Rooij, "Surface micromachining", Technical Digest of The 3rd Workshop on Micromachining, Micromechanics and Microsystems, MME '92, Leuven, Belgium, June 1992, pp. 43-55.
- M.-A. Grétillat, C. Linder and N.F. de Rooij, "Multilayer Polysilicon Resonators Including Shielding for Excitation and Detection", Digest of Technical Papers of the 7th International Conference on Solide-State Sensors and Actuators, Transducers '93, Yokohama, Japan, June 1993, pp. 292-295.
- M.-A. Grétillat, P. Thiébaud, N. F. de Rooij and C. Linder, "Electrostatic polysilicon microrelays integrated with MOSFETs", Proceedings of the 7th IEEE Workshop on Micro Electro Mechanical Systems, MEMS '94, Oiso, Japan, January 1994, pp. 97-101.
- M.-A. Grétillat, P. Thiébaud, C. Linder and N. F. de Rooij, "IC Compatible Electrostatic Polysilicon Microrelays", Technical Digest of The 5th Workshop on Micromachining, Micromechanics and Microsystems, MME '94, Pisa, Italy, September 1994, pp. 137-140.
- C. Marxer, M.-A. Grétillat, V. P. Jaecklin, R. Baettig, O. Anthamatten, P. Vogel and N. F. de Rooij, "MHz Opto-mechanical Modulator", Digest of Technical Papers of the 8th International Conference on Solide-State Sensors and Actuators, Transducers '95, Stockholm, Sweden, June 1995, vol.1: pp. 289-292.

- F. Paoletti, M.-A. Grétillat and N. F de Rooij, "A Silicon Micromachined Vibrating Gyroscope with Piezoresistive Detection and Electromagnetic Excitation", Proceedings of the 9th IEEE Workshop on Micro Electro Mechanical Systems, MEMS '96, San Diego, CA, February 1996, pp. 162-167.
- R Baettig, O. Anthamatten, B. Valk, C. Marxer, M. A. Grétillat, N. de Rooij, "A Reflective Modulator Based on Silicon Micromechanics", Proceedings of the IEE Colloquium on Optical and Hybrid access networks, BT Laboratories, Digest No: 1996/052, Ipswich, March 1996, pp. 10/1-10/4.
- R. K. Bättig, O. Anthamatten, J-Ch. Roulet, M. Fitzpatrick, B. Valk, P. Vogel, C. Marxer, M.-A. Grétillat, N. F. de Rooij, "Design Considerations and Optical Characterization of a Silicon-Micromechanical Light Modulator for Telecommunication Applications", Proceedings of the Topical Meeting of the European Optical Society (EOS), Engelberg, Switzerland, April 1996, pp. 40-41.
- C. Marxer, M.A Grétillat and N. F. de Rooij, "Breakdown Mechanisms of Electrostatic Polysilicon Actuators using as an Exemple the REMO Component", Digest of IEEE/LEOS 1996, Summer Topical Meeting, Optical MEMS and their Applications, Keystone, CO, August 1996, pp. 15-16.
- O. Anthamatten, R. Bättig, B. Valk, P. Vogel, C. Marxer, M.-A. Grétillat and N. F. de Rooij, "Packaging of a Reflective Optical Duplexer Based on Silicon Micromechanics", Digest of IEEE/LEOS 1996, Summer Topical Meeting, Optical MEMS and their Applications, Keystone, CO, August 1996, pp. 61-62.
- C. Marxer, M.-A. Grétillat, R. Baettig, O. Anthamatten, B. Valk, P. Vogel and N. F. de Rooij, "Reliability Considerations for Electrostatic Polysilicon Actuators using as an Example the REMO-Component", Proceedings of the 10th European Conference on Solide-State Transducers, Eurosensor X, Leuven, Belgium, September 1996, pp. 1117-1121.
- F. Paoletti, M.-A. Grétillat and N. F de Rooij, "A Silicon Micromachined Tuning Fork Gyroscope", Proceedings of Symposium Gyro Technology 1996, Stuttgart, Germany, September 1996, pp. 5.0-5.8.

- M.-A Grétillat, F. Paoletti, P. Thiébaud, S. Roth, M. Koudelka-Hep and N.F. de Rooij, "A New Fabrication Method of Borosilicate Glass Capillary Tubes with Lateral Inlets and Outlets", Proceedings of the 10th European Conference on Solide-State Transducers, Eurosensor X, Leuven, Belgium, September 1996, pp. 259-262.
- O. Anthamatten, R. Bättig, B. Valk, C. Marxer, M. A. Grétillat and N. F. de Rooij, "Telecommunications technology for telemetry", Proceedings of the Opto '96 Congress, Leipzig, Germany, September 1996, pp. 331-336.
- M.-A Grétillat, F. Paoletti, P. Thiébaud, S. Roth, M. Koudelka-Hep and N.F. de Rooij, "A New Fabrication Method of Borosilicate Glass Capillary Tubes with Lateral Inlets and Outlets", Proceedings of Miniaturized Total Analysis Systems, μ-TAS96, Analytical Methods & Instrumentation, Basel, Switzerland, November 1996, p. 214.
- F. Paoletti, M.-A. Grétillat and N. F. de Rooij, "A Silicon Micromachined Tuning Fork Gyroscope", Technical digest of the IEE colloquium on Silicon Fabricated Inertial Instruments, Digest N° 1996/227, London, England, December 1996, pp. 3/1-3/6.
- C. Marxer, M.-A Grétillat, O. Anthamatten, R. Baettig, B. Valk, P. Vogel and N. F. de Rooij, "Vertical Mirrors Fabricated By Reactive Ion Etching For Fiber Optical Switching Applications", Proceedings of the 10th IEEE Workshop on Micro Electro Mechanical Systems, MEMS '97, Nagoya, Japan, January 1997, pp. 49-54.
- Ph. Luginbuhl, S. D. Collins, G.-A. Racine, M.-A. Grétillat, N. F. de Rooij, K. G. Brooks and N. Setter, "Flexural-plate-wave actuators based on PZT thin film", Proceedings of the 10th IEEE Workshop on Micro Electro Mechanical Systems, MEMS '97, Nagoya, Japan, January 1997, pp. 327-332.
- M.-A. Grétillat, Y. J. Yang, E. S. Hung, V. Rabinovich, G. K. Anathasuresh, N. F. de Rooij and S. D. Senturia, "Nonlinear Electromechanical Behavior of an Electrostatic Microrelay", Digest of Technical Papers of the 9th International Conference on Solide-State Sensors and Actuators, Transducers '97, Chicago, IL, June 1997, pp. 1141-1144.
- Y. J. Yang, M.-A. Grétillat and S. D. Senturia, "Effect of Air Damping on the Dynamics of Nonuniform Deformations of Microstructures", Digest of Technical Papers of the 9th International Conference on Solide-State Sensors and Actuators, Transducers '97, Chicago, IL, June 1997, pp. 1093-1096.

- M.-A. Grétillat, C. Linder, A. Dommann, G. Staufert, N. F. de Rooij and M.-A. Nicolet, "Surface-Micromachined Ta-Si-N Beams for Use in Micromechanics", Technical Digest of The 8th Workshop on Micromachining, Micromechanics and Microsystems, MME '97, Southampton, UK, September 1997, pp. 63-66.
- C. Marselli, H.P. Amann, F. Pellandini, F. Grétillat, M.-A. Grétillat and N. F de Rooij, "Error Modelling of a Silicon Angular Rate Sensor", Proceedings of Symposium Gyro Technology 1997, Stuttgart, Germany, September 1997, pp.4.0-4.9.

Unpublished contribution:

- M.-A. Grétillat, "Réalisation de structures résonnantes - Méthodes d'excitation et de détection", Diploma work, Institute of Microtechnology, University of Neuchâtel, 1991.